Table of Contents

Experimental

Spectroscopic Investigations

Vibrational spectra were recorded from 2–5 milligrams of the compounds with an ALPHA FT–IR spectrometer from Bruker optics (ATR module) using OPUS software.

Absorption Spectra were measured on solid–state products using a standard Agilent Cary 5000 UV–VIS–NIR spectrophotometer with a Praying Mantis accessory, which had been mounted and aligned for use with the DRP–ASC ambient chamber. The source, detector, and grating changeovers were at the standard position of 350, 800, and 800 nm, respectively, for all studied compounds except ₁[Nd(2–PyPzH)$_2$Cl$_3$] (**2**) and [Dy(2–PyPzH)$_2$Cl$_3$] (**13**), the detector and grating changeovers were set to 850 nm. For ₁[Nd(2–PyPzH)$_2$Cl$_3$] (**2**), β–[Sm$_2$(2–PyPzH)$_4$Cl$_6$] (**8**), and [Ce(2–PyPzH)$_3$Cl$_3$] (**11**), the source has been set to 380, 330, and 320 nm, respectively. The reference spectrum was collected on PTFE and the reference and samples were packed in the ambient chamber within the glovebox under inert conditions. Water has absorption bands in the NIR region at around 1370 and 1850 nm, which interferes with the absorption of our Ln^{3+} ions. In order to avoid these interferences, we carried out the measurements up to 1300 nm.

Photoluminescence spectra were recorded for ground solid samples after filling them in quartz glass tubes under argon. Measurements were performed at room temperature as well as 77 K (the latter using the liquid nitrogen–filled assembly FL–1013 of HORIBA) with a HORIBA Jobin Yvon Spex Fluorolog 3 spectrometer equipped with a 450 W Xe short–arc lamp (USHIO), double–grated excitation, emission monochromators, and a photomultiplier tube (R928P) using the FluoroEssence™ software. Excitation and emission spectra were corrected for the spectral response of the monochromators and detector using spectral corrections provided by the constructor. In addition, a photodiode reference detector was used to correct the excitation spectra for the spectral distribution of the lamp intensity. An R5509–73 detector was used to collect the data in the NIR region. When needed, data collection was performed using an edge filter (Newport 20CGA–345, 395, 495 for the visible range and Reichmann Optics RG 830 longpass for the NIR range). Emission spectra with gating were recorded using a xenon flashlamp with a pulse repetition rate of 41 ms.

Photoluminescence overall decay process times were determined using the aforementioned HORIBA Jobin Yvon Spex Fluorolog 3 spectrometer equipped with a dual lamp housing (FL–1040A), a UV–xenon flashlamp (Exelitas FX–1102), and a TCSPC (time–correlated single–photon counting) upgrade, or pulsed picosecond laser diode. Emission decays were recorded using DataStation software. Exponential tail fitting was used to calculate the resulting intensity decay using Decay Analysis Software 6. The quality of the fit was confirmed by χ^2 values being below 1.2.

Photoluminescence quantum yields were determined using a second similar instrument HORIBA Jobin Yvon Spex Fluorolog 3 spectrometer equipped with a HORIBA Quanta–ϕ Integrating Sphere. For the measurements, solid samples were filled into Starna Micro Cell cuvettes 18–F/ST/C/Q/10 (fluorescence with ST/C closed–cap, material UV quartz glass Spectrosil Q, pathlength 10 mm, matched). Magnesium oxide was used as reference material. Each sample was measured at least three times and then the quantum yield values with standard deviation were evaluated. The Quanta–ϕ Integrating Sphere was checked with a standard (sodium salicylate as a powder, λ_{ex} = 340 nm, λ_{em} = 365–600 nm, measured QY = 52%, literature: 53%) [77].

Thermal analysis

Simultaneous DTA/TG (NETZSCH STA 409–PC) coupled to a mass spectrometer (NETZSCH QMS 403 Aëolos) in a constant argon flow of 50 mL·min^{-1} with a heating rate of 5 K·min^{-1} from room temperature to 1000 °C was used to determine the thermal properties. The DTA curve was baseline–corrected after the measurement using the Origin™ software.

CHN analysis

A Thermo Scientific Flash EA–1112 was used to perform the CHN analyses. The samples were placed in a tin crucible with at least one mass equivalent of V_2O_5. The samples were prepared and stored under inert conditions until the measurements.

Synthesis of (1*H*–pyrazol–3–yl)pyridines, the general method

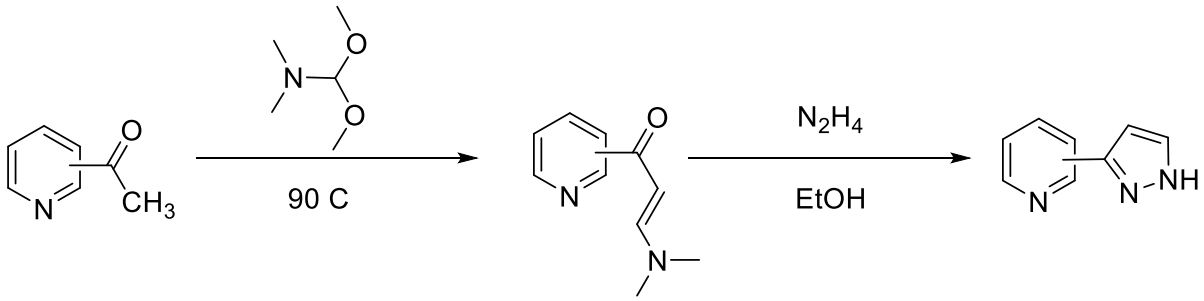

A mixture of acetylpyridine (15g, 124 mmol) and DMF–DMA (30mL, 26.9g, 225 mmol) was stirred at 90 °C using an oil bath. MeOH was removed *via* a short Vigreux column (10 cm) with an attached descending condenser. The reaction was stopped as soon as the distillation of MeOH ceased (7–8 h) and the mixture was cooled to room temperature overnight. Afterward, 30 mL of hexane was added and the resulting suspension was stirred for 30 min and then filtered. All solids were dried to a constant weight and were used without further purification. The products are darkening under atmospheric conditions and should be used shortly after preparation or stored in a freezer at −18 °C.

(E/Z)–3–(dimethylamino)–1–(pyridin–2–yl)prop–2–en–1–one.

To a stirred warm (40°C) solution of 19.3 g (110 mmol) of the corresponding aminoketone in 150 mL of 96% ethanol N_2H_4*H_2O (100%, 8 mL, 160 mmol) was added in one portion and the resulting mixture was refluxed for 6 h with gentle stirring and then cooled to room temperature. Yellow crystals with a yield of 19.6 g (89%) were obtained. Further separation of (1H–pyrazol–3–yl)pyridines was varied for different isomers.

2–(1*H*–pyrazol–3–yl)pyridine / 3–(2–pyridyl)pyrazole (2–PyPzH)

The cooled reaction mixture was dried under diminished pressure and the resulting solid was dissolved in 200mL of $CHCl_3$. The organic solution was washed twice by 20 mL portions of brine, dried over $MgSO_4$, and the solvent was evaporated. The resulting solid was suspended in 20 mL of hexane, filtered, and the crystals were dried. The yield is 12.8 g (80%) of yellow solid. M.p. 118–119 °C (lit. 119–120°C.

^{1}H NMR (300 MHz, $CDCl_3$) δ 11.24 (br. s, 1H), 8.54 (d, J = 4.7 Hz, 1H), 7.78 (t, J = 8.1 Hz, 1H), 7.31 (d, J = 7.7 Hz, 1H), 7.60 (d, J = 2.4 Hz, 1H), 7.06 (t, J = 5.6 Hz, 1 H), 6.78 (s, 1H).

Crystallographic Data

CCDC 2208098 (**1**), 2208099 (**2**), 2208100 (**3**), 2208101 (**5**), 2208102 (**6**), 2208103 (**7**), 2208104 (**8**), 2208105 (**9**), 2208106 (**10**), 2208107 (**11**), 2208108 (**12**), 2208109 (**13**), 2208110 (**14**), 2208111 (**15**), 2208112 (**16**), 2208113 (**17**), 2208114 (**18**) contain the supplementary crystallographic data. These data are provided free of charge by the Cambridge Crystallographic Data Centre.

Table S1. Crystallographic data of ∞[Ln_2(2–PyPzH)$_4Cl_6$], Ln = La (**1**), Nd (**2**), and Sm (**3**).

Compound	**∞[La_2(2–PyPzH)$_4Cl_6$]**	**∞[Nd_2(2–PyPzH)$_4Cl_6$]**	**∞[Sm_2(2–PyPzH)$_4Cl_6$]**
CCDC number	2208098	2208099	2208100
Empirical formula	$C_{16}H_{14}N_6Cl_3La$	$C_{16}H_{14}N_6Cl_3Nd$	$C_{16}H_{14}N_6Cl_3Sm$
M_r / g·mol^{-1}	535.59	540.92	547.03
T / K	100(2)	200(2)	100(2)
λ / pm	71.073, Mo–K_α	71.073, Mo–K_α	71.073, Mo–K_α
Crystal system	Monoclinic	Monoclinic	Monoclinic
Space group	*C*2/*c*	*C*2/*c*	*C*2/*c*
a / pm	2033.6(1)	2031.3(1)	1993.4(1)
b / pm	1190.2(1)	1186.3(1)	1192.3(1)
c / pm	2489.7(2)	2466.6(2)	2449.5(1)
α / °	90	90	90
β / °	92.802(2)	92.326(2)	92.519(2)
γ / °	90	90	90
V / 10^6 pm^3	6018.7(5)	5939.0(6)	5816.5(5)
Z	12	12	12
ρ_{calc} / g·cm^{-3}	1.773	1.815	1.874
μ / mm^{-1}	2.541	3.040	3.455
F(000)	3120	3156	3180
Crystal size / mm^3	0.059 x 0.035 x 0.031	0.172 x 0.114 x 0.077	0.604 x 0.108 x 0.082
θ_{min} / °	1.983	2.007	2.175
θ_{max} / °	27.589	30.582	26.731
Reflections collected	214731	62094	58706
Independent reflections	6998	9066	6173
R(int)	0.0613	0.1365	0.0756
No. Of parameters	454	430	442
GOF	1.119	0.990	1.166
Final *R* indices [$I > 2\sigma$(I)]	R_1 = 0.0319, wR_2 = 0.0752	R_1 = 0.0450, wR_2 = 0.0651	R_1 = 0.0445, wR_2 = 0.0789
R indices (all data)	R_1 = 0.0403, wR_2 = 0.0794	R_1 = 0.0938, wR_2 = 0.0753	R_1 = 0.0574, wR_2 = 0.0819
$\Delta\rho_{max}$, $\Delta\rho_{min}$ / e·10^{-6}·pm^{-3}	2.571, −1.170	1.115, −1.334	2.160, −2.454

Table S2. Crystallographic data of α–[Ln_2(2–PyPzH)$_4Cl_6$], Ln = Eu (**5**), Gd (**6**), and Tb (**7**).

Compound	**α–[Eu_2(2–PyPzH)$_4Cl_6$]**	**α–[Gd_2(2–PyPzH)$_4Cl_6$]**	**α–[Tb_2(2–PyPzH)$_4Cl_6$]**
CCDC number	2208101	2208102	2208103
Empirical formula	$C_{16}H_{14}N_6Cl_3Eu$	$C_{16}H_{14}N_6Cl_3Gd$	$C_{16}H_{14}N_6Cl_3Tb$
M_r / g·mol^{-1}	548.64	553.93	555.60
T / K	100(2)	100(2)	100(2)
λ / pm	71.073, Mo–K_α	71.073 Mo–K_α	71.073, Mo–K_α
Crystal system	Monoclinic	Monoclinic	Monoclinic
Space group	$P2_1/c$	$P2_1/c$	$P2_1/c$
a / pm	811.5(1)	809.1(1)	809.5(1)
b / pm	2380.2(2)	2376.4(2)	2368.7(1)
c / pm	1055.4(1)	1053.3(1)	1054.2(1)
α / °	90	90	90
β / °	112.34(1)	112.19(1)	112.437(1)
γ / °	90	90	90
V / 10^6 pm^3	1885.6(2)	1875.2(3)	1868.31(9)
Z	4	4	4
ρ_{calc} / g·cm^{-3}	1.933	1.962	1.975
μ / mm^{-1}	3.764	3.977	4.227
F(000)	1064	1068	1072
Crystal size / mm^3	0.035 x 0.033 x 0.032	0.067 x 0.038 x 0.023	0.423 x 0.376 x 0.152
θ_{min} / °	2.255	2.257	2.260
θ_{max} / °	26.020	27.136	37.032
Reflections collected	33885	46710	122560
Independent reflections	3695	4156	9509
R(int)	0.0781	0.0956	0.0573
No. Of parameters	299	329	235
GOF	1.048	1.054	1.112
Final R indices [$I > 2\sigma$(I)]	R_1 = 0.0326, wR_2 = 0.0638	R_1 = 0.0409, wR_2 = 0.0895	R_1 = 0.0241, wR_2 = 0.0500
R indices (all data)	R1 = 0.0511, wR2 = 0.0724	R_1 = 0.0694, wR_2 = 0.1066	R_1 = 0.0331, wR_2 = 0.0524
$\Delta\rho_{max}$, $\Delta\rho_{min}$ / e·10^{-6}·pm^{-3}	2.119, −1.824	3.501, −2.013	1.961, −1.527

Table S3. Crystallographic data of β–[Ln_2(2–PyPzH)$_4Cl_6$], Ln = Sm (**8**), Eu (**9**), Gd (**10**) and [Ce(2–PyPzH)$_3Cl_3$] (**11**).

Compound	**β–[Sm_2(2–PyPzH)$_4Cl_6$]**	**β–[Eu_2(2–PyPzH)$_4Cl_6$]**	**β–[Gd_2(2–PyPzH)$_4Cl_6$]**	**[Ce(2–PyPzH)$_3Cl_3$]**
CCDC number	2208104	2208105	2208106	2208107
Empirical formula	$C_{16}H_{14}N_6Cl_3Sm$	$C_{16}H_{14}N_6Cl_3Eu$	$C_{16}H_{14}N_6Cl_3Gd$	$C_{24}H_{21}N_9Cl_3Ce$
M_r / g·mol^{-1}	547.03	548.64	553.93	681.97
T / K	100(2)	100(2)	100(2)	100(2)
λ / pm	71.073, Mo–K_α	71.073, Mo–K_α	71.073, Mo–K_α	71.073, Mo–K_α
Crystal system	Triclinic	Triclinic	Triclinic	Orthorhombic
Space group	$P\bar{1}$	$P\bar{1}$	$P\bar{1}$	*Pbca*
a / pm	832.3(1)	831.4(1)	830.1(2)	1329.8(1)
b / pm	1045.6(1)	1045.6(2)	1050.6(3)	1916.0(1)
c / pm	1226.0(1)	1224.2(2)	1229.9(3)	2051.1(1)
α / °	74.63(1)	74.60(1)	75.20(1)	90
β / °	86.96(1)	86.88(1)	86.95(1)	90
γ / °	68.71(1)	68.64(1)	68.34(1)	90
V / 10^6 pm^3	957.5(1)	954.5(2)	962.9(4)	5226.1(5)
Z	2	2	2	8
ρ_{calc} / g·cm^{-3}	1.897	1.909	1.910	1.734
μ / mm^{-1}	3.497	3.718	3.872	2.082
F(000)	530	532	534	2696
Crystal size / mm^3	0.027 x 0.026 x 0.015	0.050 x 0.036 x 0.019	0.061 x 0.047 x 0.014	0.021 x 0.032 x 0.074
θ_{min} / °	2.387	2.169	1.714	2.112
θ_{max} / °	27.253	27.170	27.308	27.132
Reflections collected	95185	33424	21316	94436
Independent reflections	4281	4211	4281	5784
R(int)	0.1488	0.0560	0.0624	0.1012
No. Of parameters	235	235	236	334
GOF	1.040	0.874	1.167	1.040
Final R indices [$I > 2\sigma$(I)]	R_1 = 0.0262, wR_2 = 0.0444	R_1 = 0.0274, wR_2 = 0.0956	R_1 = 0.0398, wR_2 = 0.0816	R_1 = 0.0309, wR_2 = 0.0645
R indices (all data)	R_1 = 0.0393, wR_2 = 0.0473	$R1$ = 0.0332, $wR2$ = 0.1021	$R1$ = 0.0499, $wR2$ = 0.0846	R_1 = 0.0412, wR_2 = 0.0709
$\Delta\rho_{max}$, $\Delta\rho_{min}$ / e·10^{-6}·pm^{-3}	1.683, −0.804	1.007, −1.368	1.235, −0.900	1.764, −0.595

Table S4. Crystallographic data of [Ln(2–PyPzH)$_2$Cl$_3$], Ln = Tb (**12**), Dy (**13**), Ho (**14**), and Eu (**15**).

Compound	**[Tb(2–PyPzH)$_2$Cl$_3$]**	**[Dy(2–PyPzH)$_2$Cl$_3$]**	**[Ho(2–PyPzH)$_2$Cl$_3$]**	**[Er(2–PyPzH)$_2$Cl$_3$]**
CCDC number	2208108	2208109	2208110	2208111
Empirical formula	$C_{16}H_{14}N_6Cl_3Tb$	$C_{16}H_{14}N_6Cl_3Dy$	$C_{16}H_{14}N_6Cl_3Ho$	$C_{16}H_{14}N_6Cl_3Er$
M_r / g·mol^{-1}	555.60	559.18	561.61	563.94
T / K	100(2)	100(2)	100(2)	100(2)
λ / pm	71.073, Mo–K$_\alpha$	71.073, Mo–K$_\alpha$	71.073, Mo–K$_\alpha$	71.073, Mo–K$_\alpha$
Crystal system	Monoclinic	Monoclinic	Monoclinic	Monoclinic
Space group	$P2_1/c$	$P2_1/c$	$P2_1/c$	$P2_1/c$
a / pm	1072.9(1)	1070.9(2)	1072.0(1)	1073.0(1)
b / pm	1221.8(1)	1222.1(2)	1220.1(1)	1218.5(1)
c / pm	1467.1(1)	1466.1(2)	1465.3(1)	1464.6(1)
α / °	90	90	90	90
β / °	92.66(1)	92.32(1)	91.989(3)	91.761
γ / °	90	90	90	90
V / 10^6 pm^3	1921.2(2)	1917.1(5)	1915.43(14)	1913.9(1)
Z	4	4	4	4
ρ_{calc} / g·cm^{-3}	1.921	1.937	1.948	1.957
μ / mm^{-1}	4.111	4.328	4.562	4.816
F(000)	1072	1076	1080	1084
Crystal size / mm^3	0.131 x 0.022 x 0.014	0.112 x 0.059 x 0.033	0.224 x 0.201 x 0.137	0.196 x 0.081 x 0.034
θ_{min} / °	1.900	1.903	2.530	2.175
θ_{max} / °	26.413	25.578	34.969	38.565
Reflections collected	32112	61699	75143	107396
Independent reflections	3944	3596	8419	10826
R(int)	0.0894	0.0759	0.1273	0.0845
No. Of parameters	235	235	235	235
GOF	1.038	1.068	1.065	1.026
Final R indices [$I > 2\sigma$(I)]	$R1$ = 0.0360, $wR2$ = 0.0639	R_1 = 0.0263, wR_2 = 0.0583	R_1 = 0.0600, wR_2 = 0.1190	R_1 = 0.0303, wR_2 = 0.0514
R indices (all data)	$R1$ = 0.0556, $wR2$ = 0.0705	R_1 = 0.0345, wR_2 = 0.0618	R_1 = 0.1137, wR_2 = 0.1377	R_1 = 0.0531, wR_2 = 0.0565
$\Delta\rho_{max}$, $\Delta\rho_{min}$ / e·10^{-6}·pm^{-3}	1.628, −0.890	1.631, −1.113	5.536, −2.807	2.231, −1.785

Table S5. Crystallographic data of $[Gd_2(2–PyPzH)_3(2–PyPz)Cl_5]$ (**16**), $[Gd_3(2–PyPzH)_8Cl_8]Cl$ (**17**), and $[PyH][Tb(2–PyPzH)_2Cl_4]$ (**18**).

Compound	**$[Gd_2(2–PyPzH)_3(2–PyPz)Cl_5]$**	**$[Gd_3(2–PyPzH)_8Cl_8]Cl$**	**$[PyH][Tb(2–PyPzH)_2Cl_4]$**
CCDC number	2208112	2208113	2208114
Empirical formula	$C_{32}H_{27}N_{12}Cl_5Gd_2$	$C_{64}H_{56}N_{24}Cl_9Gd_3$	$C_{21}H_{20}N_7Cl_4Tb$
M_r / g·mol^{-1}	1071.40	1952.12	671.16
T / K	100(2)	100(2)	200(2)
λ / pm	71.073 Mo–K_α	71.073, Mo–K_α	71.073, Mo–K_α
Crystal system	Monoclinic	Triclinic	Orthorhombic
Space group	$P2_1/n$	$P\bar{1}$	$Pbcn$
a / pm	1047.5(1)	994.2(2)	1205.5(1)
b / pm	1982.9(1)	1963.5(3)	1230.6(1)
c / pm	1914.4(1)	2016.1(3)	1762.2(2)
α / °	90	69.87(1)	90
β / °	102.37(1)	88.81(1)	90
γ / °	90	78.39(1)	90
V / 10^6 pm^3	3883.8(4)	3614.6(8)	2614.1(2)
Z	4	2	4
ρ_{calc} / g·cm^{-3}	1.832	1.794	1.705
μ / mm^{-1}	3.771	3.112	3.137
F(000)	2064	1906	1312
Crystal size / mm^3	0.31 x 0.102 x 0.027	0.076 x 0.038 x 0.036	0.285 x 0.150 x 0.122
θ_{min} / °	2.054	2.056	2.633
θ_{max} / °	27.193	27.103	27.133
Reflections collected	76683	163558	32818
Independent reflections	8618	15930	2895
R(int)	0.1076	0.0890	0.0496
No. Of parameters	460	1001	177
GOF	1.074	1.100	1.069
Final R indices [$I > 2\sigma$(I)]	R_1 = 0.0454, wR_2 = 0.0968	R_1 = 0.0463, wR_2 = 0.0869	R_1 = 0.0197, wR_2 = 0.0365
R indices (all data)	R_1 = 0.0800, wR_2 = 0.1109	R_1 = 0.0678, wR_2 = 0.0935	R_1 = 0.0320, wR_2 = 0.0406
$\Delta\rho_{max}$, $\Delta\rho_{min}$ / e·10^{-6}·pm^{-3}	2.264, −1.227	1.537, −1.340	0.369, −0.488

Interatomic distances and Angles

Table S6. Selected interatomic distances (pm) and angles (°) of $^{1}_{\infty}$[Ln_2(2–PyPzH)$_4Cl_6$], Ln= La (**1**), Nd (**2**), and Sm (**3**). Symmetry operations: I -x+1,y,-z+1/2.

Compound	$^{1}_{\infty}$[La_2(2–PyPzH)$_4Cl_6$]	$^{1}_{\infty}$[Nd_2(2–PyPzH)$_4Cl_6$]	$^{1}_{\infty}$[Sm_2(2–PyPzH)$_4Cl_6$]
Ln1–Cl1	290.4(1)	287.7(1)	283.9(1)
Ln1–Cl2	281.6(1)	275.0(1)	272.0(2)
Ln1–Cl3	277.5(1)	272.4(1)	269.6(2)
Ln1–Cl4	292.4(1)	289.2(1)	285.6(2)
Ln2–Cl4	294.5(1)	292(1)	288.8(2)
Ln2–Cl5	280.3(1)	273.8(1)	270.6(2)
Ln1–N1	273.9(3)	268.6(3)	265.5(5)
Ln1–N2	262.2(3)	256.1(3)	253.2(5)
Ln1–N4	275.5(3)	270.3(4)	267.0(5)
Ln1–N5	263.3(3)	257.0(3)	254.2(5)
Ln2–N7	269(2)	267(1)	265(1)
Ln2–N8	266(2)	260(1)	255(1)
Cl1–Ln1–Cl2	78.6(1)	78.1(1)	78.0(1)
Cl1–Ln1–Cl3	78.1(1)	78.0(1)	78.0(1)
Cl3–Ln1–Cl2	92.2(1)	92.7(1)	94.2(1)
Cl1–Ln1–Cl4	151.4(1)	150.1(1)	149.0(1)
Cl2–Ln1–Cl4	75.7(1)	75.6(1)	75.9(1)
Cl3–Ln1–Cl4	90.8(1)	89.1(1)	87.7(1)
Cl4– Ln2–Cl4^{I}	132.9(1)	132.7(1)	133.3(1)
Cl5–Ln2–Cl4	79.9(1)	79.6(1)	79.0(1)
Cl5^{I}–Ln2–Cl4	76.6(1)	76.5(1)	76.5(1)
Cl5–Ln2–Cl5^{I}	118.8(1)	117.8(1)	115.2(1)
N1–Ln1–Cl1	75.8(1)	76.1(1)	76.0(1)
N1–Ln1–Cl2	150.5(1)	149.5(1)	147.5(2)
N1–Ln1–Cl3	96.4(1)	97.6(1)	98.9(1)
N1–Ln1–Cl4	132.1(1)	133.0(1)	133.9(2)
N2–Ln1–Cl1	125.1(1)	125.6(1)	125.5(1)
N2–Ln1–Cl2	148.2(1)	148.5(1)	149.7(1)
N2–Ln1–Cl3	75.1(1)	75.1(1)	75.2(1)
N2–Ln1–Cl4	75.6(1)	75.3(1)	75.4(1)
N4–Ln1–Cl1	128.1(1)	129.5(1)	131.2(1)
N4–Ln1–Cl2	112.6(1)	111.3(1)	109.6(1)
N4–Ln1–Cl3	145.9(1)	145.6(1)	144.8(1)
N4–Ln1–Cl4	74.2(1)	74.3(1)	74.1(2)
N5–Ln1–Cl1	70.6(1)	71.3(1)	72.0(2)
N5–Ln1–Cl2	84.7(1)	82.4(1)	80.8(1)
N5–Ln1–Cl3	148.5(1)	149.2(1)	150.0(1)
N5–Ln1–Cl4	118.5(1)	118.5(1)	119.1(1)
N7–Ln2–Cl4	81.8(2)	81.1(2)	80.8(2)

N7^{I}–Ln2–Cl4	136.0(2)	82.8(3)	137.5(2)
N7–Ln2–Cl5	145.0(3)	144.4(3)	143.8(3)
N7^{I}–Ln2–Cl5	85.2(4)	85.9(4)	88.4(3)
N8–Ln2–Cl4	135.8(3)	135.0(2)	134.5(3)
N8^{I}–Ln2–Cl4	75.1(2)	75(2)	74.7(2)
N8^{I}–Ln2–Cl5	76.8(4)	75.9(3)	76.0(3)
N8^{I}–Ln2–Cl5^{I}	144.3(3)	145.1(2)	146.2(3)
N2–Ln1–N1	61.1(1)	61.9(1)	62.7(2)
N2–Ln1–N4	71.6(1)	71.6(1)	71.3(2)
N4–Ln1–N1	73.8(1)	74.4(1)	74.9(2)
N5–Ln1–N1	73.4(1)	74.1(1)	73.1(2)
N5–Ln1–N2	121.2(1)	122.5(1)	122.2(2)
N5–Ln1–N4	60.9(1)	61.8(1)	62.4(2)
N7^{I}–Ln2–N7	87.6(8)	88.2(7)	86.6(6)
N8–Ln2–N7	61.2(2)	62.2(2)	62.9(2)
N8^{I}–Ln2–N7	69.7(5)	70.3(5)	69.8(5)
N8^{I}– Ln2–N8	110.0(6)	112.1(5)	113.3(5)

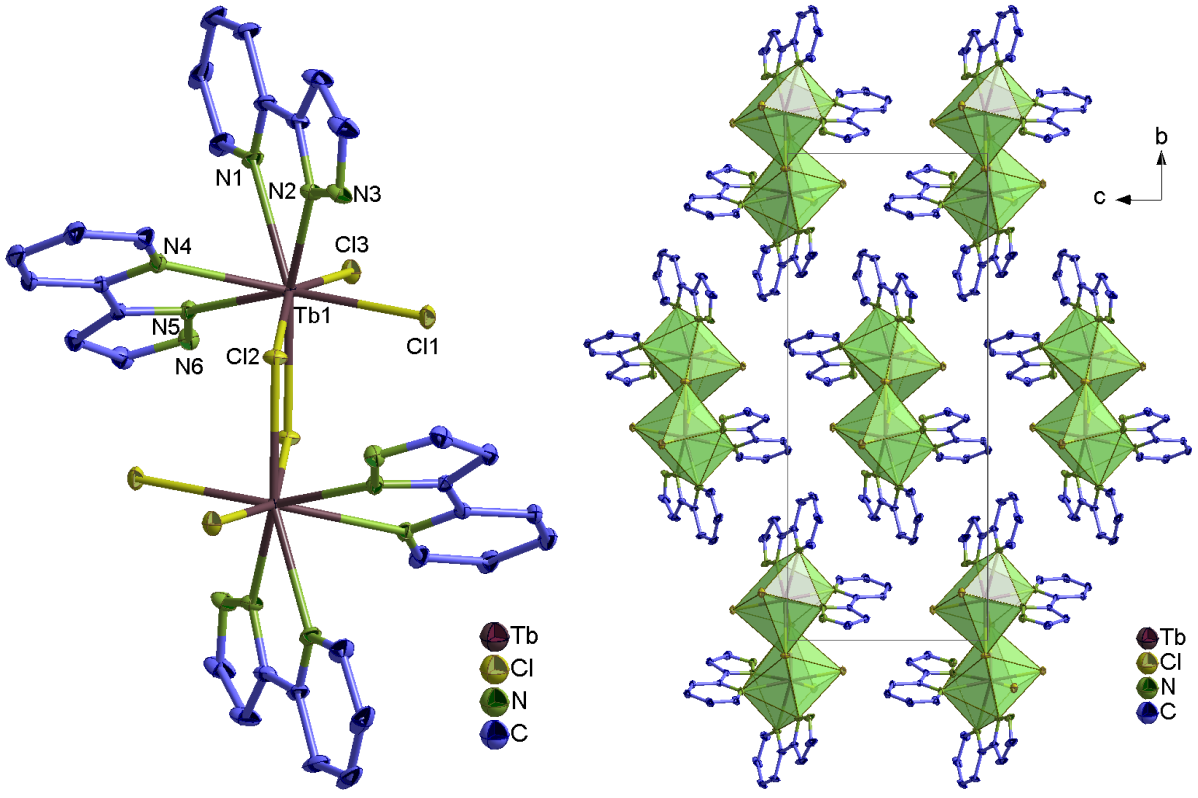

(**a**) (**b**)

Figure S1. (**a**) Extended coordination sphere of Tb^{3+} ion in α–$[Tb_2(2–PyPzH)_4Cl_6]$ (**7**) representing the isotypic complexes **4**–**7**. (**b**) Packing structure of **7** with a view along [100]. In all figures, the hydrogen atoms are omitted for clarity and the coordination polyhedra around Ln^{3+} are shown in green, with thermal ellipsoids shown with a probability of 50%.

Table S7. Selected interatomic distances (pm) and angles (°) of α–[Ln_2(2–PyPzH)$_4Cl_6$], Ln=Eu (**6**), Gd (**7**), and Tb (**8**).

Compound	**α–[Eu_2(2–PyPzH)$_4Cl_6$]**	**α–[Gd_2(2–PyPzH)$_4Cl_6$]**	**α–[Tb_2(2–PyPzH)$_4Cl_6$]**
Ln1–Cl1	277.6(2)	266.5(2)	266.0(1)
Ln1–Cl2	270.8(2)	276.7(2)	275.8(1)
Ln1–Cl3	266.9(2)	269.9(2)	269.2(1)
Ln1–N1	265.1(4)	266.0(2)	262.5(2)
Ln1–N2	248.7(5)	249.0(2)	247.3(2)
Ln1–N4	262.0(2)	264.6(5)	262.7(2)
Ln1–N5	250.0(2)	247.4(6)	246.0(2)
Cl1–Ln1–Cl2	87.0(1)	83.7(1)	83.1(1)
Cl1–Ln1–Cl3	84.1(1)	80.7(1)	80.8(1)
Cl3–Ln1–Cl2	81.1(1)	87.0(1)	87.5(1)
N1–Ln1–Cl1	104.2(1)	116.2(4)	118.7(1)
N1–Ln1–Cl2	131.5(1)	151.0(3)	148.0(1)
N1–Ln1–Cl3	146.1(1)	76.5(4)	74.6(1)
N2–Ln1–Cl1	73.9(1)	76.8(5)	79.6(1)
N2–Ln1–Cl2	76.3(1)	146.7(3)	148.5(1)
N2–Ln1–Cl3	148.9(2)	115.7(5)	115.1(1)
N4–Ln1–Cl1	144.0(3)	146.1(2)	146.0(1)
N4–Ln1–Cl2	71.4(6)	104.5(2)	104.2(1)
N4–Ln1–Cl3	119.1(7)	131.8(2)	132.0(1)
N5–Ln1–Cl1	152.6(4)	148.8(2)	148.0(1)
N5–Ln1–Cl2	114.9(6)	74.0(2)	73.9(1)
N5–Ln1–Cl3	83.4(6)	76.7(2)	76.5(1)
N2–Ln1–N1	62.7(2)	62.1(4)	63.1(1)
N2–Ln1–N4	73.2(5)	79.2(6)	77.6(1)
N4–Ln1–N1	72.7(7)	71.4(5)	71.6(1)
N5–Ln1–N1	74.4(7)	79.1(4)	76.3(1)
N5–Ln1–N2	125.5(5)	132.7(4)	130.6(1)
N5–Ln1–N4	62.7(4)	62.8(2)	63.3(1)

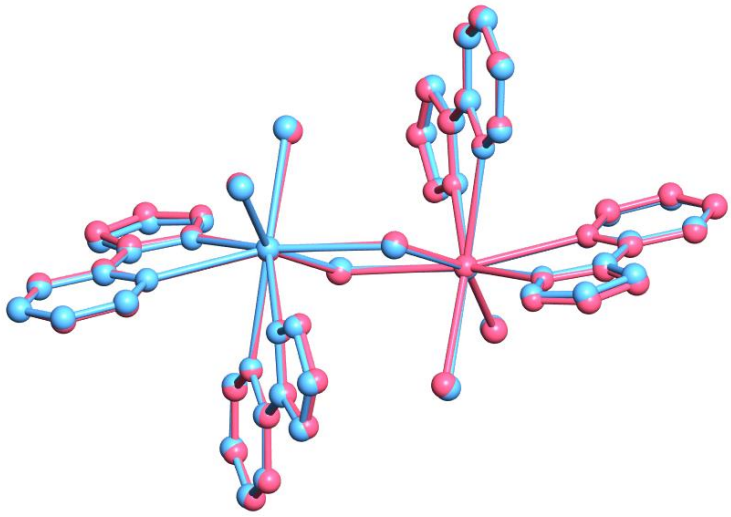

Figure S2. Overlay of the molecular structures of α–[Eu_2(2–PyPzH)$_4Cl_6$] (red) (**5**) and β–[Eu_2(2–PyPzH)$_4Cl_6$] (blue) (**9**).

Table S8. Selected interatomic distances (pm) and angles (◦) of β–[Ln_2(2–PyPzH)$_4Cl_6$], Ln= Sm (**8**), Eu (**9**), and Gd (**10**).

Compound	**β–[Sm_2(2–PyPzH)$_4Cl_6$]**	**β–[Eu_2(2–PyPzH)$_4Cl_6$]**	**β–[Gd_2(2–PyPzH)$_4Cl_6$]**
Ln1–Cl1	272.8(1)	272(1)	271.1(2)
Ln1–Cl2	269.2(1)	268.5(1)	267.7(2)
Ln1–Cl3	277.6(1)	276.2(1)	276.0(2)
Ln1–N1	265.1(3)	264.6(4)	264.1(5)
Ln1–N2	251.1(3)	251.2(3)	249.0(5)
Ln1–N4	267.0(3)	266.0(4)	265.5(5)
Ln1–N5	250.0(3)	249.1(3)	247.6(5)
Cl1–Ln1–Cl2	82.1(1)	81.9(1)	81.4(1)
Cl1–Ln1–Cl3	86.7(1)	87.0(1)	86.6(1)
Cl3–Ln1–Cl2	86.1(1)	86.2(1)	86.5(1)
N1–Ln1–Cl1	130.5(1)	130.8(1)	130.9(1)
N1–Ln1–Cl2	145.9(1)	145.8(1)	145.9(1)
N1–Ln1–Cl3	103.2(1)	103.2(1)	103.9(1)
N2–Ln1–Cl1	74.5(1)	74.7(1)	75.1(1)
N2–Ln1–Cl2	150.4(1)	150.3(1)	150.5(1)
N2–Ln1–Cl3	74.7(1)	74.6(1)	74.9(1)
N4–Ln1–Cl1	77.0(1)	76.7(1)	76.8(1)
N4–Ln1–Cl2	114.9(1)	114.9(1)	114.1(2)
N4–Ln1–Cl3	150.7(1)	150.6(1)	150.7(2)
N5–Ln1–Cl1	119.1(1)	118.7(1)	119.1(2)
N5–Ln1–Cl2	77.3(1)	77.0(1)	77.0(2)
N5–Ln1–Cl3	146.4(1)	146.2(1)	146.2(1)
N2–Ln1–N1	62.3(1)	62.6(1)	62.5(2)

N2–Ln1–N4	77.6(1)	77.6(1)	77.6(2)
N4–Ln1–N1	71.3(1)	71.5(1)	71.3(2)
N5–Ln1–N1	77.3(1)	77.5(1)	76.8(2)
N5–Ln1–N2	130.2(1)	130.6(1)	130.2(2)
N5–Ln1–N4	62.0(1)	62.4(1)	62.4(2)

Table S9. Selected interatomic distances (pm) and angles (◦) of [Ce(2–PyPzH)$_3$Cl$_3$] (**11**).

Atoms	**[Ce(2–PyPzH)$_3$Cl$_3$]**	**Atoms**	**[Ce(2–PyPzH)$_3$Cl$_3$]**
Ce1–Cl1	279.9(2)	N1–Ce1–Cl2	77.03(9)
Ce1–Cl2	279.7(2)	N2–Ce1–Cl1	70.0(1)
Ce1–Cl3	283.2(1)	N2–Ce1–Cl2	128.9(1)
Ce1–N1	271.5(4)	N5–Ce1–Cl1	137.2(1)
Ce1–N2	264.6(4)	N5–Ce1–Cl2	134.4(1)
Ce1–N4	282.6(4)	N8–Ce1–Cl1	74.3(1)
Ce1–N5	260.7(4)	N8–Ce1–Cl2	71.1(1)
Ce1–N7	280.4(4)	N1–Ce1–N4	68.7(1)
Ce1–N8	261.1(4)	N1–Ce1–N7	137.3(1)
Cl1–Ce1–Cl3	86.5(1)	N2–Ce1–N1	60.8(2)
Cl2–Ce1–Cl3	146.7(1)	N2–Ce1–N4	110.7(2)
N1–Ce1–Cl3	132.2(1)	N2–Ce1–N7	138.3(2)
N2–Ce1–Cl3	72.1(1)	N5–Ce1–N1	80.5(2)
N4–Ce1–Cl3	125.5(1)	N5–Ce1–N2	67.8(2)
N5–Ce1–Cl3	74.1(1)	N5–Ce1–N4	59.5(1)
N7–Ce1–Cl3	75.8(1)	N5–Ce1–N7	78.4(2)
N8–Ce1–Cl3	76.1(1)	N5–Ce1–N8	133.5(2)
Cl1–Ce1–N4	147.4(1)	N7–Ce1–N4	68.6(1)
Cl1–Ce1–N7	133.7(1)	N8–Ce1–N1	144.6(2)
Cl2–Ce1–N4	75.4(1)	N8–Ce1–N2	133.0(2)
Cl2–Ce1–N7	92.1(1)	N8–Ce1–N4	115.9(2)
N1–Ce1–Cl1	85.5(1)	N8–Ce1–N7	60.1(2)

Table S10. Selected interatomic distances (pm) and angles (◦) of [Ln(2–PyPzH)$_2$Cl$_3$], Ln= Tb (**12**), Dy (**13**), Ho (**14**), and Er (**15**).

Compound	**[Tb(2–PyPzH)$_2$Cl$_3$]**	**[Dy(2–PyPzH)$_2$Cl$_3$]**	**[Ho(2–PyPzH)$_2$Cl$_3$]**	**[Er(2–PyPzH)$_2$Cl$_3$]**
Ln1–Cl1	263.1(2)	261.7(1)	261.1(2)	260.2(1)
Ln1–Cl2	262.2(2)	261.4(1)	260(2)	259.1(1)
Ln1–Cl3	267.3(2)	265.7(1)	265.4(2)	264.5(1)
Ln1–N1	256.7(4)	255.6(3)	253.7(5)	253.2(2)
Ln1–N2	244.2(4)	242.9(3)	242.2(5)	240.5(2)
Ln1–N4	255.9(4)	255.1(3)	253.6(5)	252.7(2)
Ln1–N5	245.4(4)	244.6(3)	243.7(5)	241.9(2)

Cl1–Ln1–Cl2	94.4(1)	95.1(1)	95.4(1)	95.5(1)
Cl1–Ln1–Cl3	161.9(1)	162.1(1)	162.1(1)	162.1(1)
Cl3–Ln1–Cl2	92.0(1)	91.1(1)	91.0(1)	90.5(1)
N1–Ln1–Cl1	85.5(1)	85.6(1)	85.4(1)	85.4(1)
N1–Ln1–Cl2	85.6(1)	85.7(1)	85.4(1)	85.5(1)
N1–Ln1–Cl3	78.1(1)	78.2(1)	78.5(1)	78.3(1)
N2–Ln1–Cl1	84.1(1)	83.8(1)	83.5(1)	83.5(1)
N2–Ln1–Cl2	150.7(1)	151.3(1)	151.3(2)	151.7(1)
N2–Ln1–Cl3	82.0(1)	82.8(1)	82.9(1)	83.3(1)
N4–Ln1–Cl1	75.4(1)	75.3(1)	75.4(1)	75.5(1)
N4–Ln1–Cl2	81.9(1)	81.6(1)	81.4(1)	81.1(1)
N4–Ln1–Cl3	122.3(1)	122.3(1)	122.1(1)	122.2(1)
N5–Ln–Cl1	112.3(1)	112.0(1)	111.7(1)	112.2(1)
N5–Ln1–Cl2	127.8(1)	127.3(1)	127.4(1)	127.1()
N5–Ln1–Cl3	76.3(1)	76.6(1)	76.8(1)	76.6(1)
N2–Ln1–N1	65.1(2)	65.6(1)	65.9(2)	66.3(1)
N2–Ln1–N4	125.4(2)	125.3(1)	125.5(2)	125.3(1)
N4–Ln–N1	156.2(2)	155.9(1)	155.5(2)	155.3(1)
N5–Ln1–N1	138.1(2)	138.2(1)	138.6(2)	138.4(1)
N5–Ln1–N2	78.8(2)	78.6(1)	78.5(2)	78.3(1)
N5–Ln1–N4	64.2(2)	64.4(1)	64.5(2)	64.9(1)

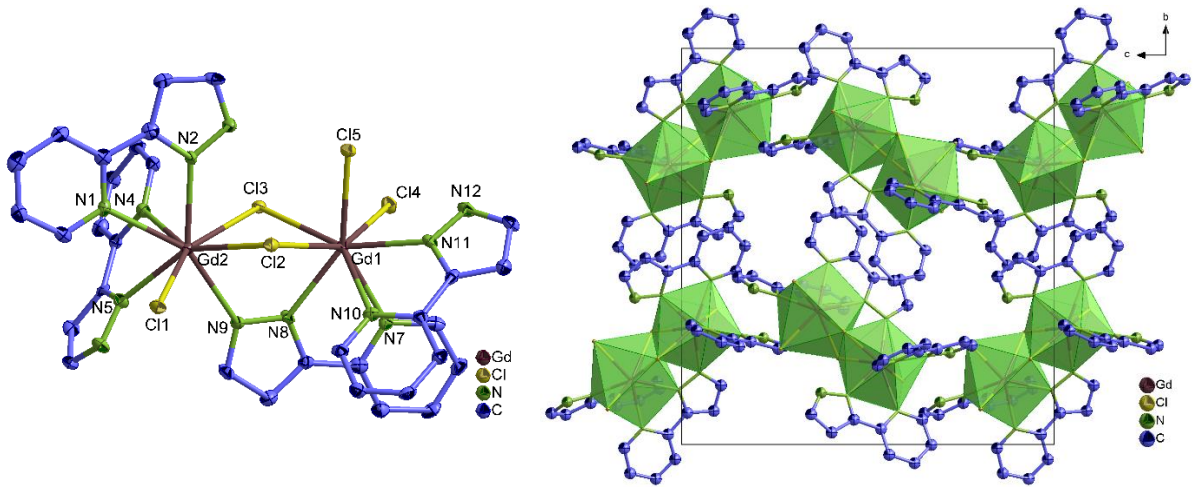

(**a**) (**b**)

Figure S3. (**a**) Extended coordination sphere of Gd^{3+} ion in $[Gd_2(2–PyPzH)_3(2–PyPz)Cl_5]$ (**16**). (**b**) Packing structure of **16** with a view along [100].

Table S11. Selected interatomic distances (pm) and angles (°) of $[Gd_2(2–PyPzH)_3(2–PyPz)Cl_5]$ (**16**).

Atoms	$[Gd_2(2–PyPzH)_3(2–PyPz)Cl_5]$	Atoms	$[Gd_2(2–PyPzH)_3(2–PyPz)Cl_5]$
Gd1–Cl1	268.3(2)	N5–Gd1–Cl3	77.1(1)
Gd1–Cl2	276.0(2)	N7–Gd2–Cl2	149.5(1)
Gd1–Cl3	281.0(2)	N7–Gd2–Cl3	76.5(1)
Gd2–Cl2	281.6(2)	N7–Gd2–Cl4	73.5(1)
Gd2–Cl3	276.1(2)	N7–Gd2–Cl5	114.9(1)
Gd2–Cl4	270.8(2)	N8–Gd2–Cl2	145.5(1)
Gd2–Cl5	278.3(2)	N8–Gd2–Cl3	85.4(2)
Gd1–N1	261.9(5)	N8–Gd2–Cl4	76.2(2)
Gd1–N2	250.3(5)	N8–Gd2–Cl5	76.9(2)
Gd1–N4	263.5(5)	N9–Gd2–Cl1	85.4(2)
Gd1–N5	249.0(5)	N9–Gd2–Cl2	76.2(2)
Gd2–N7	257.4(5)	N9–Gd2–Cl3	76.9(2)
Gd2–N8	243.3(5)	N10–Gd2–Cl2	73.4(1)
Gd2–N9	248.5(5)	N10–Gd2–Cl3	143.4(1)
Gd2–N10	263.3(5)	N10–Gd2–Cl4	132.3(1)
Gd2–N11	247.3(5)	N10–Gd2–Cl5	110.8(1)
Cl1–Gd1–Cl2	79.1(1)	N11–Gd2–Cl2	112.9(2)
Cl1–Gd1–Cl3	153.7(1)	N11–Gd2–Cl3	152.3(1)
Cl2–Gd1–Cl3	78.0(1)	N11–Gd2–Cl4	78.9(2)
Cl3–Gd2–Cl2	77.8(1)	N11–Gd2–Cl5	76.6(1)
Cl3–Gd2–Cl5	82.3(1)	N1–Gd1–N4	74.7(2)
Cl4–Gd2–Cl3	81.4(1)	N2–Gd1–N1	63.0(2)
Cl4–Gd2–Cl2	152.2(1)	N2–Gd1–N4	81.0(2)
Cl4–Gd2–Cl5	84.5(1)	N5–Gd1–N1	77.3(2)
Cl5–Gd2–Cl2	74.7(1)	N5–Gd1–N2	132.4(2)
N1–Gd1–Cl1	74.6(1)	N5–Gd1–N4	63.2(2)
N1–Gd1–Cl2	118.1(1)	N7–Gd2–N10	67.4(2)
N1–Gd1–Cl3	128.2(1)	N8–Gd2–N7	65.0(2)
N2–Gd1–Cl1	77.5(1)	N8–Gd2–N10	78.0(2)
N2–Gd1–Cl2	135.4(1)	N8–Gd2–N11	132.9(2)
N2–Gd1–Cl3	144.8(1)	N9–Gd2–N1	151.7(2)
N4–Gd1–Cl1	79.0(1)	N9–Gd2–N2	144.8(2)
N4–Gd1–Cl2	148.2(1)	N9–Gd2–N4	108.6(2)
N4–Gd1–Cl3	115.8(1)	N9–Gd2–N5	79.4(2)
N5–Gd1–Cl1	129.2(1)	N11–Gd2–N7	76.1(2)
N5–Gd1–Cl2	118.1(1)	N11–Gd2–N10	62.7(2)

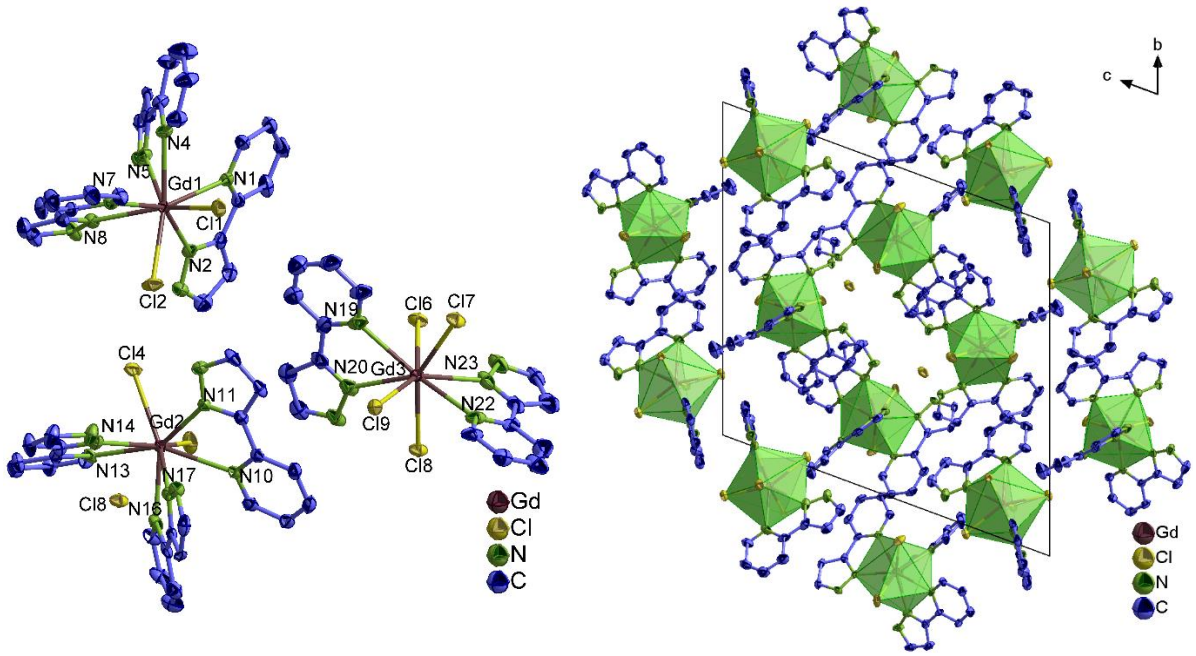

(**a**) (**b**)

Figure S4. (**a**) Extended coordination sphere of Gd^{3+} ion in $[Gd_3(2–PyPzH)_8Cl_8]Cl$ (**17**). (**b**) Packing structure of **17** with a view along [100].

Table S12. Selected interatomic distances (pm) and angles (°) of $[Gd_3(2–PyPzH)_8Cl_8]Cl$ (**17**).

Atoms	$[Gd_3(2–PyPzH)_8Cl_8]Cl$	Atoms	$[Gd_3(2–PyPzH)_8Cl_8]Cl$
Gd1–Cl1	265.5(2)	N14–Gd2–Cl5	147.5(3)
Gd1–Cl2	271.1(2)	N16–Gd2–Cl4	150.8(1)
Gd2–Cl4	271.1(2)	N16–Gd2–Cl5	83.6(1)
Gd2–Cl5	266.2(2)	N17–Gd2–Cl4	135.8(1)
Gd3–Cl6	271.5(2)	N17–Gd2–Cl5	135.5(1)
Gd3–Cl7	271.3(2)	N19–Gd3–Cl6	71.9(1)
Gd3–Cl8	276.2(2)	N19–Gd3–Cl7	78.9(2)
Gd3–Cl9	273.3(2)	N19–Gd3–Cl8	132.2(2)
Gd1–N1	268.4(5)	N19–Gd3–Cl9	75.1(1)
Gd1–N2	249.0(5)	N20–Gd3–Cl6	76.8(1)
Gd1–N4	259.7(5)	N20–Gd3–Cl7	141.0(2)
Gd1–N5	260.3(5)	N20–Gd3–Cl8	70.4(2)
Gd1–N7	259.8(5)	N20–Gd3–Cl9	81.3(1)
Gd1–N8	251.4(5)	N22–Gd3–Cl6	131.9(2)
Gd2–N10	263.3(5)	N22–Gd3–Cl7	76.5(1)
Gd2–N11	247.2(5)	N22–Gd3–Cl8	73.9(1)
Gd2–N13	259.0(2)	N22–Gd3–Cl9	80.8(2)
Gd2–N14	260.0(2)	N23–Gd3–Cl6	72.2(2)
Gd2–N16	257.9(5)	N23–Gd3–Cl7	83.4(1)
Gd2–N17	259.2(5)	N23–Gd3–Cl8	73.7(1)
Gd3–N19	266.5(5)	N23–Gd3–Cl9	141.6(2)

Gd3–N20	256.8(6)	N2–Gd1–N1	62.3(2)
Gd3–N22	264.1(6)	N2–Gd1–N5	86.5(2)
Gd3–N23	258.1(6)	N2–Gd1–N7	144.1(2)
N2–Gd1–N8	91.1(2)	N4–Gd1–N1	78.9(2)
N2–Gd1–N4	138.5(2)	N4–Gd1–N5	63.1(2)
N8–Gd1–N4	104.5(2)	N4–Gd1–N7	75.8(2)
Cl1–Gd1–Cl2	82.1(1)	N5–Gd1–N1	65.2(2)
Cl5–Gd2–Cl4	87.1(1)	N7–Gd1–N1	153.6(2)
Cl6–Gd3–Cl8	105.0(1)	N7–Gd1–N5	108.7(2)
Cl6–Gd3–Cl9	146.2(1)	N8–Gd1–N1	130.5(2)
Cl7–Gd3–Cl6	87.5(1)	N8–Gd1–N7	64.6(2)
Cl7–Gd3–Cl8	148.6(1)	N8–Gd1–N5	72.7(2)
Cl7–Gd3–Cl9	93.6(1)	N11–Gd2–N10	63.7(2)
Cl9–Gd3–Cl8	91.4(1)	N11–Gd2–N13	148.8(5)
N1–Gd1–Cl1	82.6(1)	N11–Gd2–N14	96.2(3)
N1–Gd1–Cl2	126.1(1)	N11–Gd2–N16	132.8(2)
N2–Gd1–Cl1	107.8(1)	N11–Gd2–N17	78.8(2)
N2–Gd1–Cl2	74.1(1)	N13–Gd2–N10	147.4(5)
N4–Gd1–Cl1	79.3(2)	N13–Gd2–N14	63.0(3)
N4–Gd1–Cl2	146.4(1)	N14–Gd2–N10	135.0(3)
N5–Gd1–Cl1	133.7(1)	N16–Gd2–N10	75.5(2)
N5–Gd1–Cl2	143.7(1)	N16–Gd2–N13	75.4(6)
N7–Gd1–Cl1	85.4(1)	N16–Gd2–N14	96.6(4)
N7–Gd1–Cl2	75.0(1)	N16–Gd2–N17	63.6(2)
N8–Gd1–Cl1	147(1)	N17–Gd2–N10	66.9(2)
N8–Gd1–Cl2	77.3(1)	N17–Gd2–N13	111.7(5)
N10–Gd2–Cl4	129(1)	N17–Gd2–N14	70.0(4)
N10–Gd2–Cl5	76.7(1)	N20–Gd3–N19	62.4(2)
N11–Gd2–Cl4	76.3(1)	N20–Gd3–N22	139.3(2)
N11–Gd2–Cl5	107.5(1)	N20–Gd3–N23	123.6(2)
N13–Gd2–Cl4	76.4(6)	N22–Gd3–N19	144.1(2)
N13–Gd2–Cl5	85.9(3)	N23–Gd3–N19	140.4(2)
N14–Gd2–Cl4	77.0(4)	N23–Gd3–N22	61.2(2)

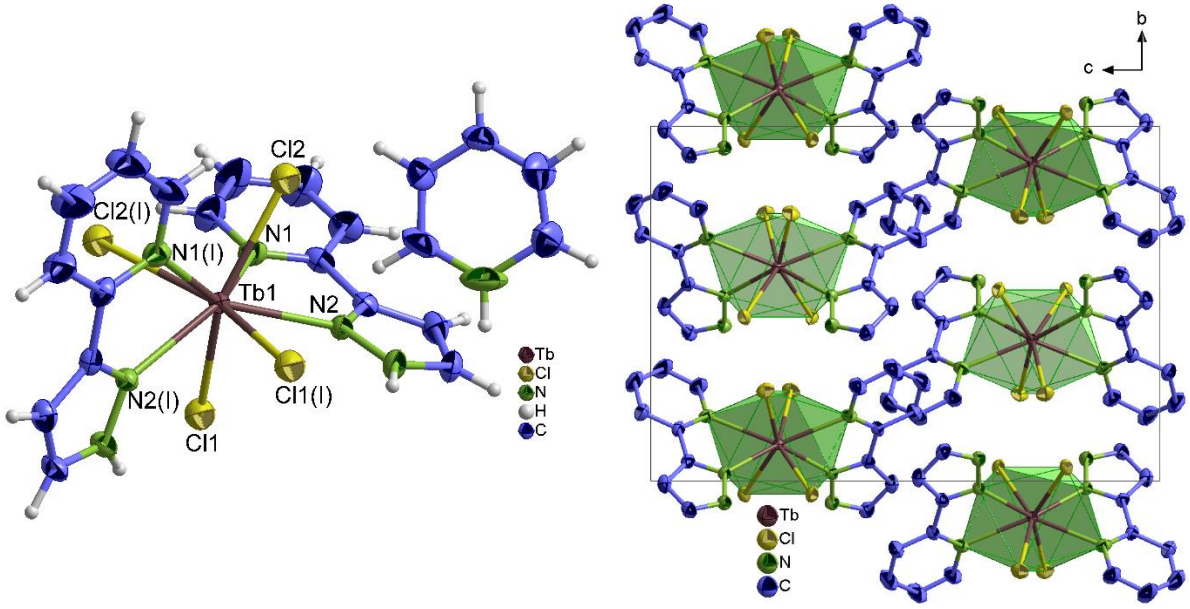

(**a**) (**b**)

Figure S5. (**a**) Extended coordination sphere of Tb^{3+} ion in [PyH][Tb(2–PyPzH)$_2$Cl$_4$] (**18**). (**b**) Packing structure of **18** with a view along [100], the protonated pyridine molecules were omitted for clarity. Symmetry operation: I -x+1,y,-z+3/2.

Table S13. Selected interatomic distances (pm) and angles (°) of [PyH][Tb(2–PyPzH)$_2$Cl$_4$] (**18**).

Atoms	**[PyH][Tb(2–PyPzH)$_2$Cl$_4$]**	**Atoms**	**[PyH][Tb(2–PyPzH)$_2$Cl$_4$]**
Tb1–Cl1	272.0(1)	N1–Tb1–Cl2	72.0(1)
Tb1–Cl2	269.8(1)	N1^{I}–Tb1–Cl2	78.7(1)
Tb1–N1	267.8(2)	N1^{I}–Tb1–N1	136.9(1)
Tb1–N2	252.2(2)	N2^{I}–Tb1–N2	132.9(1)
Cl1–Tb1–Cl1^{I}	100.7(1)	N2–Tb1–N1	62.6(1)
Cl2–Tb1–Cl1	145.0(1)	N2–Tb1–N1^{I}	138.9(1)
Cl2–Tb1–Cl1^{I}	93.4(1)	N2^{I}–Tb1–Cl2	141.3(1)
Cl2^{I}–Tb1–Cl1^{I}	145.0(1)	N2–Tb1–Cl2	76.7(1)
Cl2–Tb1–Cl2^{I}	92.9(1)		

Powder Diffraction

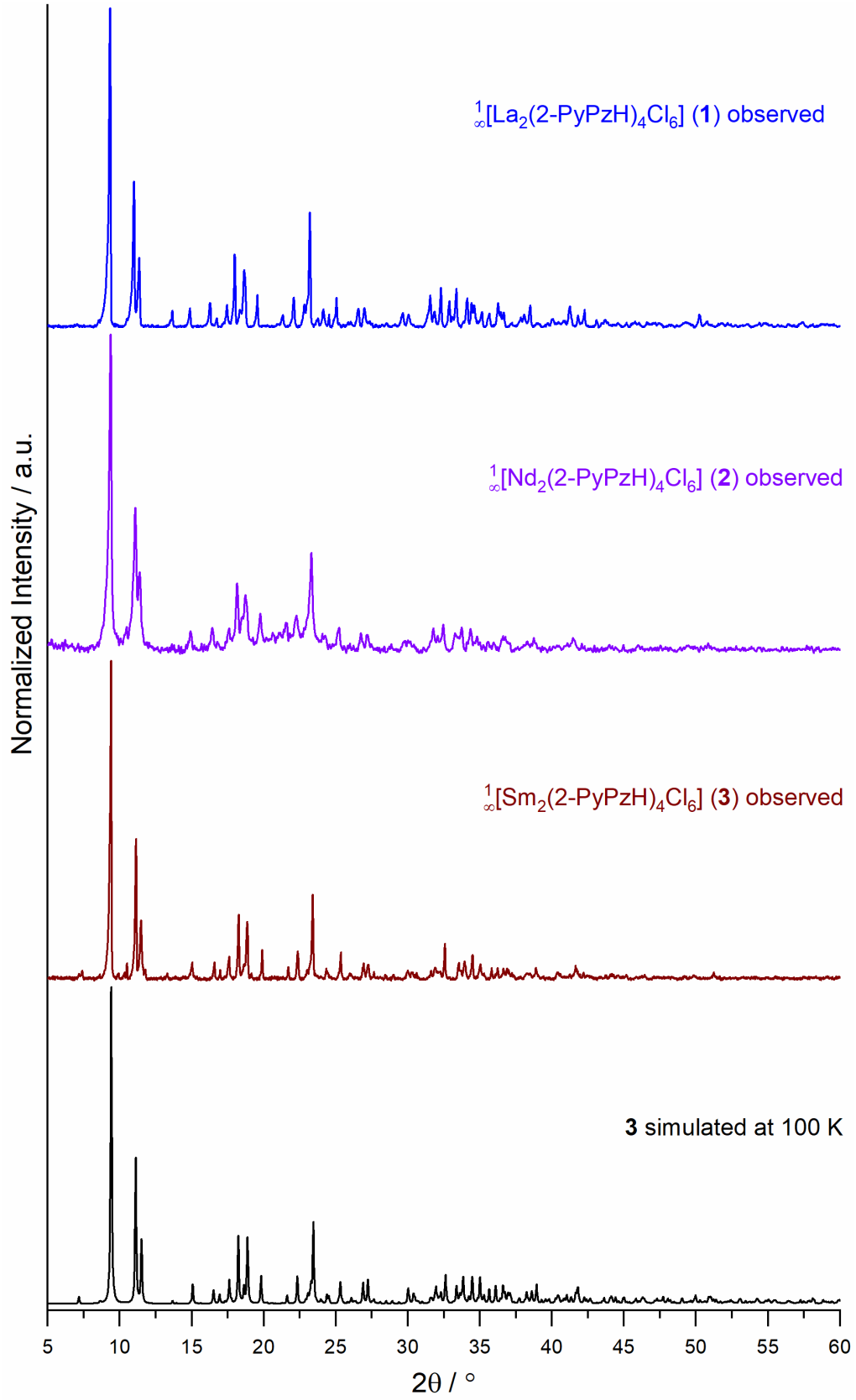

Figure S6. Comparison of the observed powder X–ray diffraction pattern (colored) of $^1_\infty$[Ln$_2$(2–PyPzH)$_4$Cl$_6$], RE = La (**1**), Nd (**2**), Sm (**3**) with the simulated diffraction pattern from the single crystal X–ray data of $^1_\infty$[Sm$_2$(2–PyPzH)$_4$Cl$_6$] (**3**) (black).

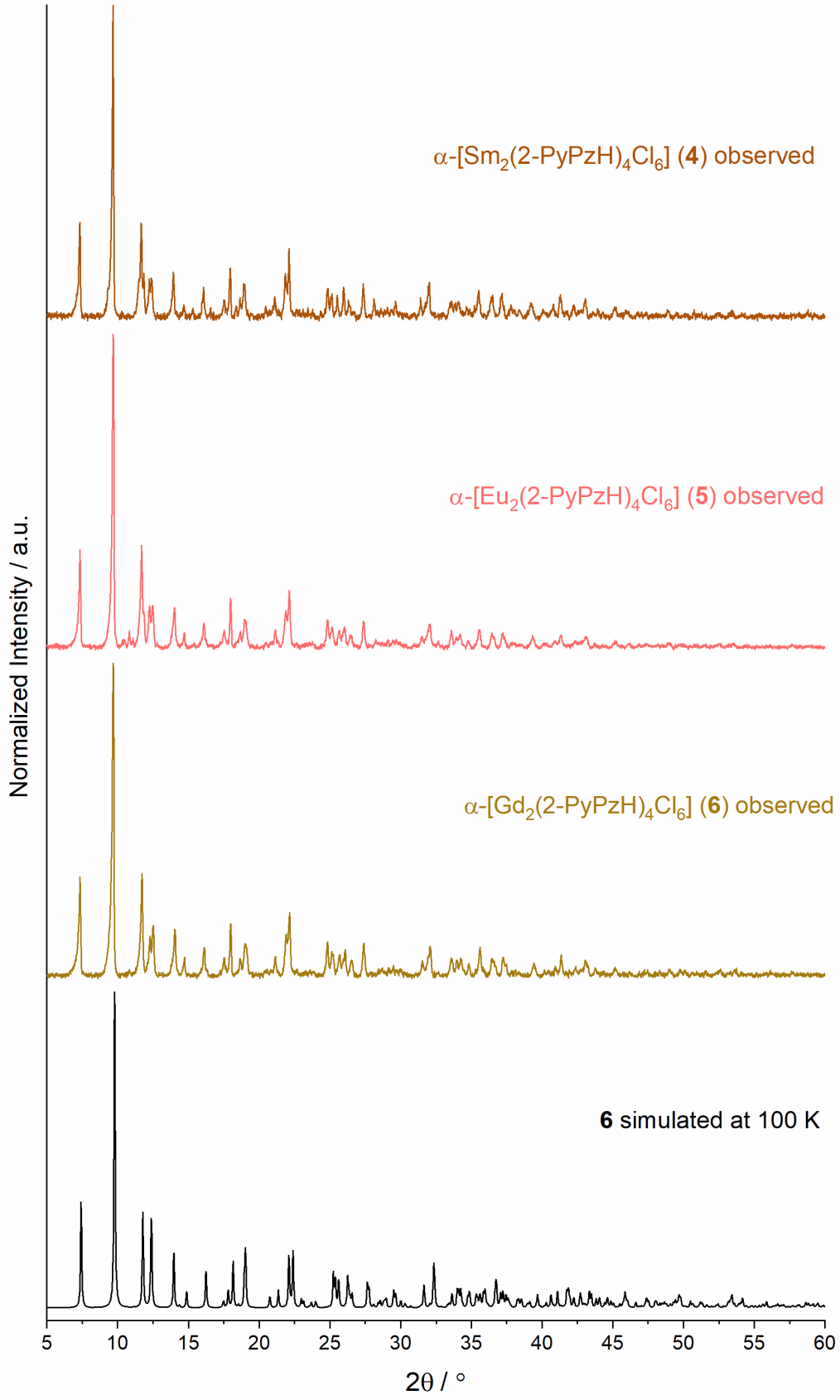

Figure S7. Comparison of the observed powder X–ray diffraction pattern (colored) of α–[Ln_2(2–PyPzH)$_4$$Cl_6$], Ln = Sm (**4**), Eu (**5**), Gd (**6**) with the simulated diffraction pattern from the single crystal X–ray data of α–[Gd_2(2–PyPzH)$_4$$Cl_6$] (**6**) (black).

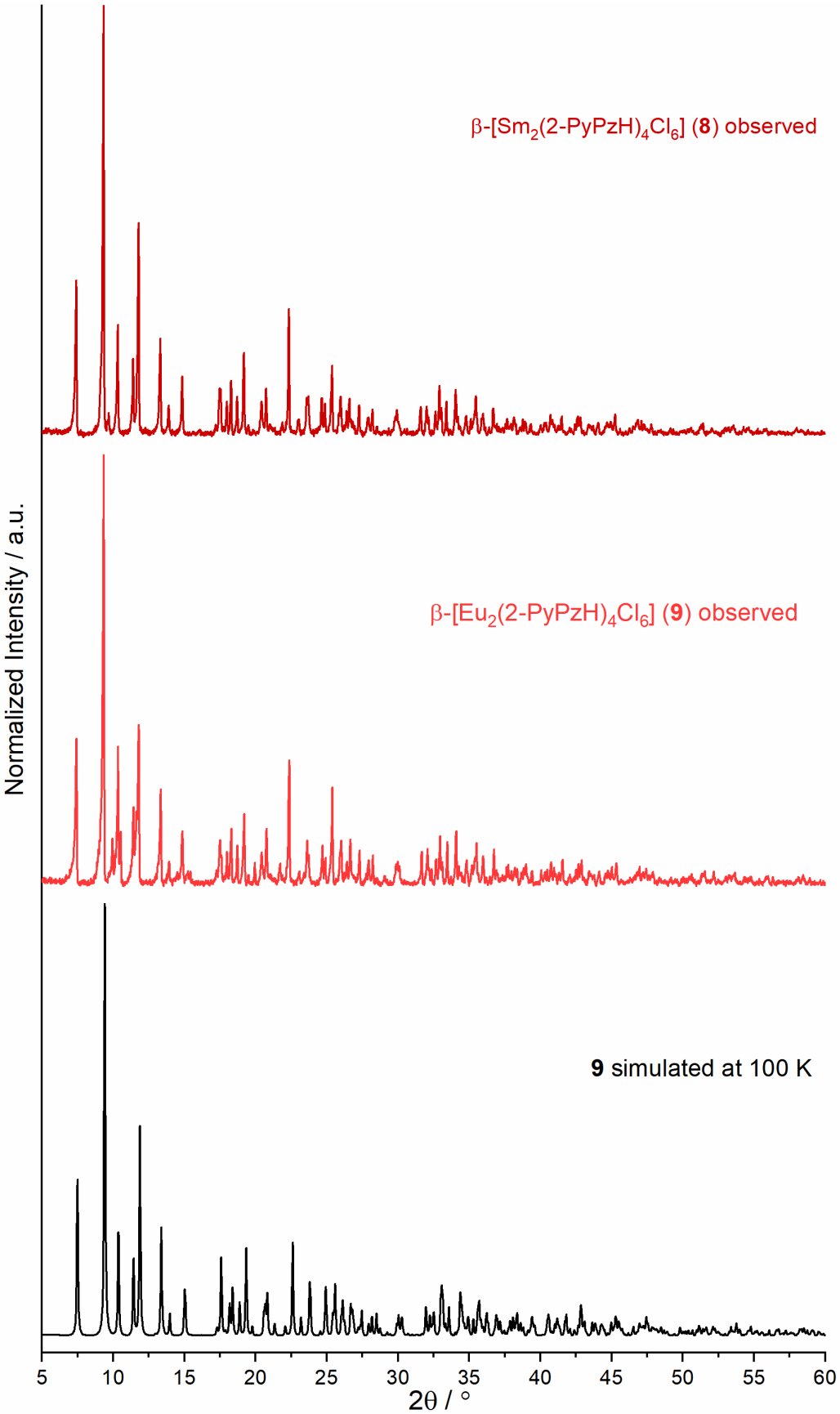

Figure S8. Comparison of the observed powder X–ray diffraction pattern (colored) of β–[Ln_2(2–PyPzH)$_4Cl_6$], Ln = Sm (**8**), Eu (**9**) with the simulated diffraction pattern from the single crystal X–ray data of β–[Eu_2(2–PyPzH)$_4Cl_6$] (**9**) (black).

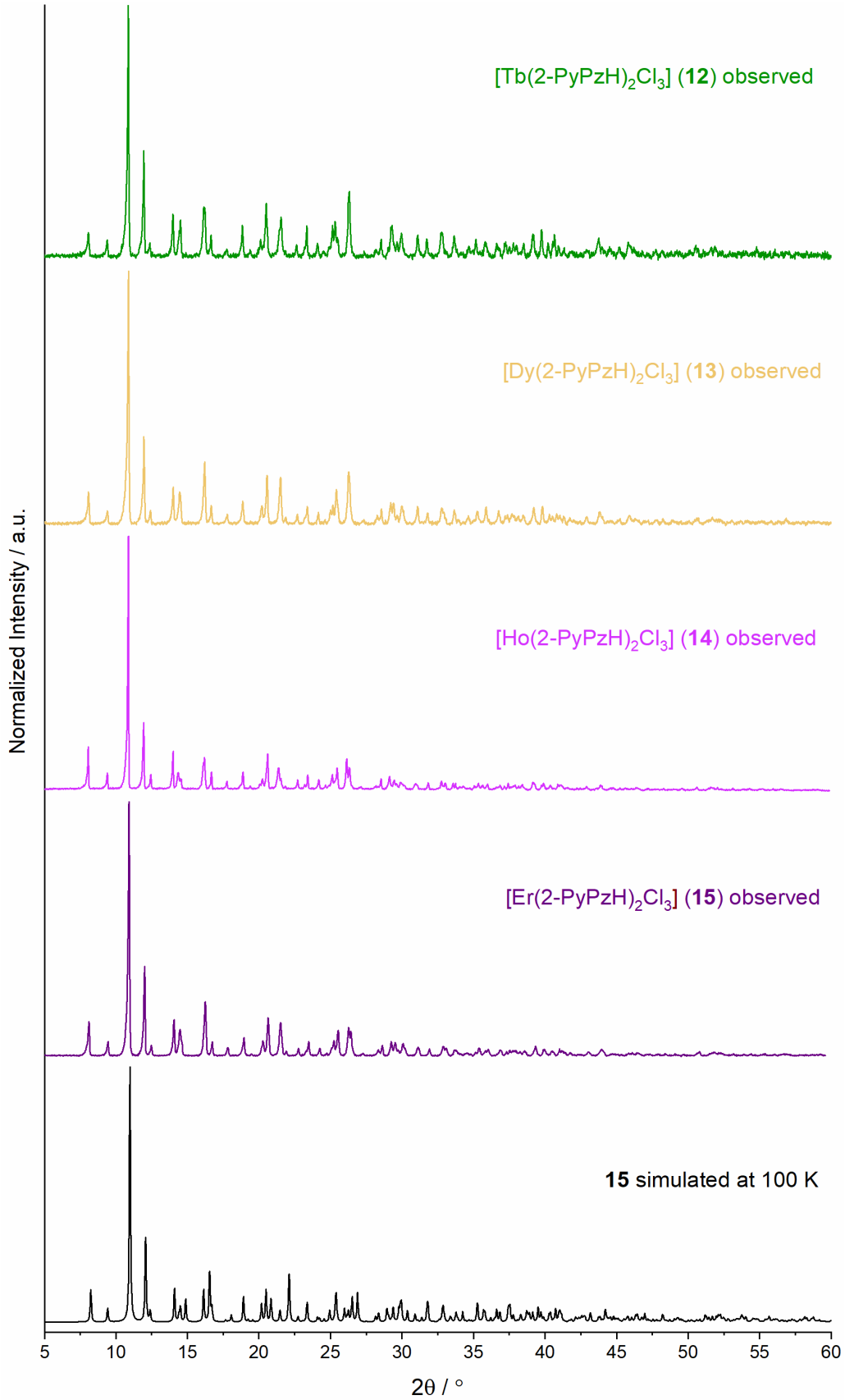

Figure S9. Comparison of the observed powder X–ray diffraction pattern (colored) of [Ln(2–PyPzH)$_2$Cl$_3$], Ln = Tb (**12**), Dy (**13**), Ho (**14**), and Er (**15**) with the simulated diffraction pattern from the single crystal X–ray data of [Er(2–PyPzH)$_2$Cl$_3$] (**15**) (black).

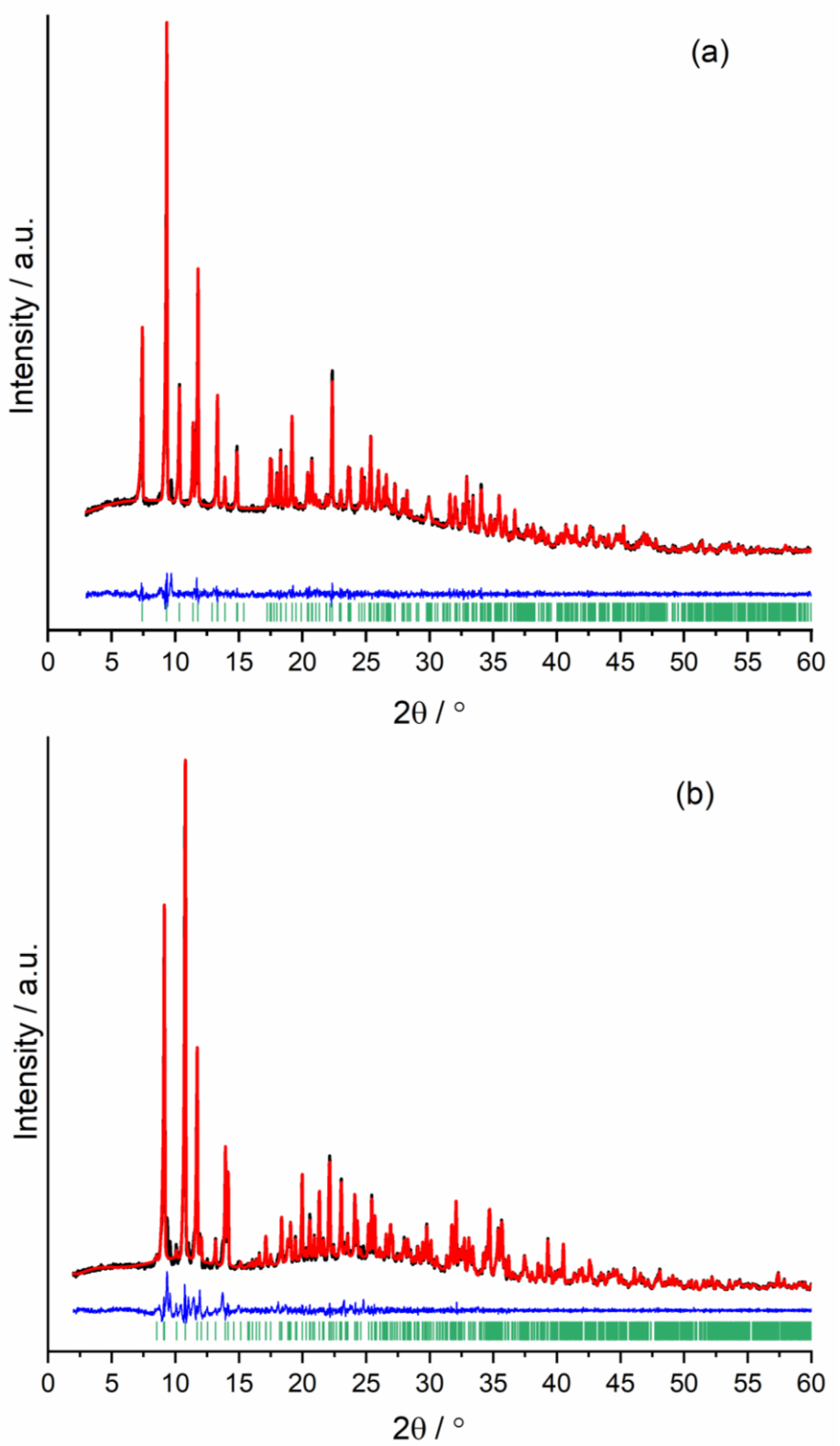

Figure S10. Pawley refinement of (**a**) β–[Sm_2(2–PyPzH)$_4Cl_6$] (**8**) with a GOF of 1.16, (**b**) [Ce(2–PyPzH)$_3Cl_3$] (**11**) with a GOF of 1.87. The experimental data are shown in black, Pawley fit in red, the corresponding difference plot in blue, and the hkl position markers in green.

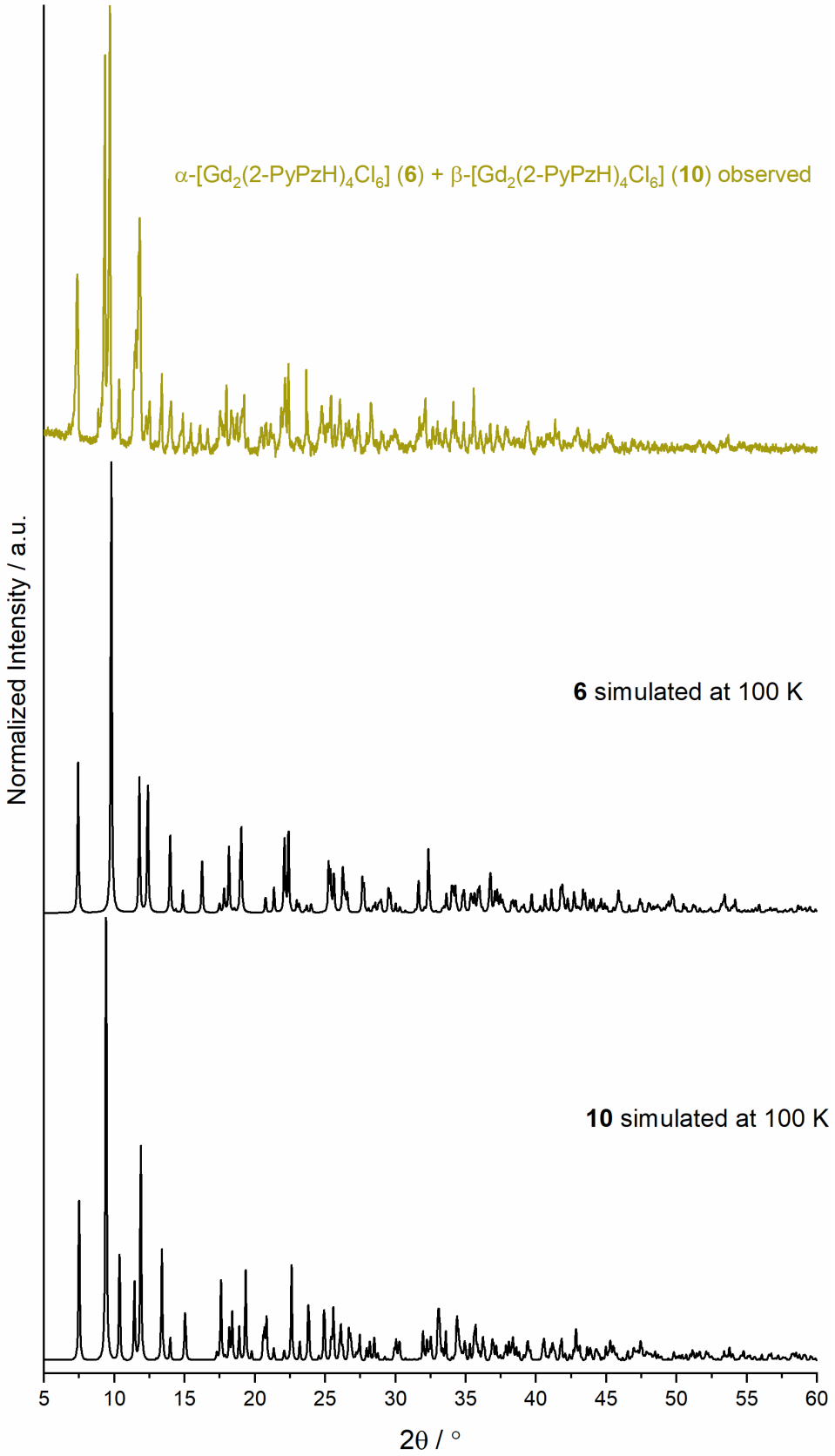

Figure S11. Comparison of the observed powder X–ray diffraction pattern (colored) of a mixture of *α*–$[Gd_2(2\text{–}PyPzH)_4Cl_6]$ (**6**) and β–$[Gd_2(2\text{–}PyPzH)_4Cl_6]$ (**10**) with the simulated diffraction pattern from the single crystal X–ray data at 100 K of *α*–$[Gd_2(2\text{–}PyPzH)_4Cl_6]$ (**6**) and β–$[Gd_2(2\text{–}PyPzH)_4Cl_6]$ (**10**) (black).

Photophysical Properties

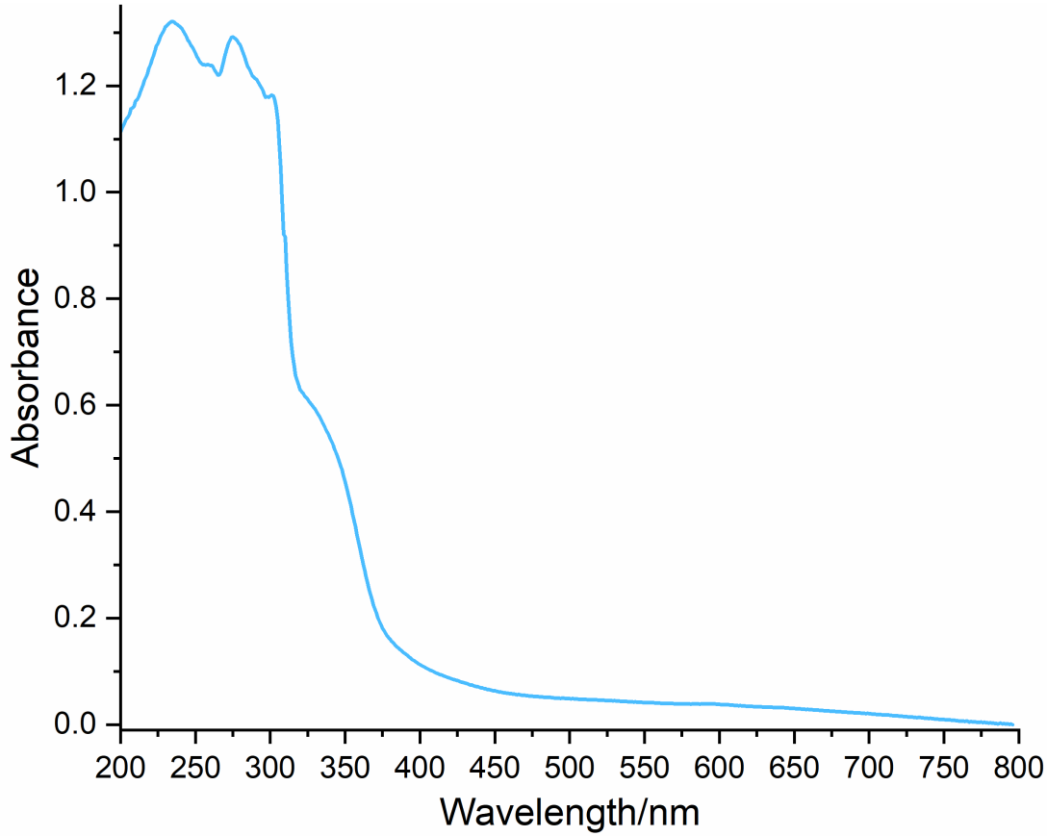

Figure S12. Absorption spectra of 2–PyPzH in the solid–state at room temperature.

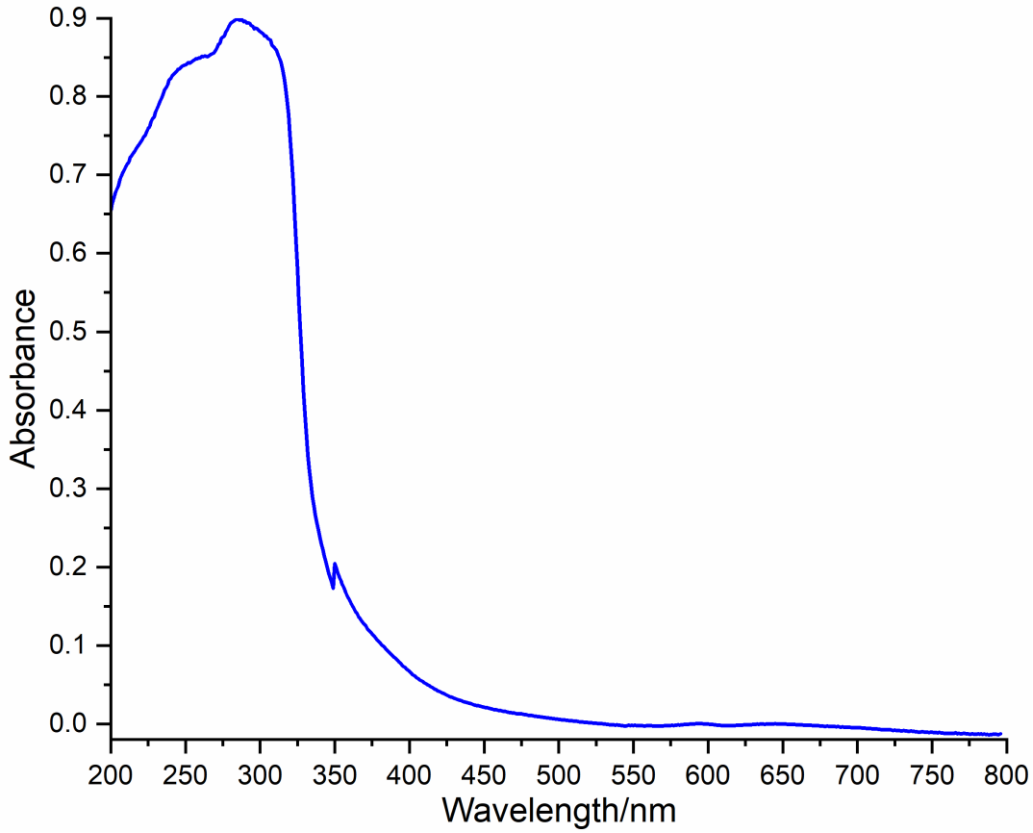

Figure S13. Absorption spectra of ∞[La_2(2–PyPzH)$_4$$Cl_6$] (**1**) in the solid–state at room temperature.

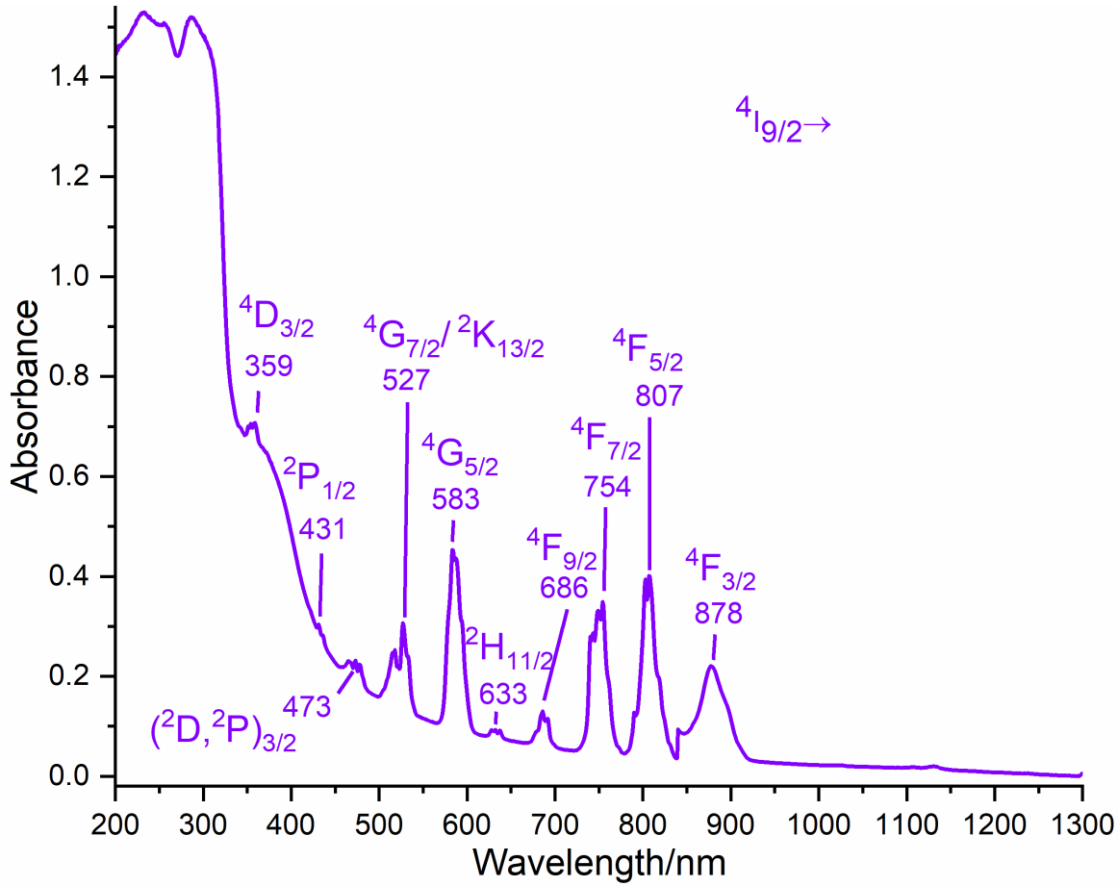

Figure S14. Absorption spectra of [Nd2(2–PyPzH)4Cl6] (**2**) in the solid–state at room temperature.

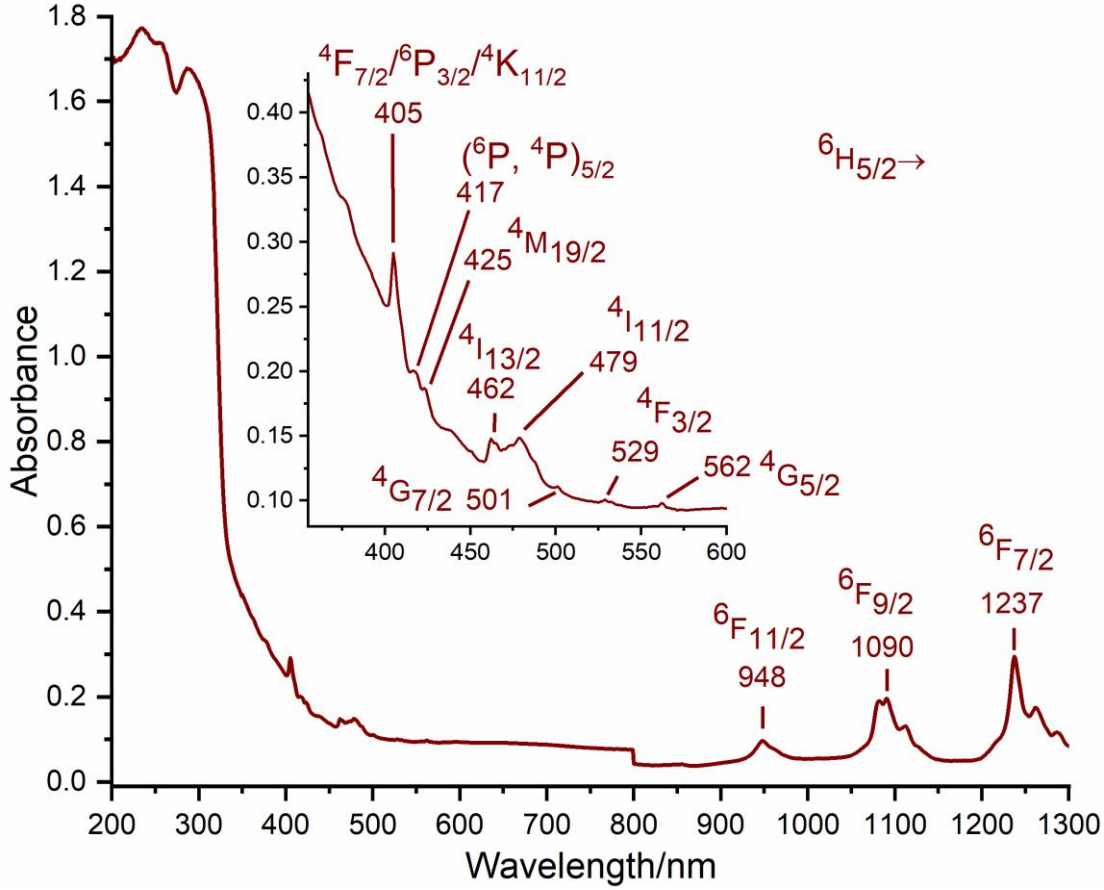

Figure S15. Absorption spectra of [Sm2(2–PyPzH)4Cl6] (**3**) in the solid–state at room temperature.

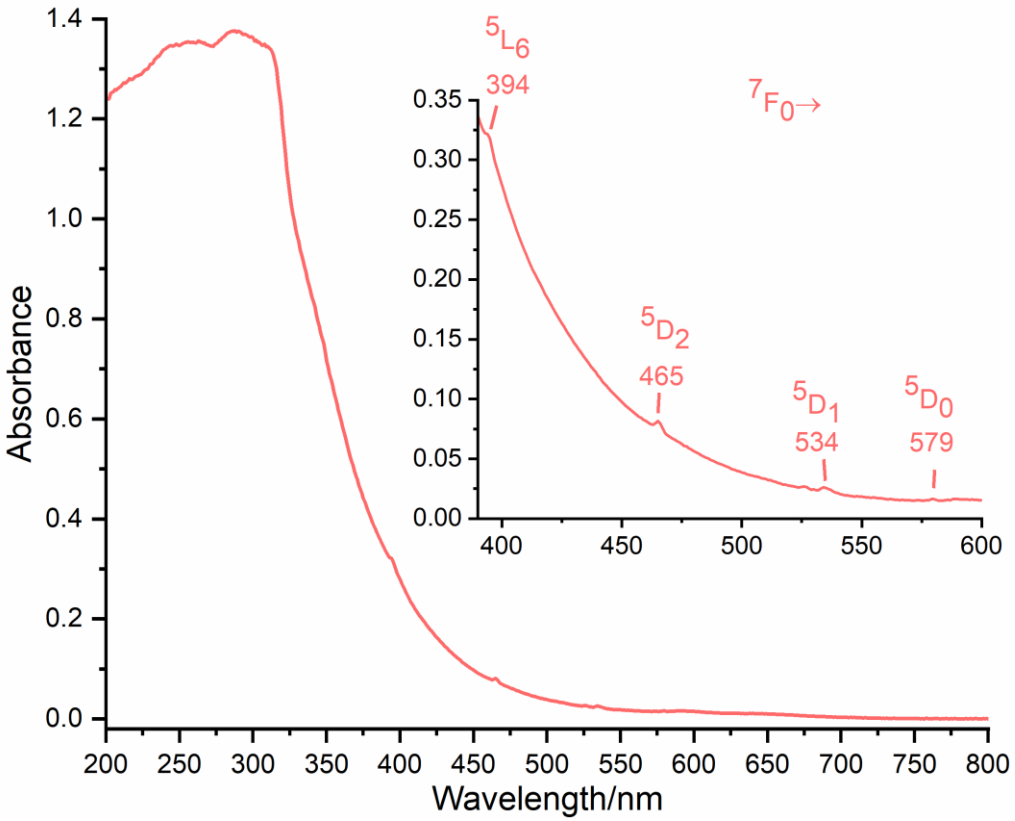

Figure S16. Absorption spectra of α–[Eu_2(2–PyPzH)$_4Cl_6$] (**5**) in the solid–state at room temperature.

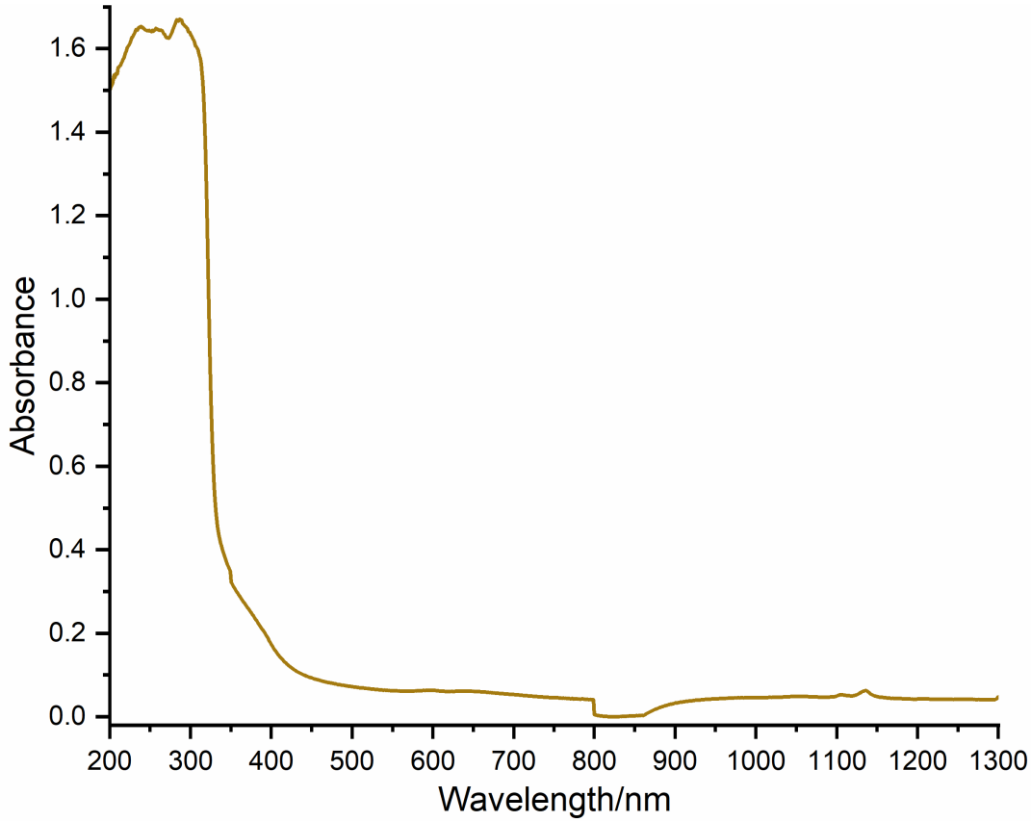

Figure S17. Absorption spectra of α–[Gd_2(2–PyPzH)$_4Cl_6$] (**6**) in the solid–state at room temperature.

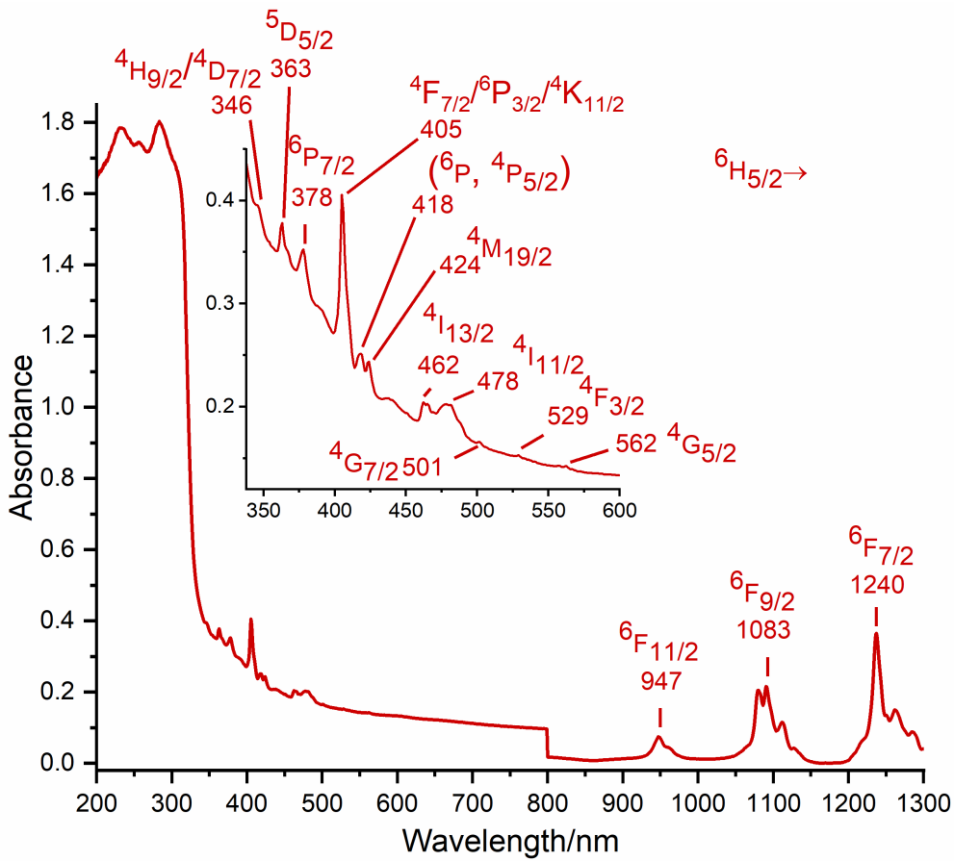

Figure S18. Absorption spectra of β–[Sm_2(2–PyPzH)$_4Cl_6$] (**8**) in the solid–state at room temperature.

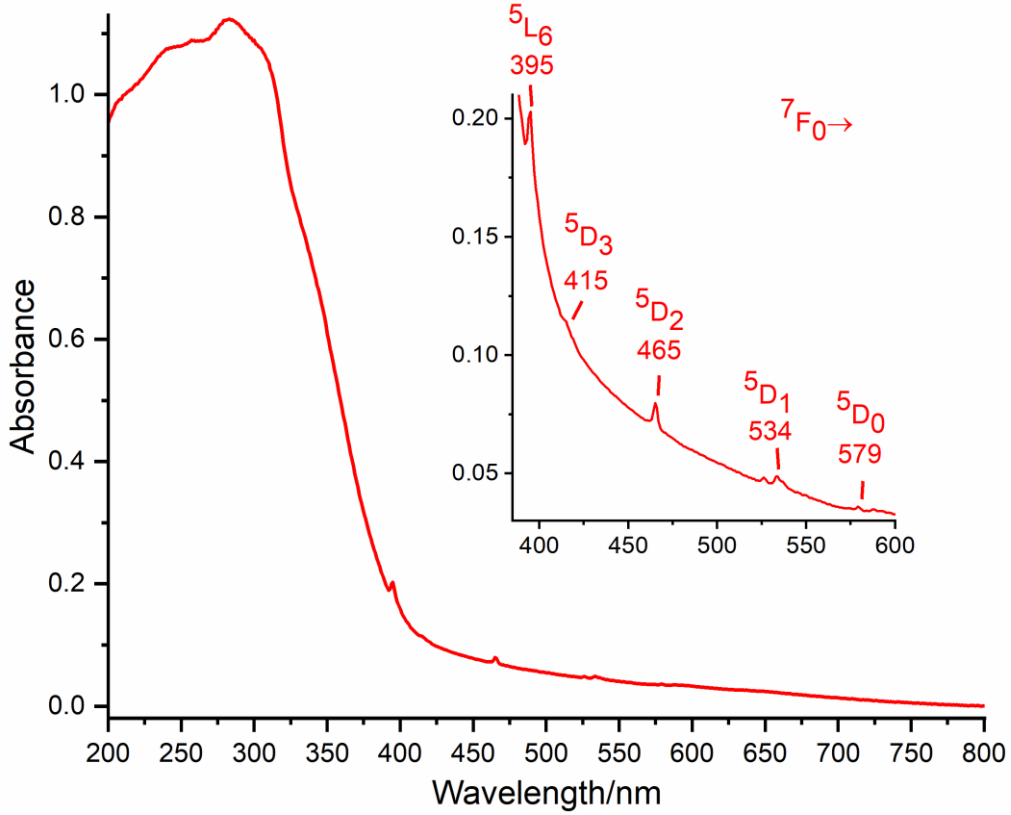

Figure S19. Absorption spectra of β–[Eu_2(2–PyPzH)$_4Cl_6$] (**9**) in the solid–state at room temperature.

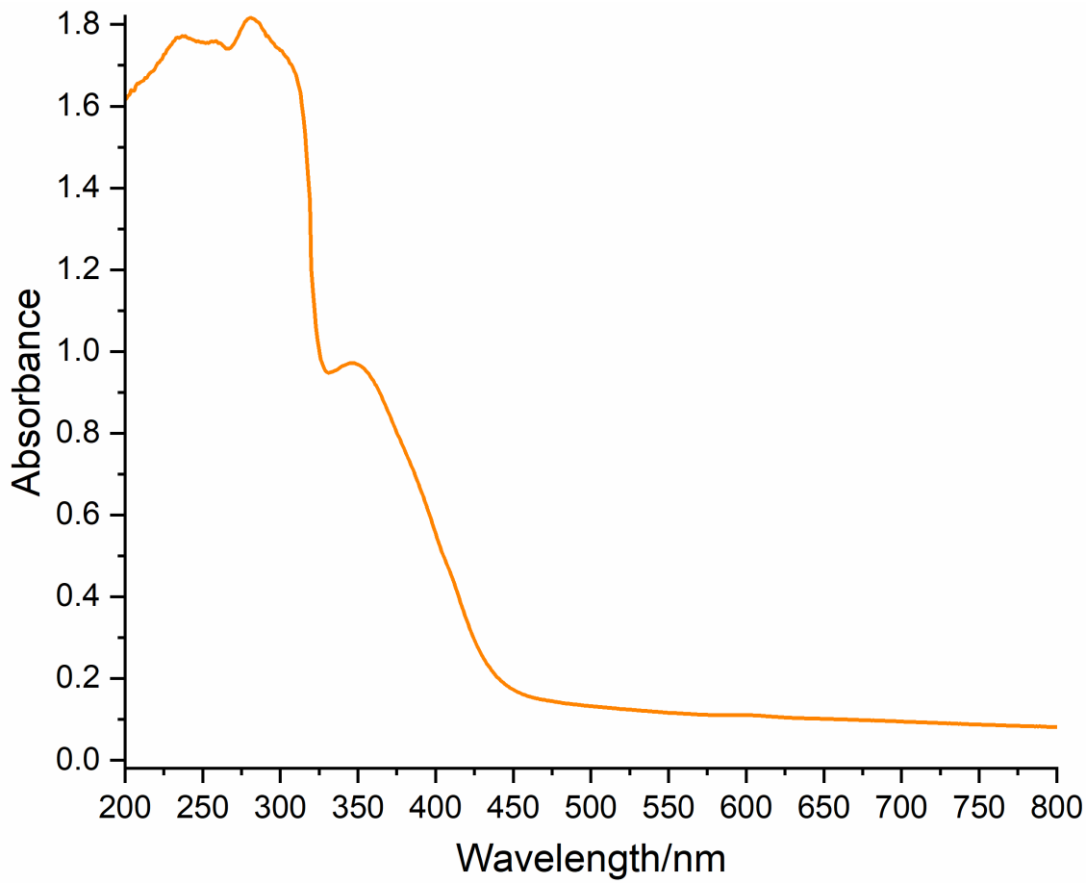

Figure S20. Absorption spectra of [Ce(2–PyPzH)$_3$Cl$_3$] (**11**) in the solid–state at room temperature.

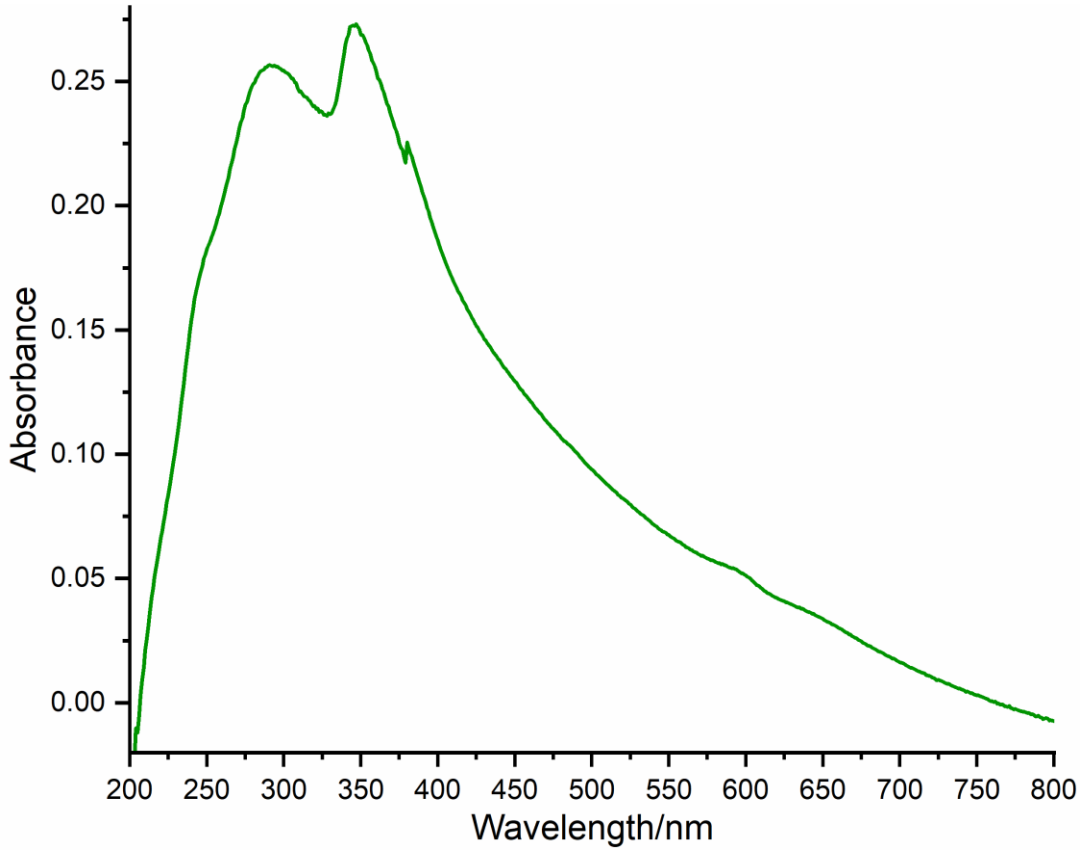

Figure S21. Absorption spectra of [Tb(2–PyPzH)$_2$Cl$_3$] (**12**) in the solid–state at room temperature.

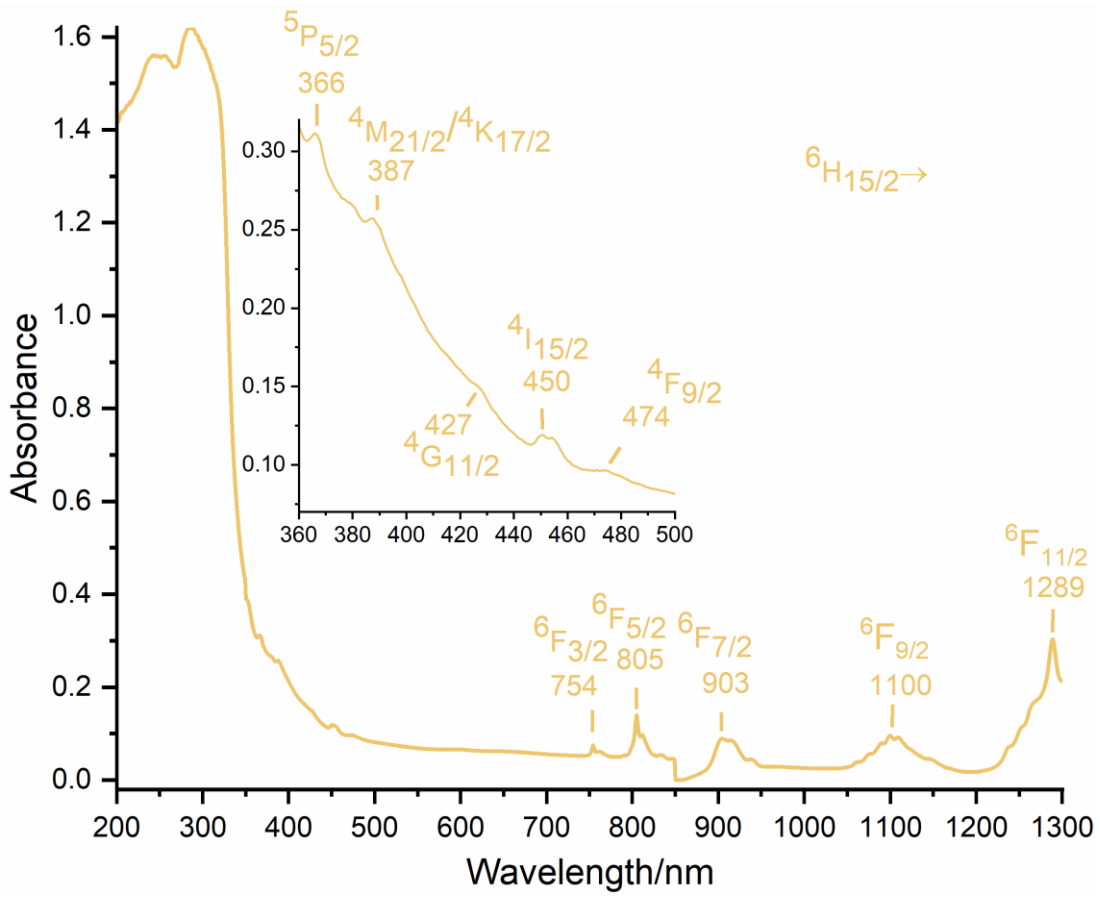

Figure S22. Absorption spectra of [Dy(2–PyPzH)$_2$Cl$_3$] (**13**) in the solid–state at room temperature.

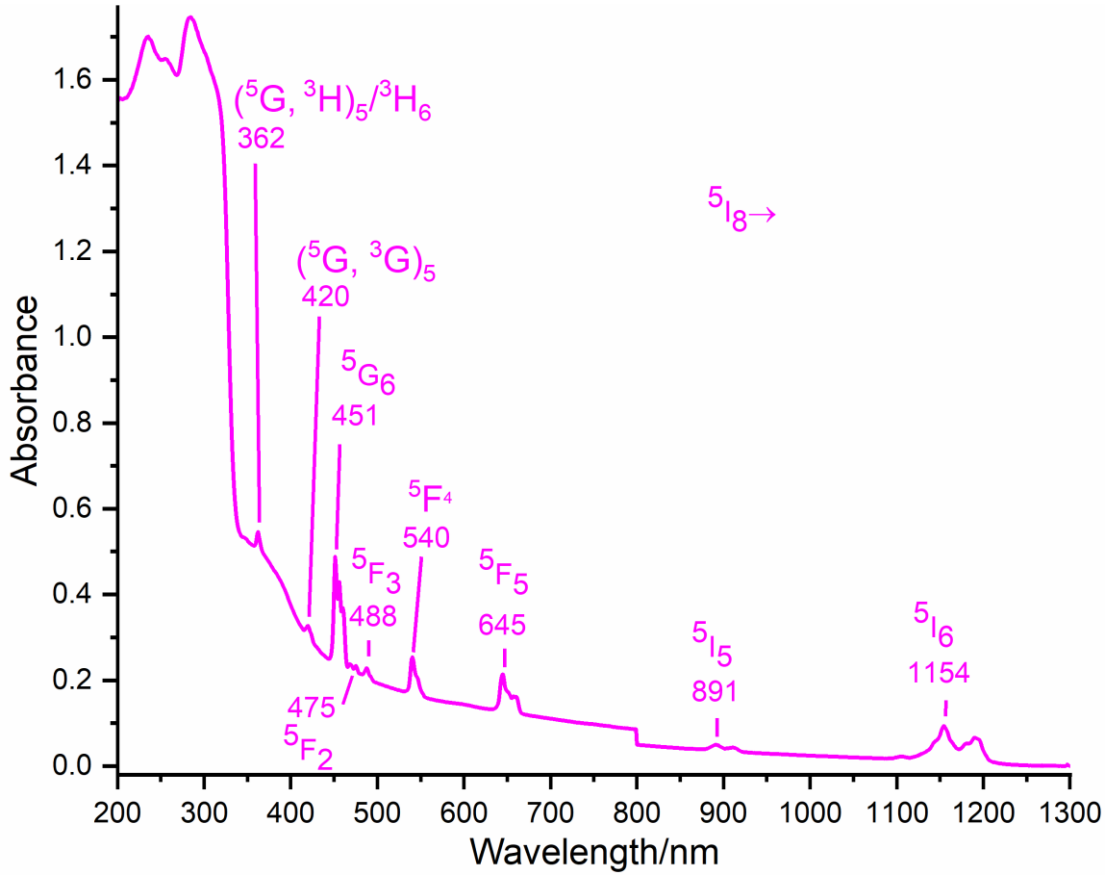

Figure S23. Absorption spectra of [Ho(2–PyPzH)$_2$Cl$_3$] (**14**) in the solid–state at room temperature.

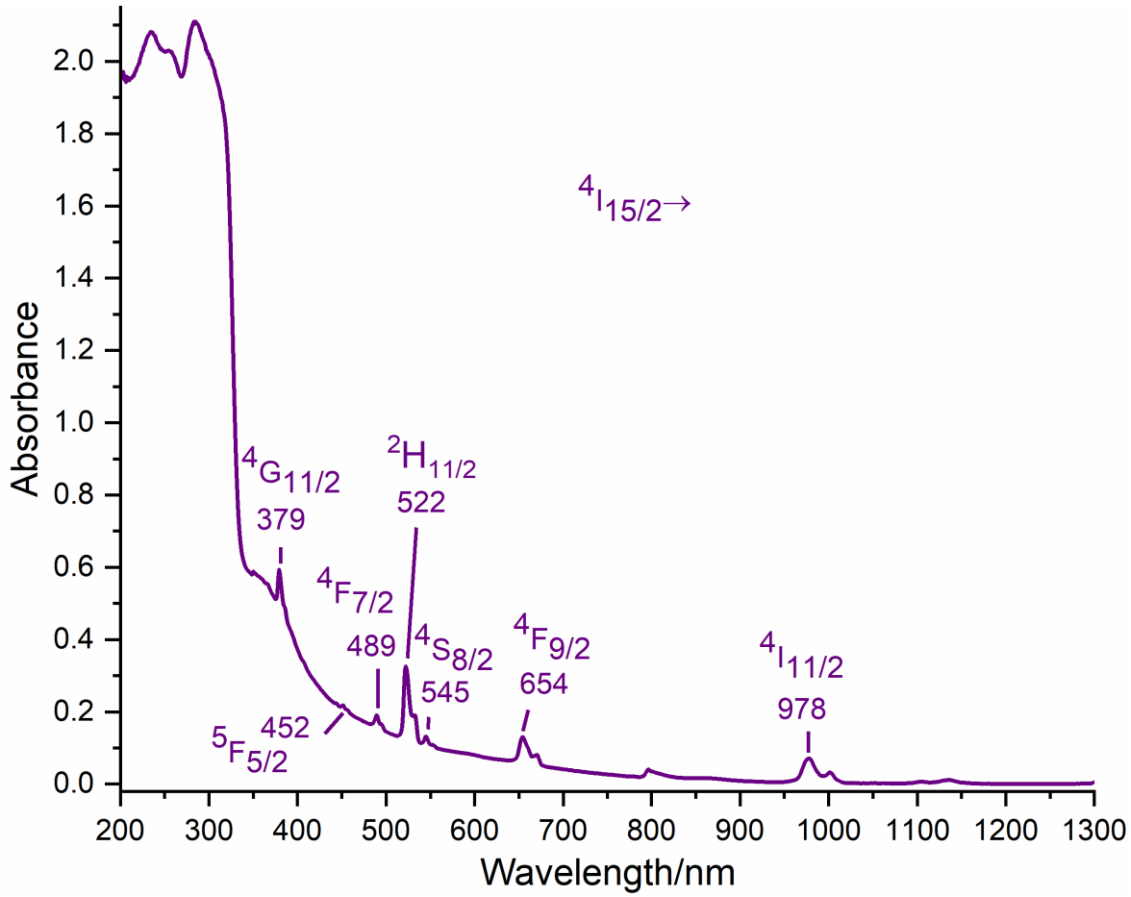

Figure S24. Absorption spectra of [Er(2–PyPzH)$_2$Cl$_3$] (**15**) in the solid–state at room temperature.

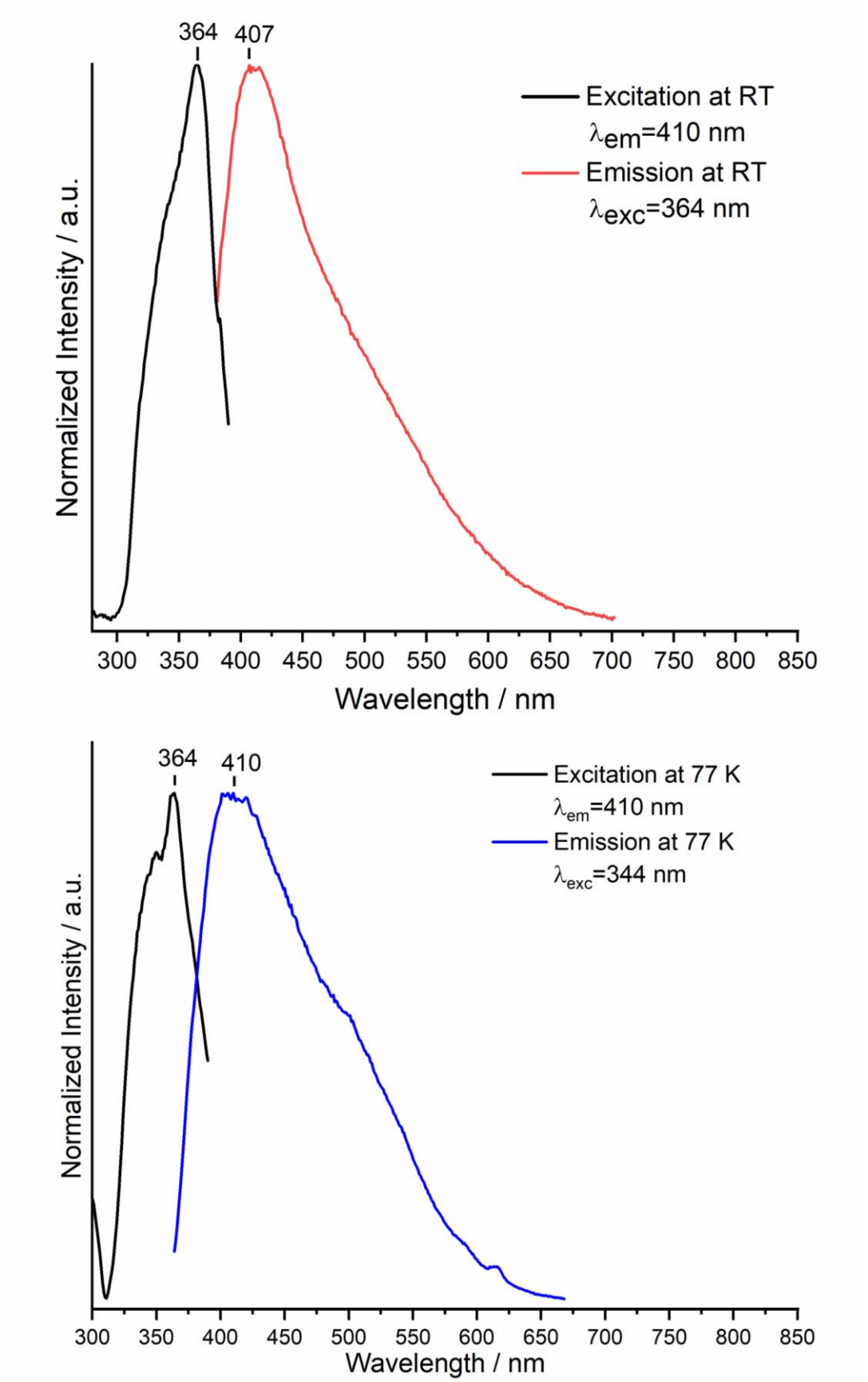

Figure S25. Normalized excitation and emission spectra of 2–PyPzH at room temperature (top) and 77 K (bottom). Wavelengths at which the spectra were recorded are reported in the legends.

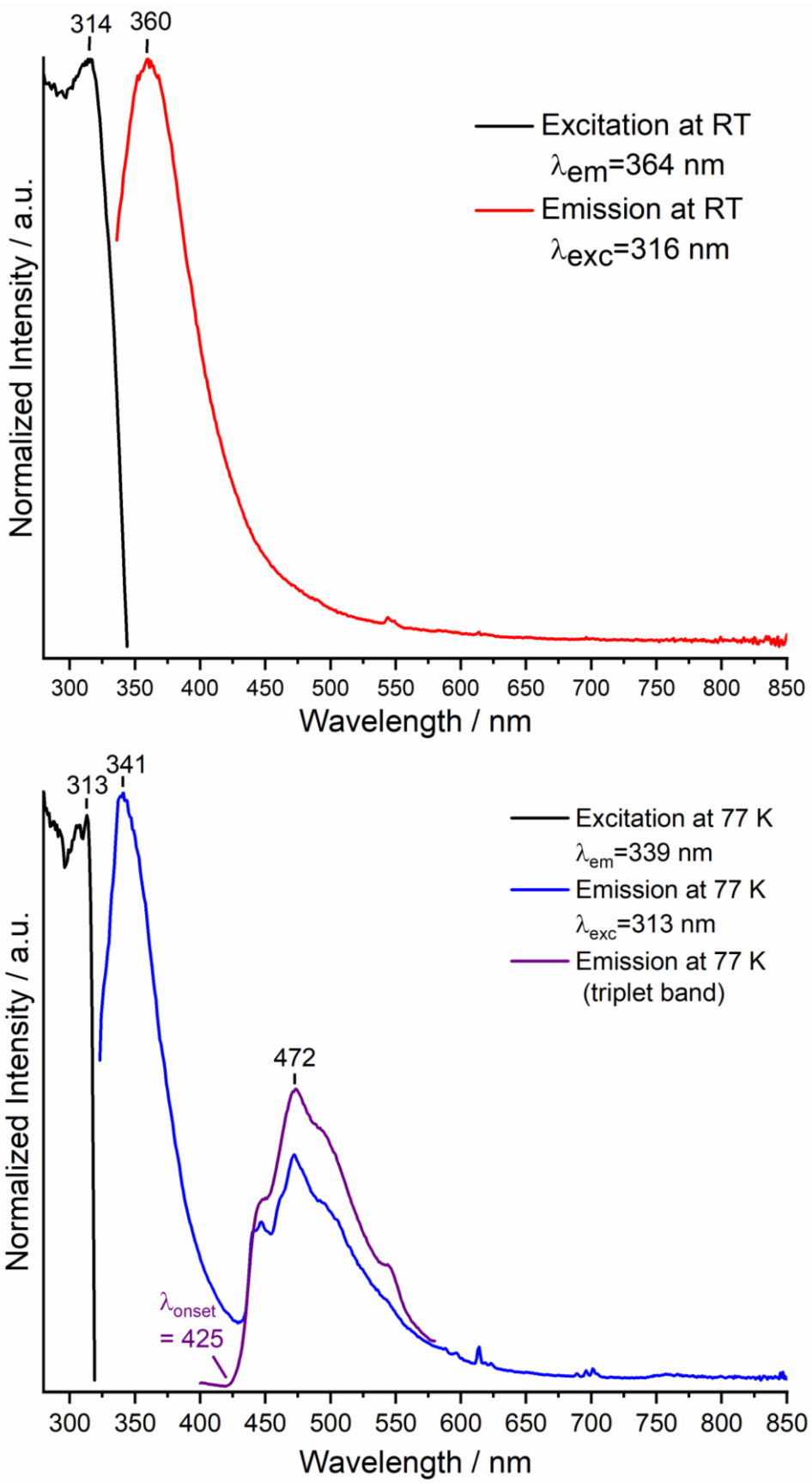

Figure S26. Normalized excitation and emission spectra of ∞[La_2(2–PyPzH)$_4$$Cl_6$] (**1**) at room temperature (top) and 77 K (bottom). Wavelengths at which the spectra were recorded are reported in the legends.

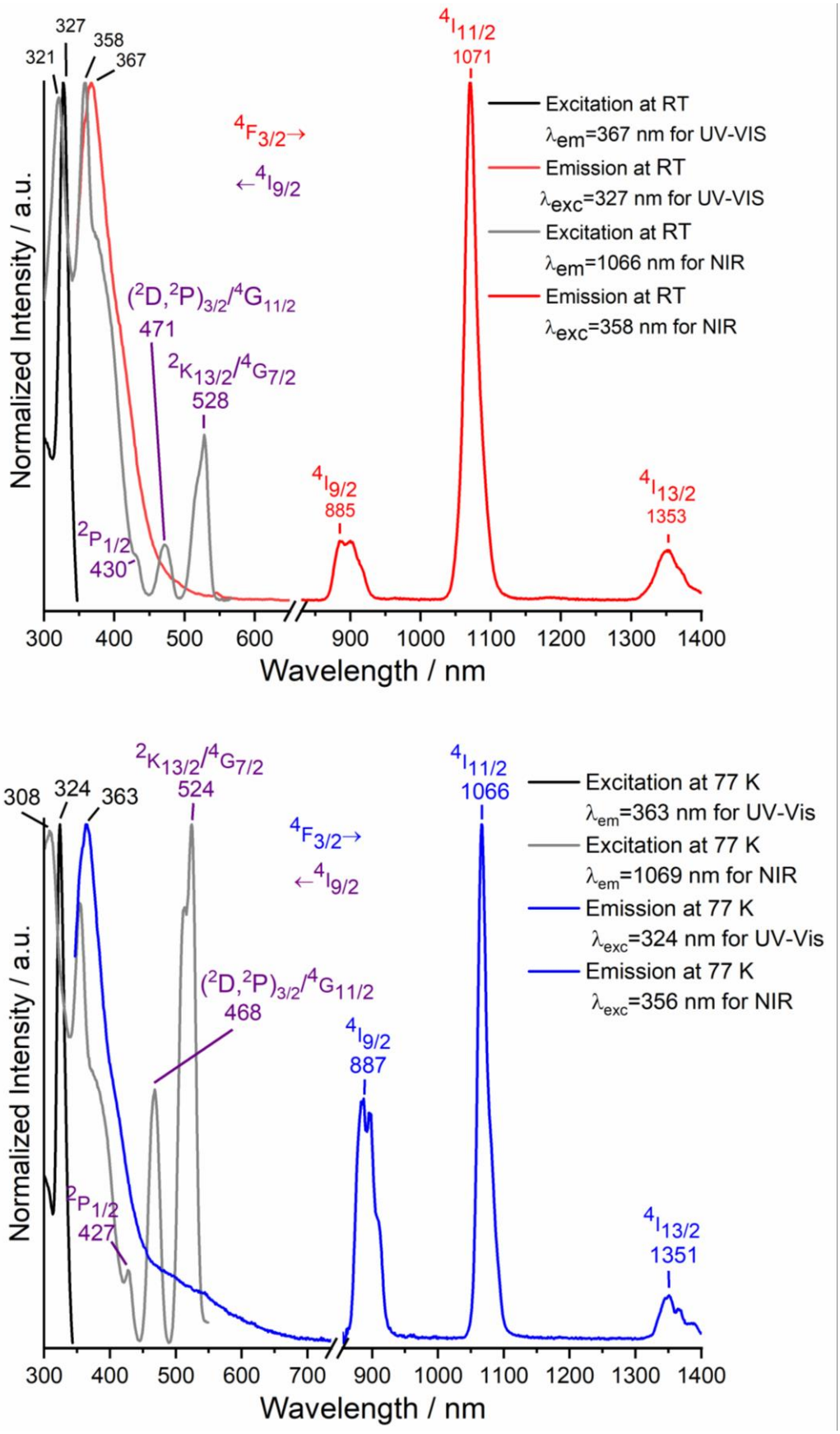

Figure S27. Normalized excitation and emission spectra of [Nd$_2$(2–PyPzH)$_4$Cl$_6$] (**2**) at room temperature (top) and 77 K (bottom). Wavelengths at which the spectra were recorded are reported in the legends.

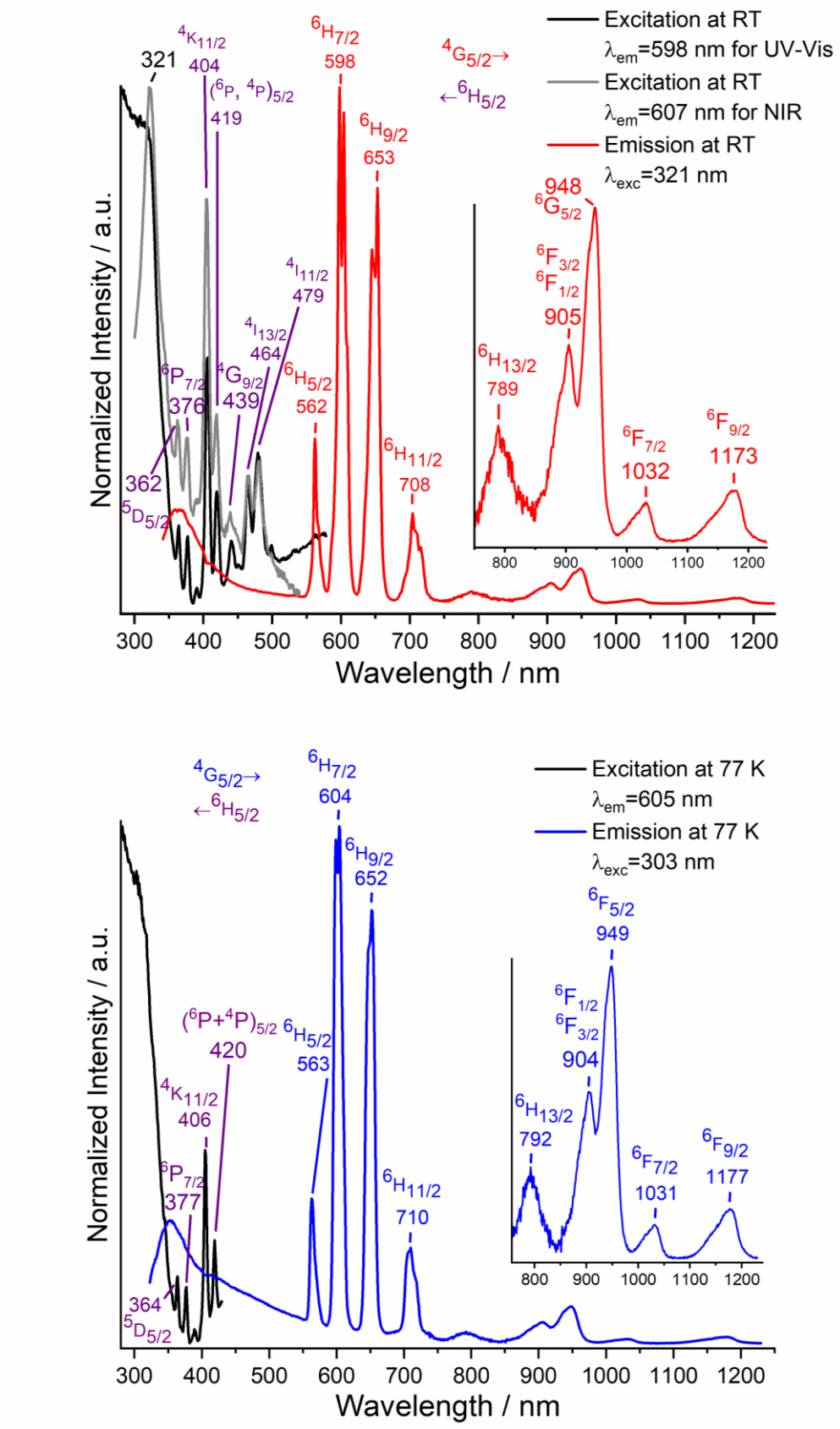

Figure S28. Normalized excitation and emission spectra of [Sm2(2–PyPzH)4Cl6] (**3**) at room temperature (top) and 77 K (bottom). Wavelengths at which the spectra were recorded are reported in the legends. Visible and NIR range emission spectra were brought to the same intensity at 708 (at RT) and 710 nm (at 77 K).

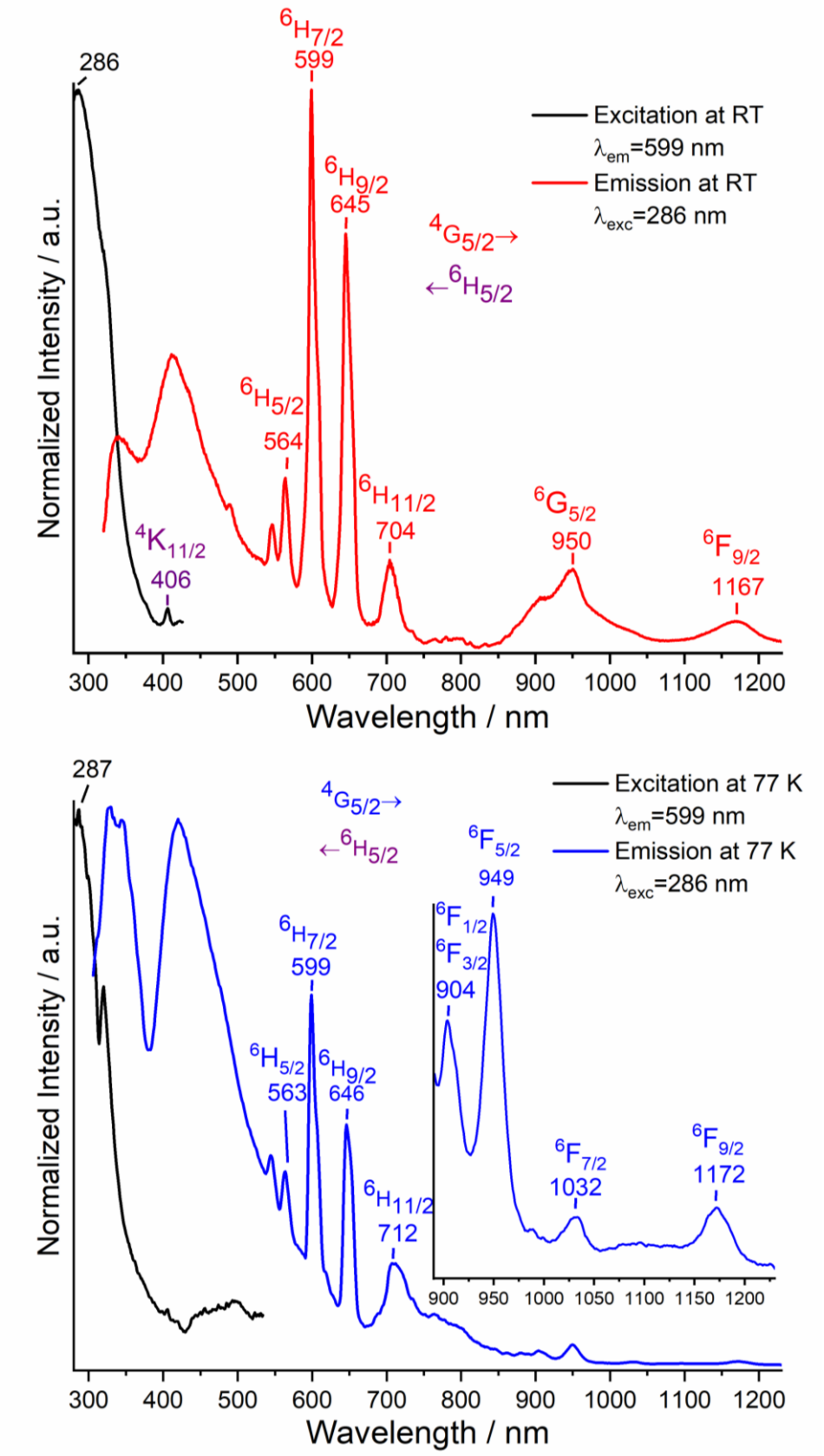

Figure S29. Normalized excitation and emission spectra of α–[Sm_2(2–PyPzH)$_4Cl_6$] (**4**) at room temperature (top) and 77 K (bottom). Wavelengths at which the spectra were recorded are reported in the legends. Visible and NIR range emission spectra were brought to the same intensity at 704 (at RT) and 712 nm (at 77 K).

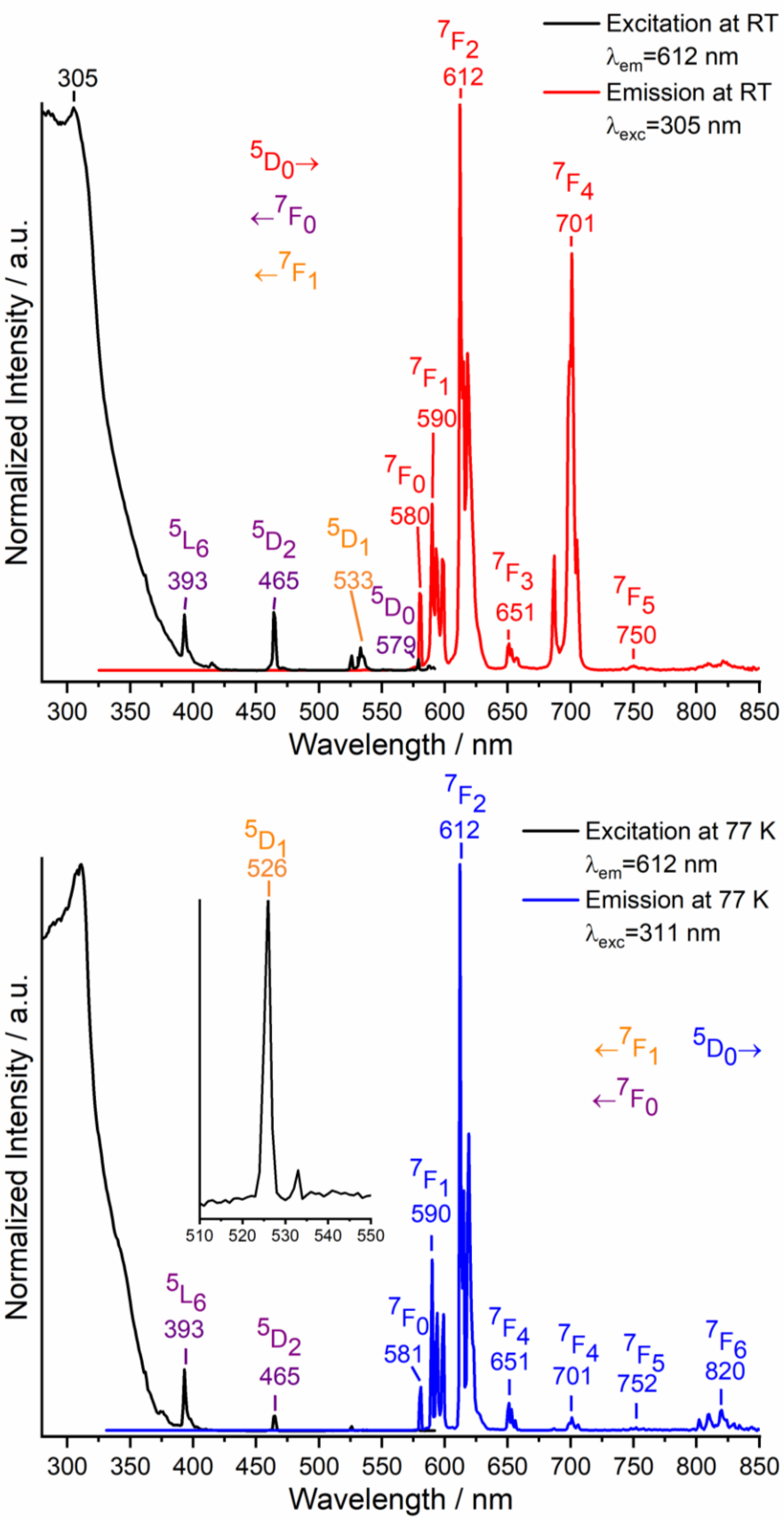

Figure S30. Normalized excitation and emission spectra of α–[Eu_2(2–PyPzH)$_4$$Cl_6$] (**5**) at room temperature (top) and 77 K (bottom). Wavelengths at which the spectra were recorded are reported in the legends.

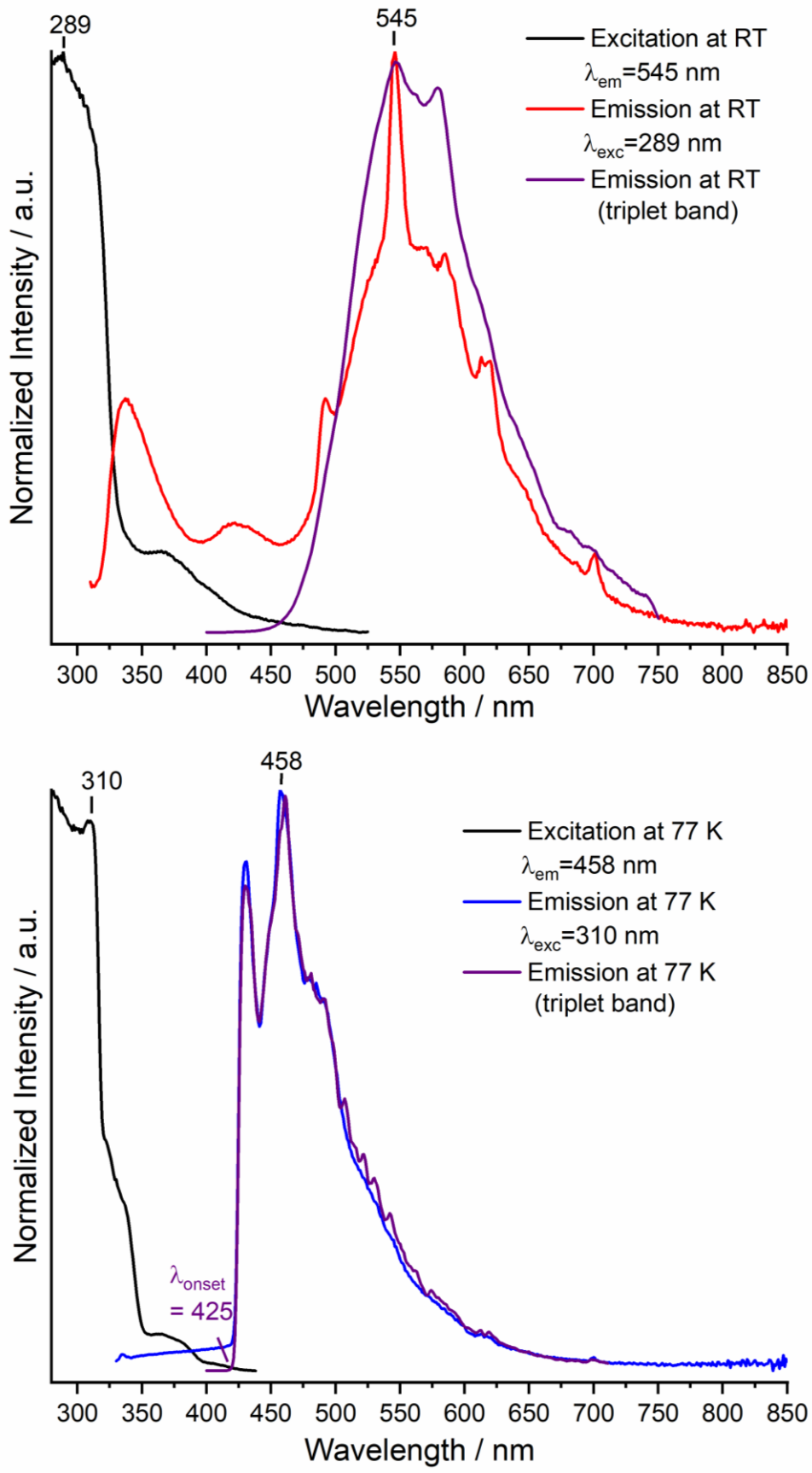

Figure S31. Normalized excitation and emission spectra of α–[Gd_2(2–PyPzH)$_4Cl_6$] (**6**) at room temperature (top) and 77 K (bottom). Wavelengths at which the spectra were recorded are reported in the legends.

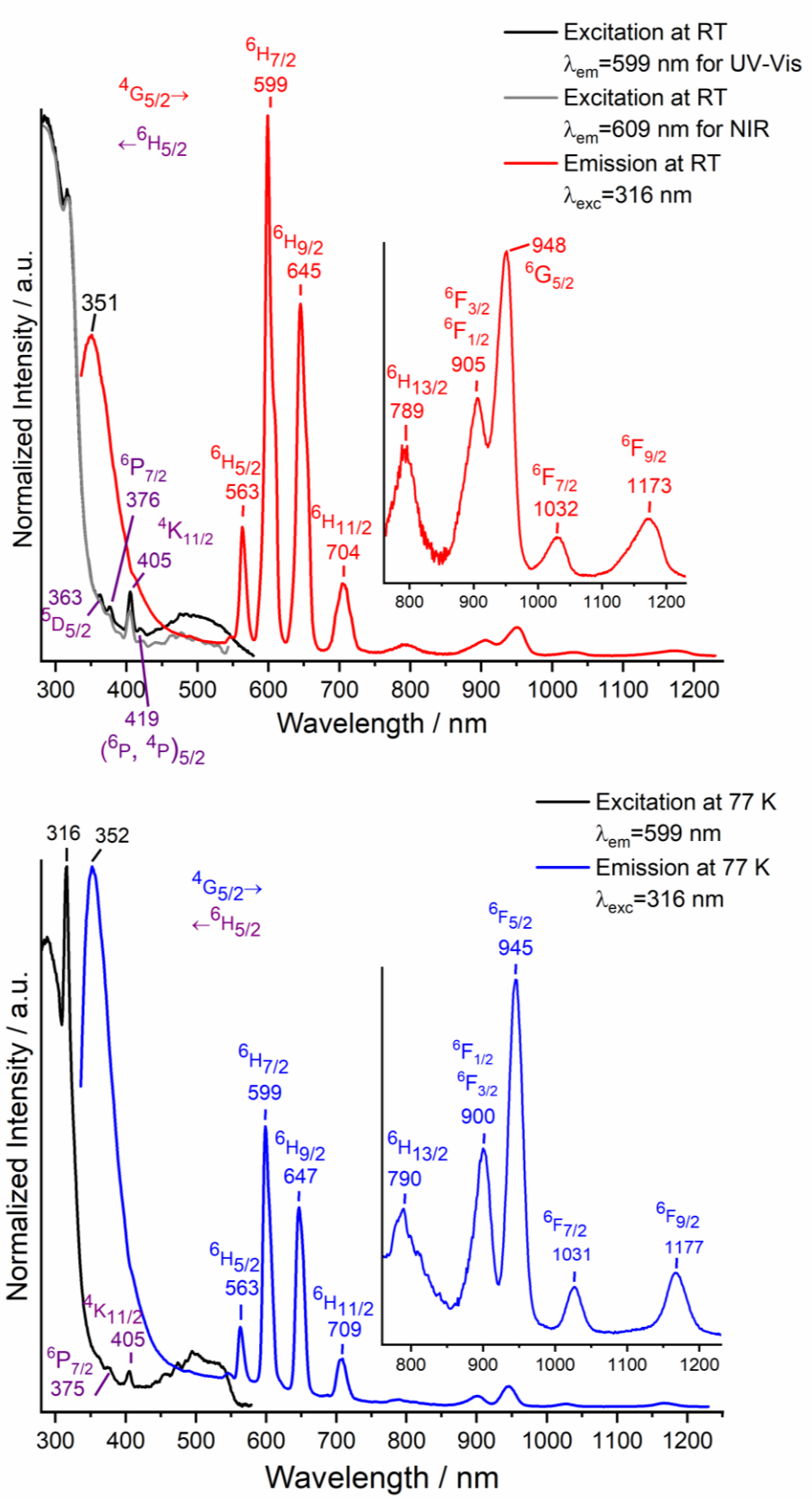

Figure S32. Normalized excitation and emission spectra of β–[Sm_2(2–PyPzH)$_4$$Cl_6$] (**8**) at room temperature (top) and 77 K (bottom). Wavelengths at which the spectra were recorded are reported in the legends. Visible and NIR range emission spectra were brought to the same intensity at 704 (at RT) and 709 (at 77 K) nm.

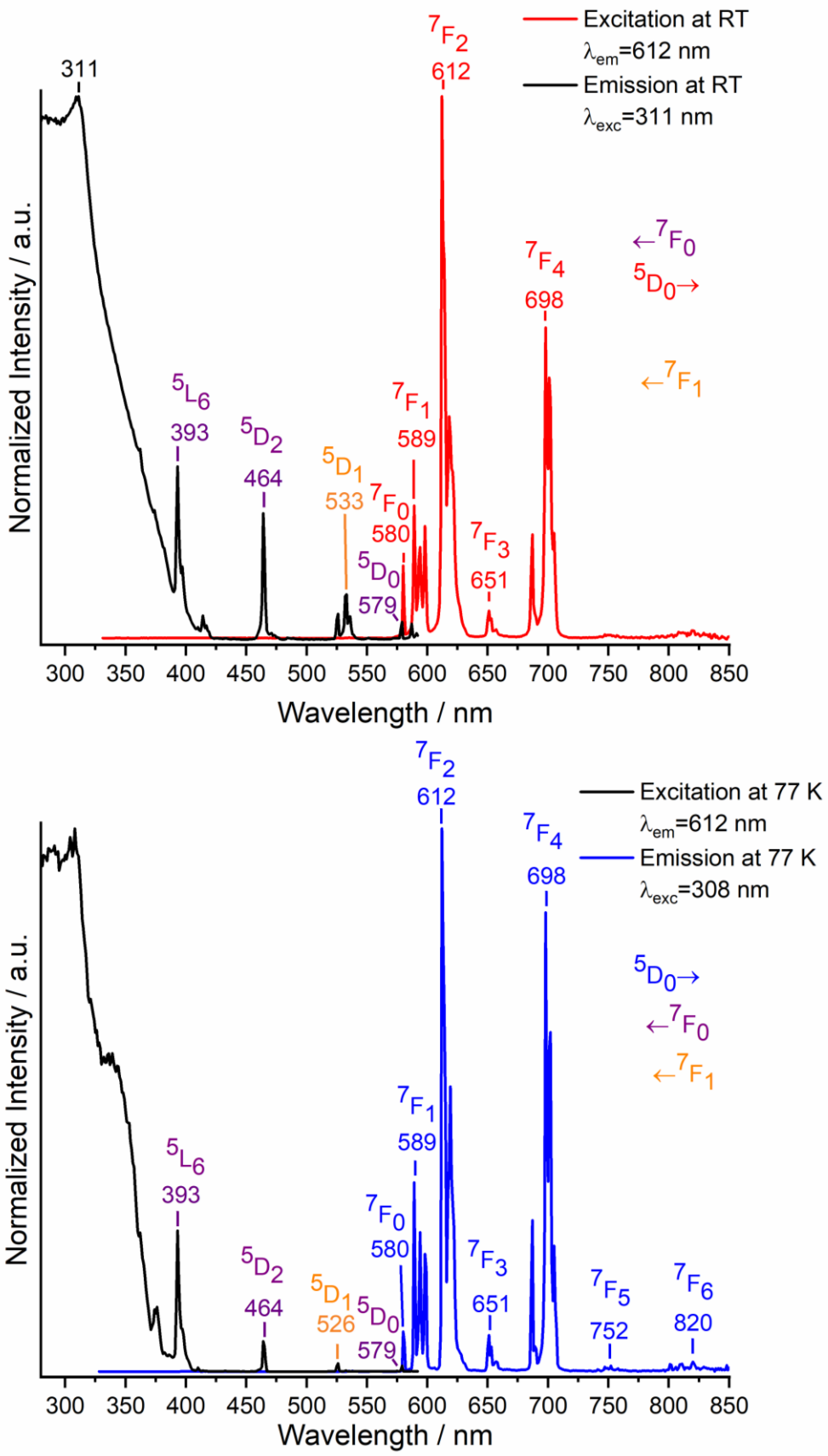

Figure S33. Normalized excitation and emission spectra of β–[Eu_2(2–PyPzH)$_4$$Cl_6$] (**9**) at room temperature (top) and 77 K (bottom). Wavelengths at which the spectra were recorded are reported in the legends.

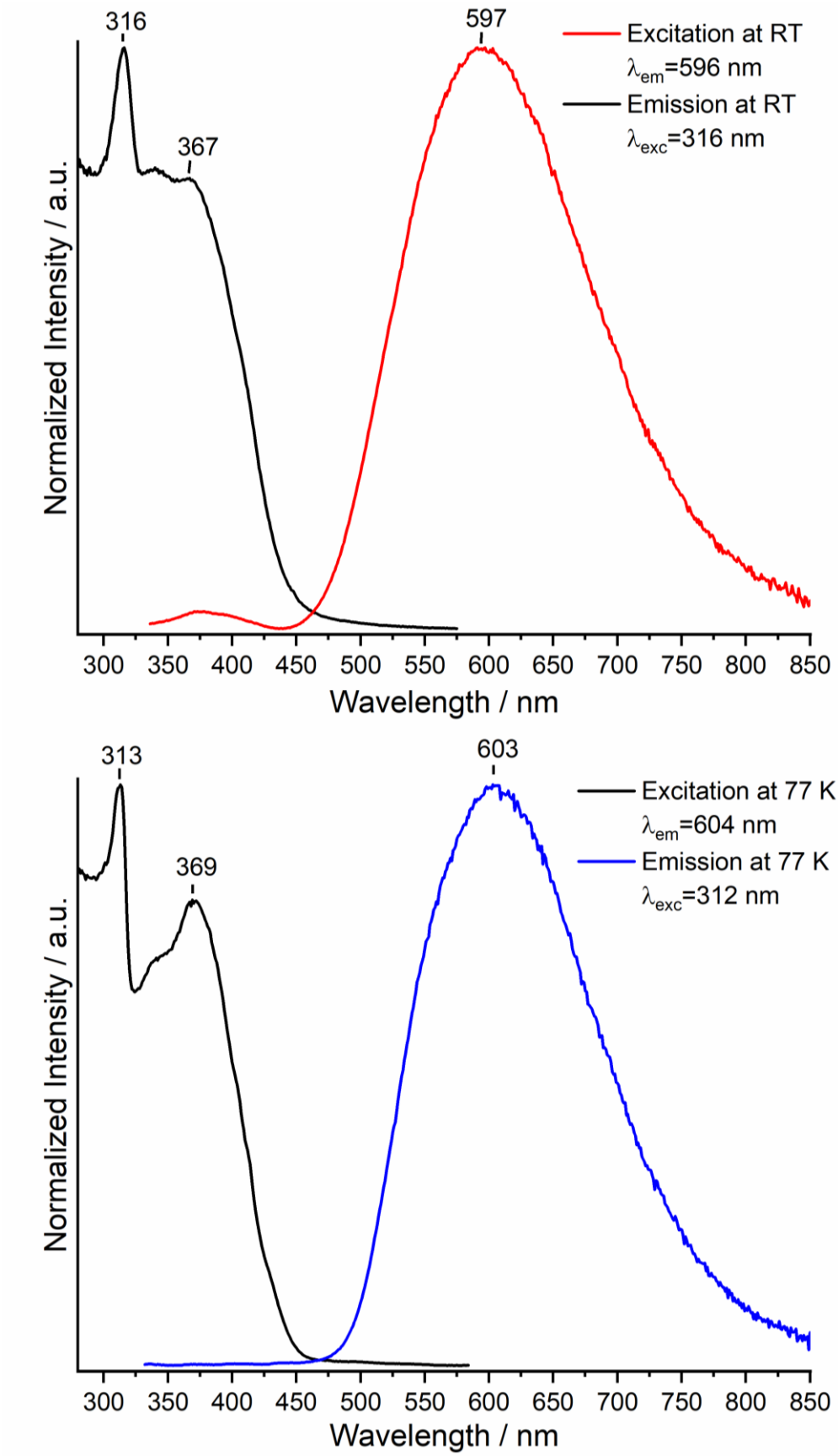

Figure S34. Normalized excitation and emission spectra of [Ce(2–PyPzH)$_3$Cl$_3$] (**11**) at room temperature (top) and 77 K (bottom). Wavelengths at which the spectra were recorded are reported in the legends.

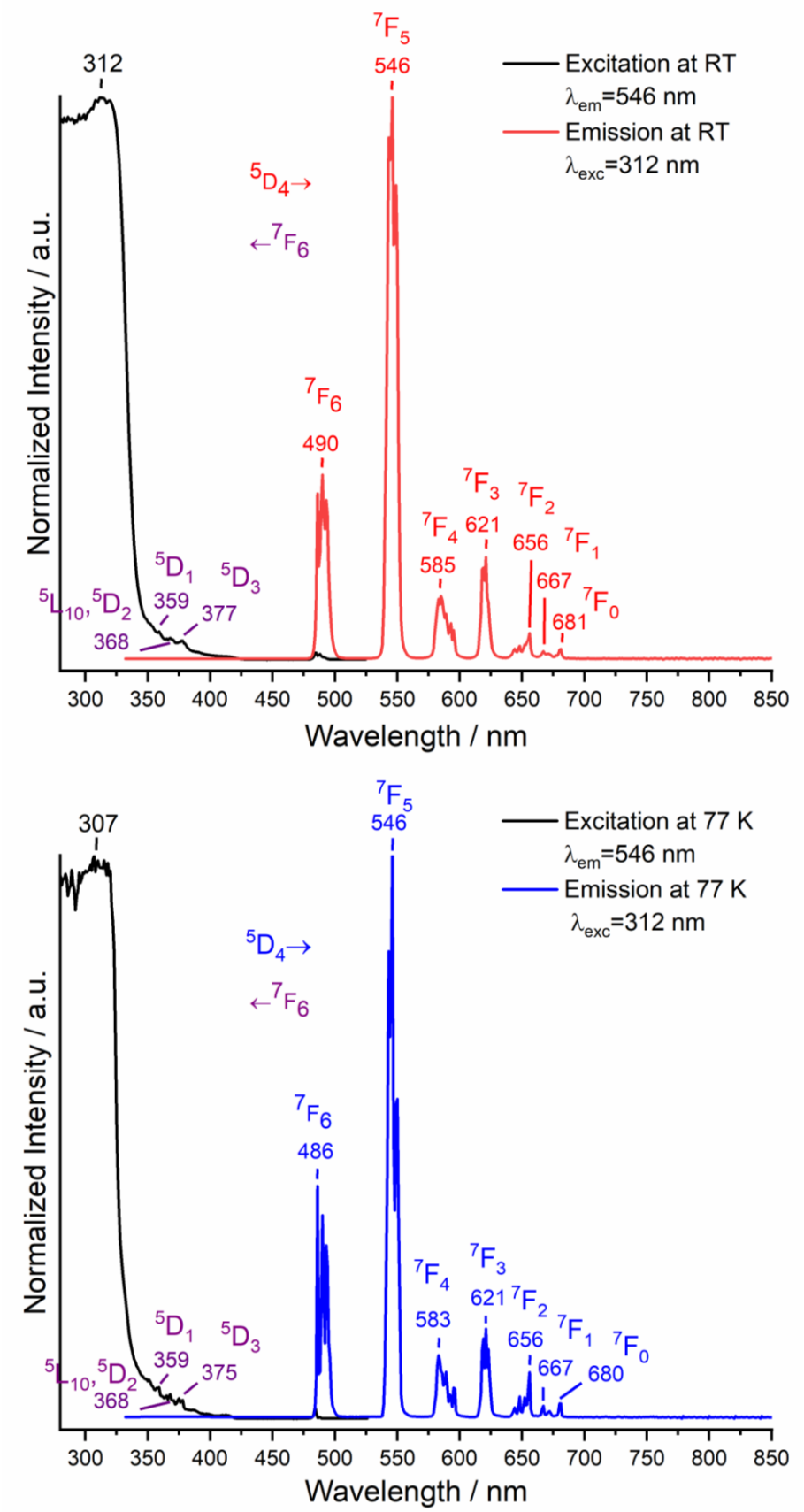

Figure S35. Normalized excitation and emission spectra of [Tb(2–PyPzH)$_2$Cl$_3$] (**12**) at room temperature (top) and 77 K (bottom). Wavelengths at which the spectra were recorded are reported in the legends.

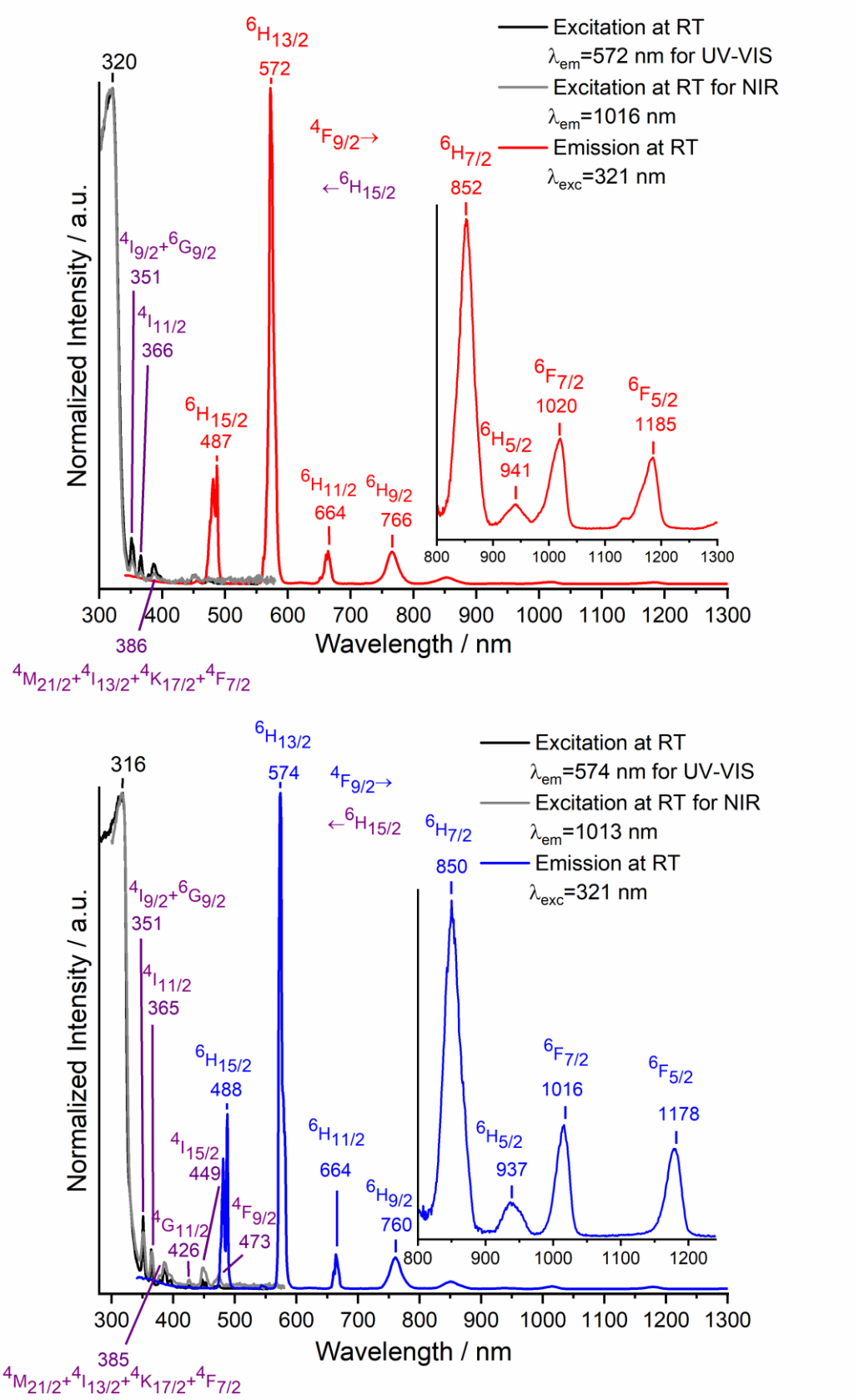

Figure S36. Normalized excitation and emission spectra of [Dy(2–PyPzH)$_2$Cl$_3$] (**13**) at room temperature (top) and 77 K (bottom). Wavelengths at which the spectra were recorded are reported in the legends. Visible and NIR range emission spectra were brought to the same intensity at 766 (at RT) and 760 (at 77 K) nm.

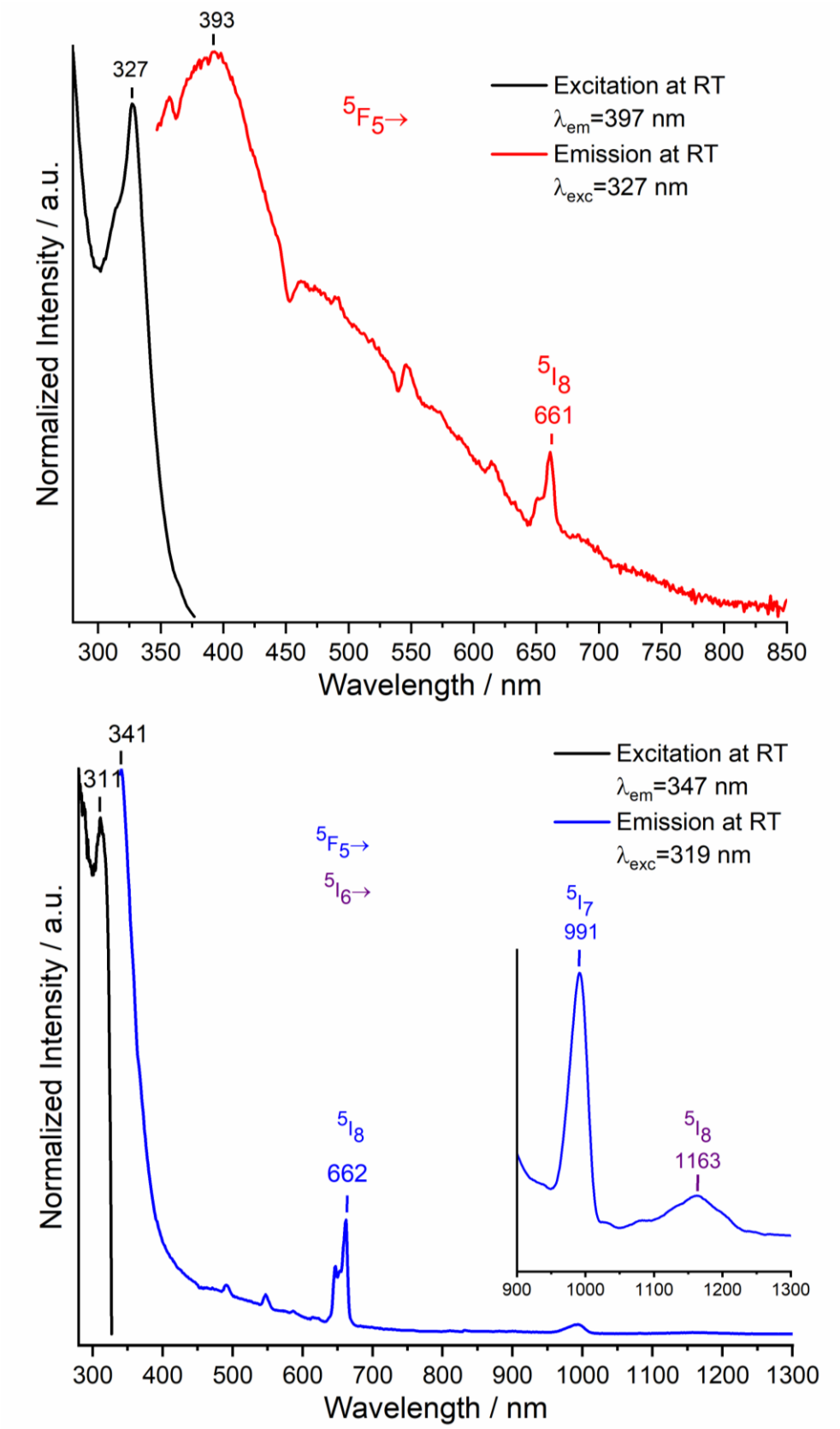

Figure S37. Normalized excitation and emission spectra of $[Ho(2–PyPzH)_2Cl_3]$ (**14**) at room temperature (top) and 77 K (bottom). Wavelengths at which the spectra were recorded are reported in the legends. Visible and NIR range emission spectra were brought to the same intensity at 662 (at 77 K) nm.

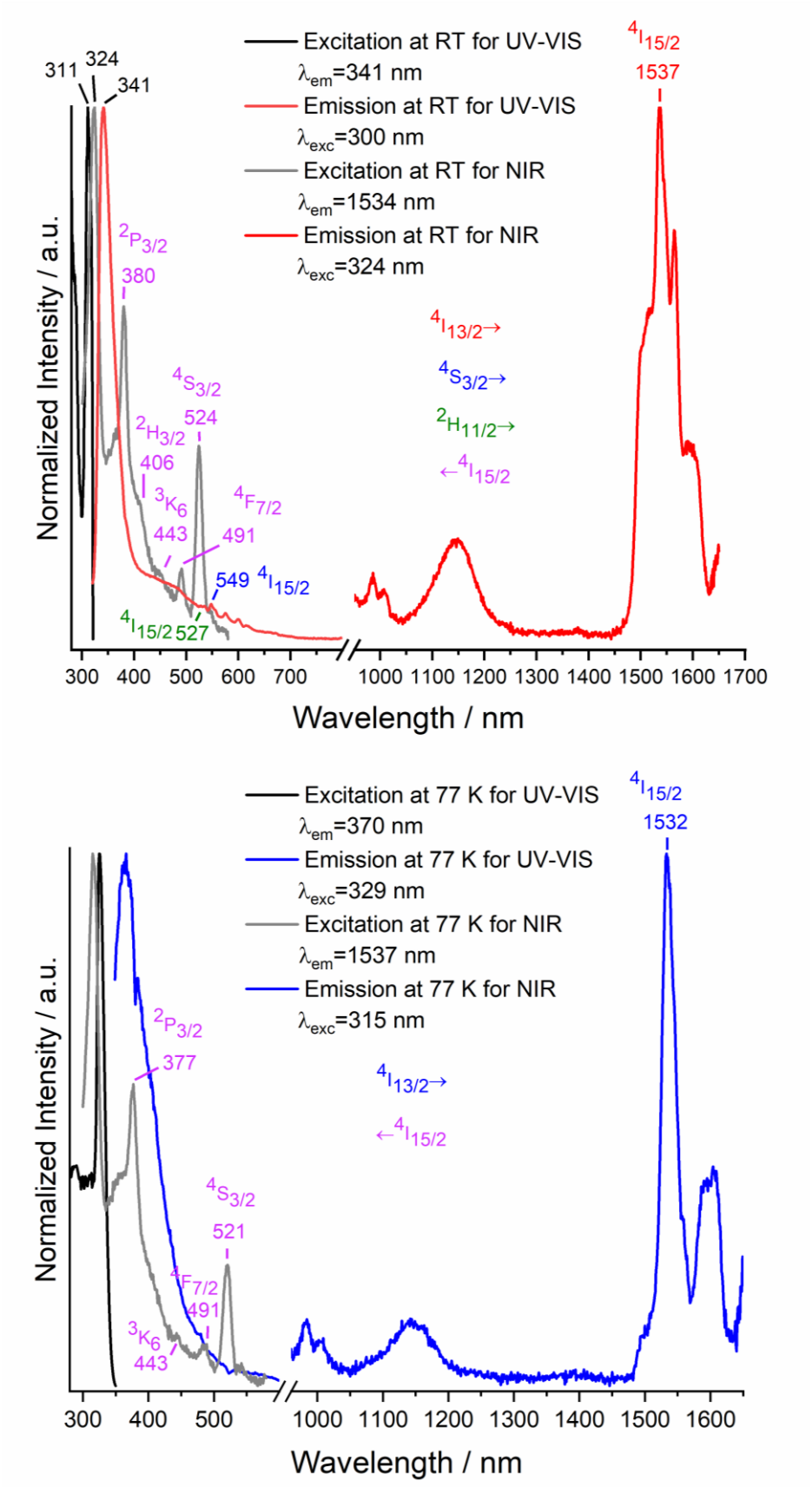

Figure S38. Normalized excitation and emission spectra of [Er(2–PyPzH)$_2$Cl$_3$] (**15**) at room temperature (top) and 77 K (bottom). Wavelengths at which the spectra were recorded are reported in the legends.

IR Spectra

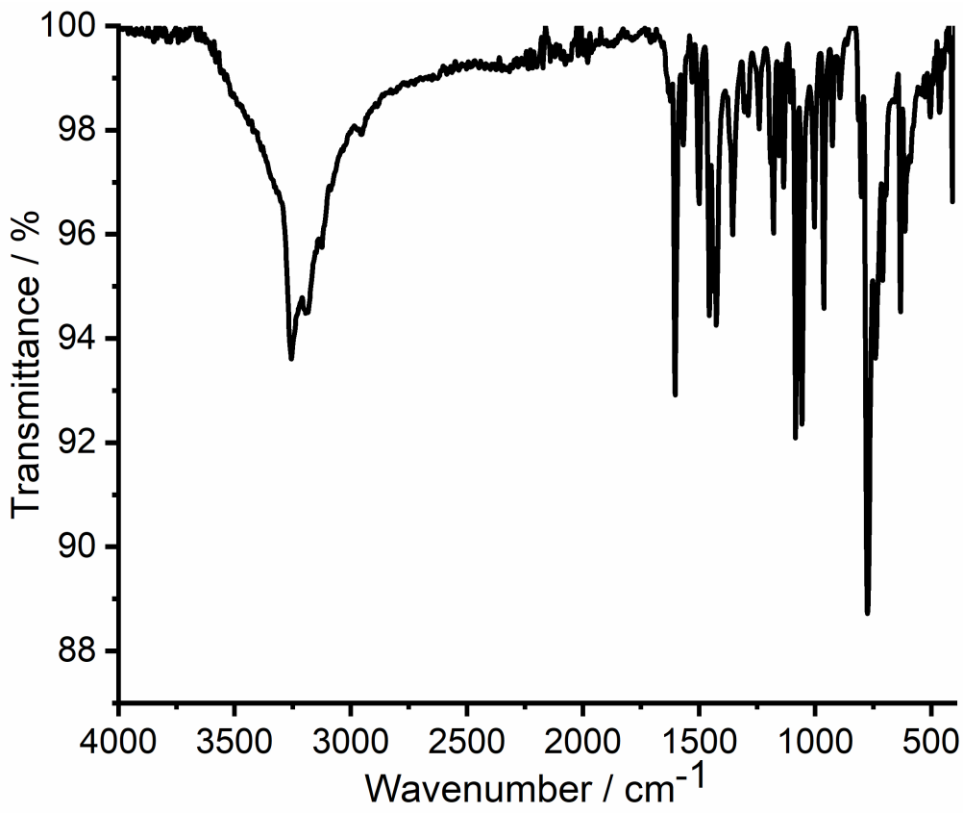

Figure S39. The infrared spectrum (ATR) of ∞[La_2(2–PyPzH)$_4$$Cl_6$] (**1**).

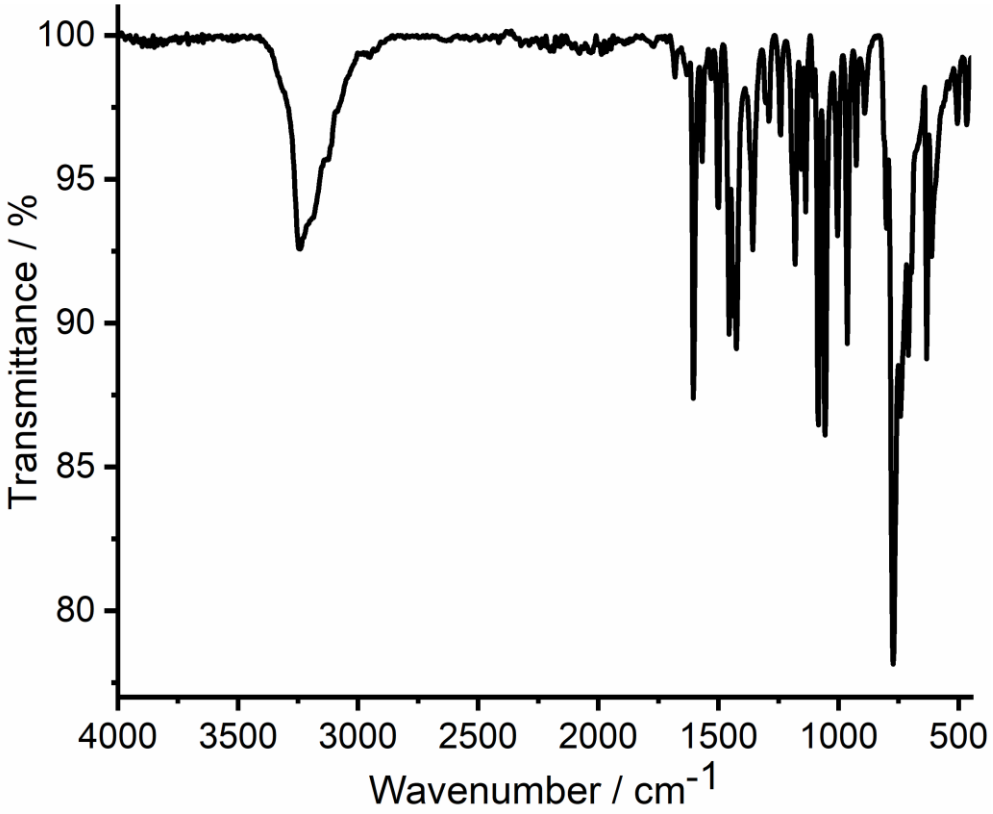

Figure S40. The infrared spectrum (ATR) of ∞[Nd_2(2–PyPzH)$_4$$Cl_6$] (**2**).

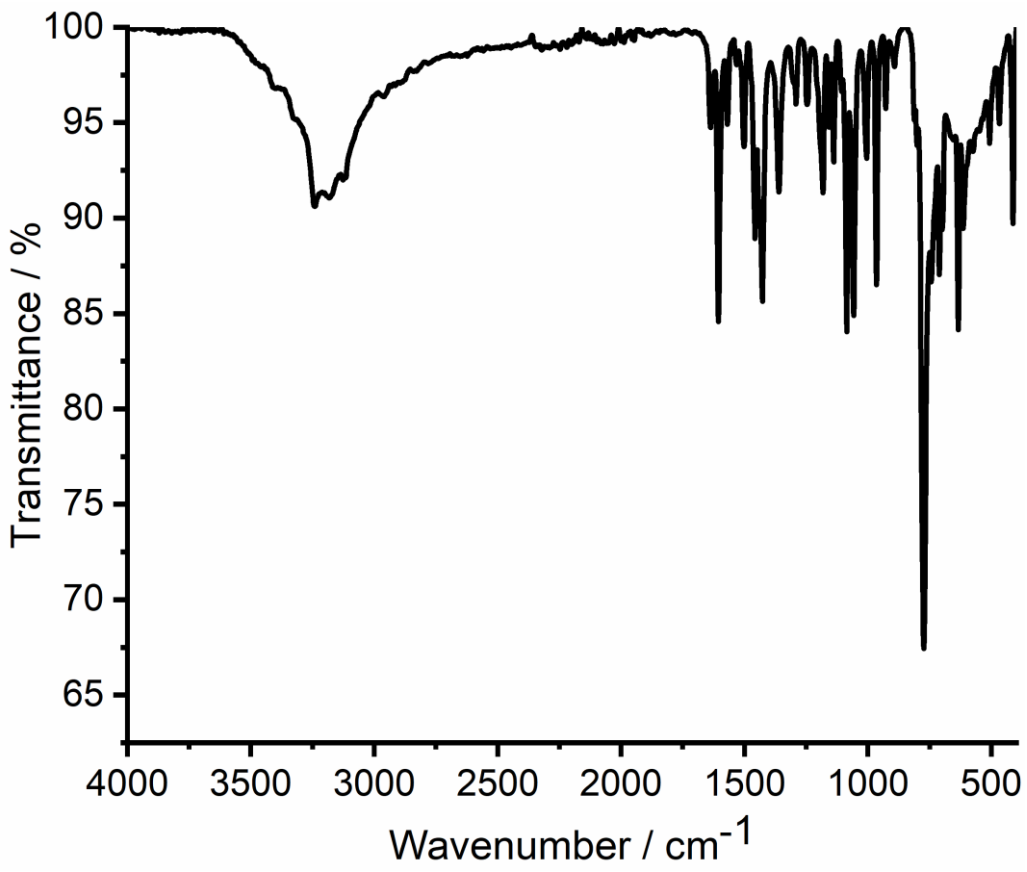

Figure S41. The infrared spectrum (ATR) of ∞[Sm_2(2–PyPzH)$_4$$Cl_6$] (**3**).

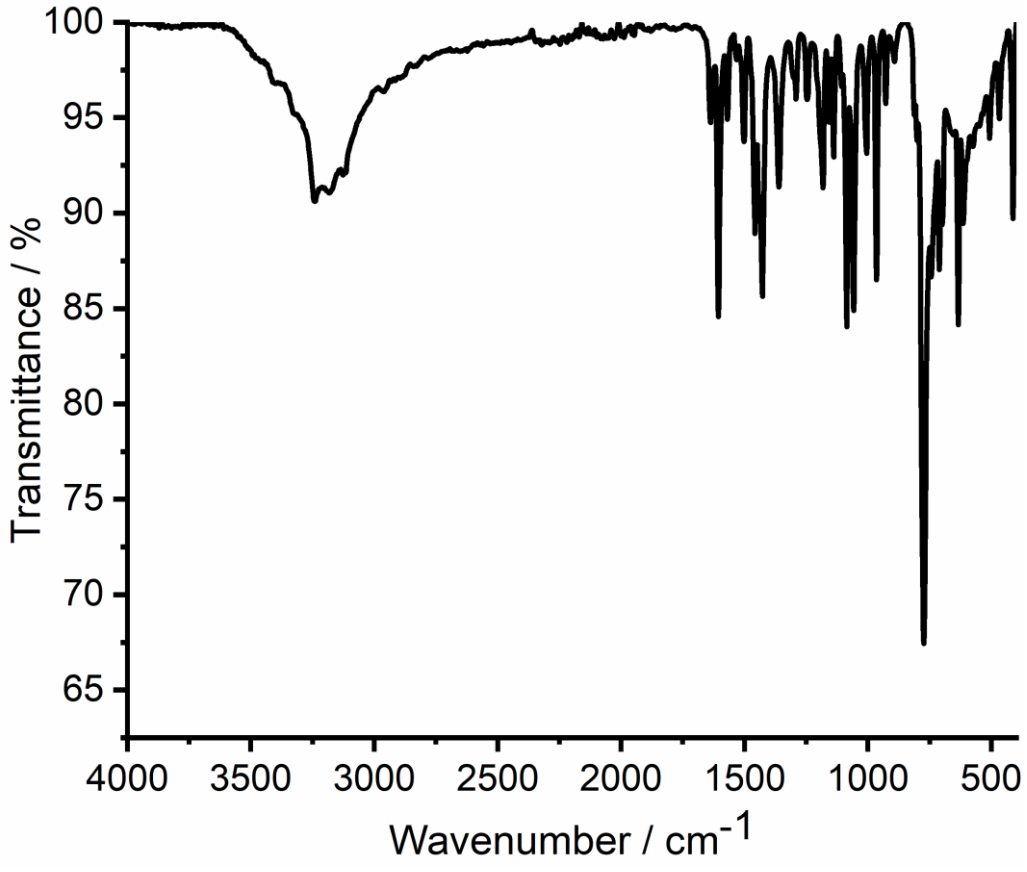

Figure S42. The infrared spectrum (ATR) of α–[Sm_2(2–PyPzH)$_4$$Cl_6$] (**4**).

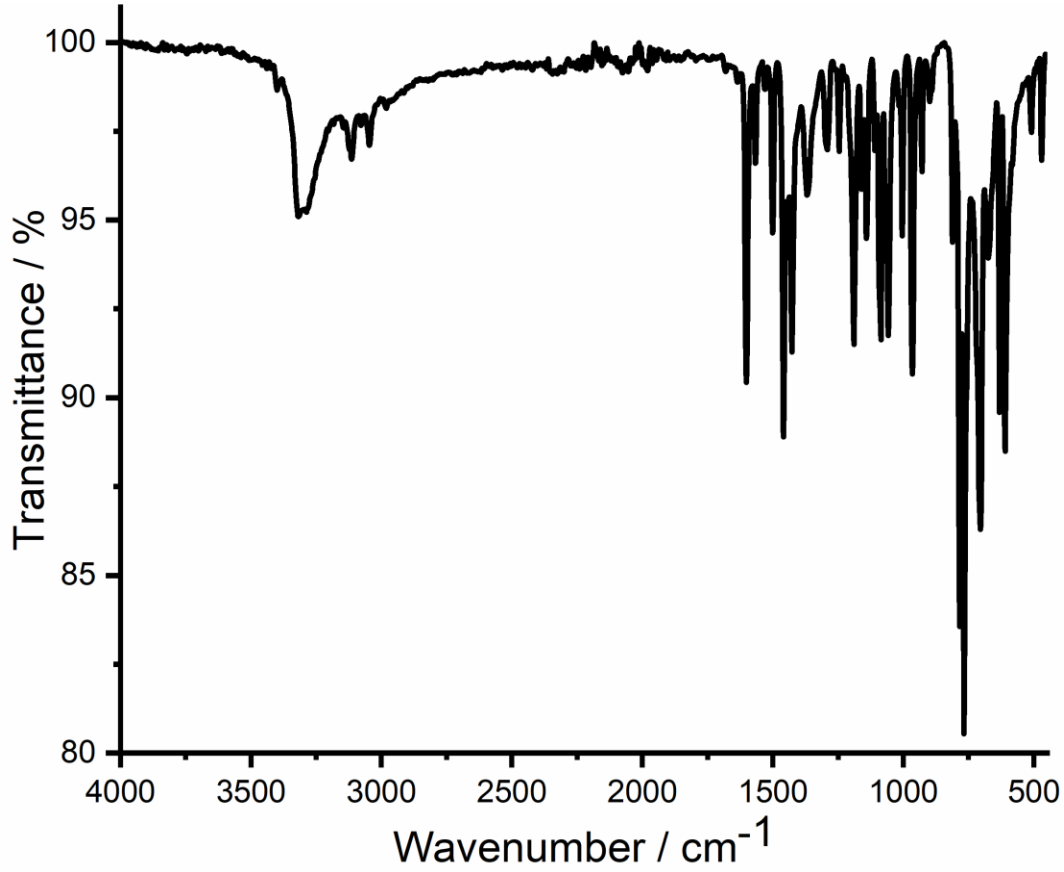

Figure S43. The infrared spectrum (ATR) of α–[Eu_2(2–PyPzH)$_4Cl_6$] (**5**).

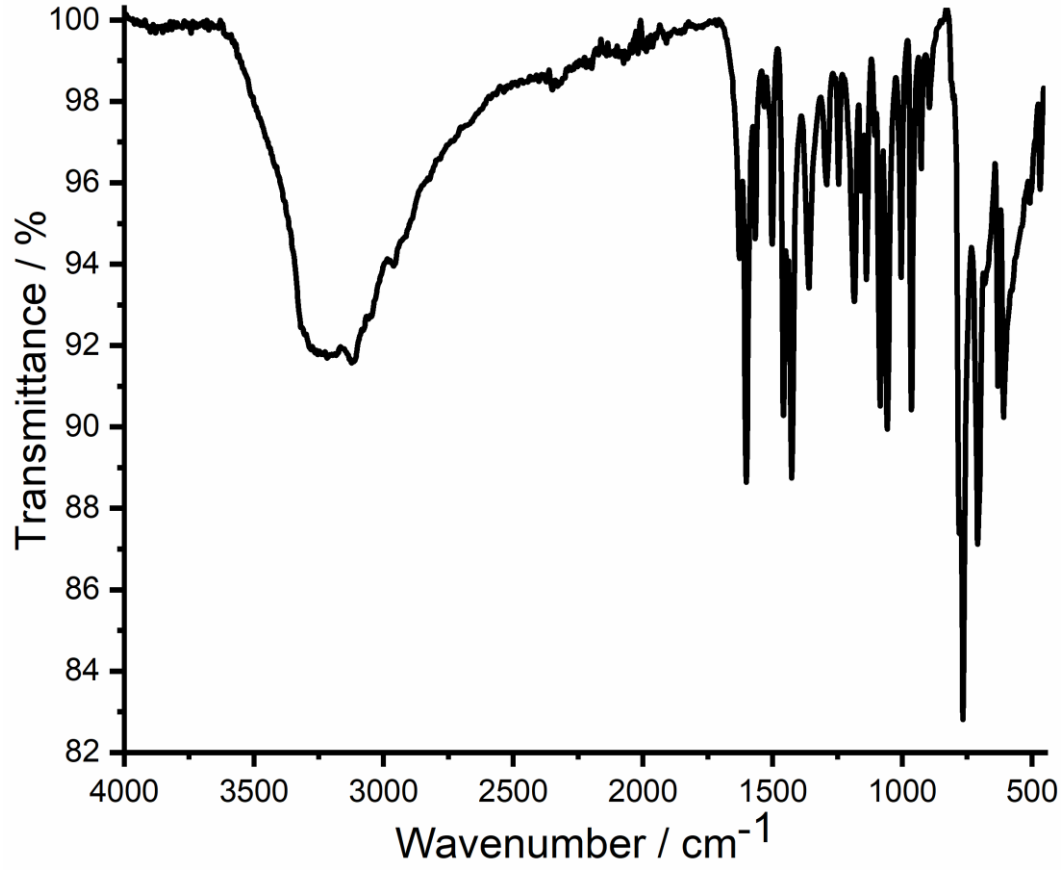

Figure S44. The infrared spectrum (ATR) of α–[Gd_2(2–PyPzH)$_4Cl_6$] (**6**).

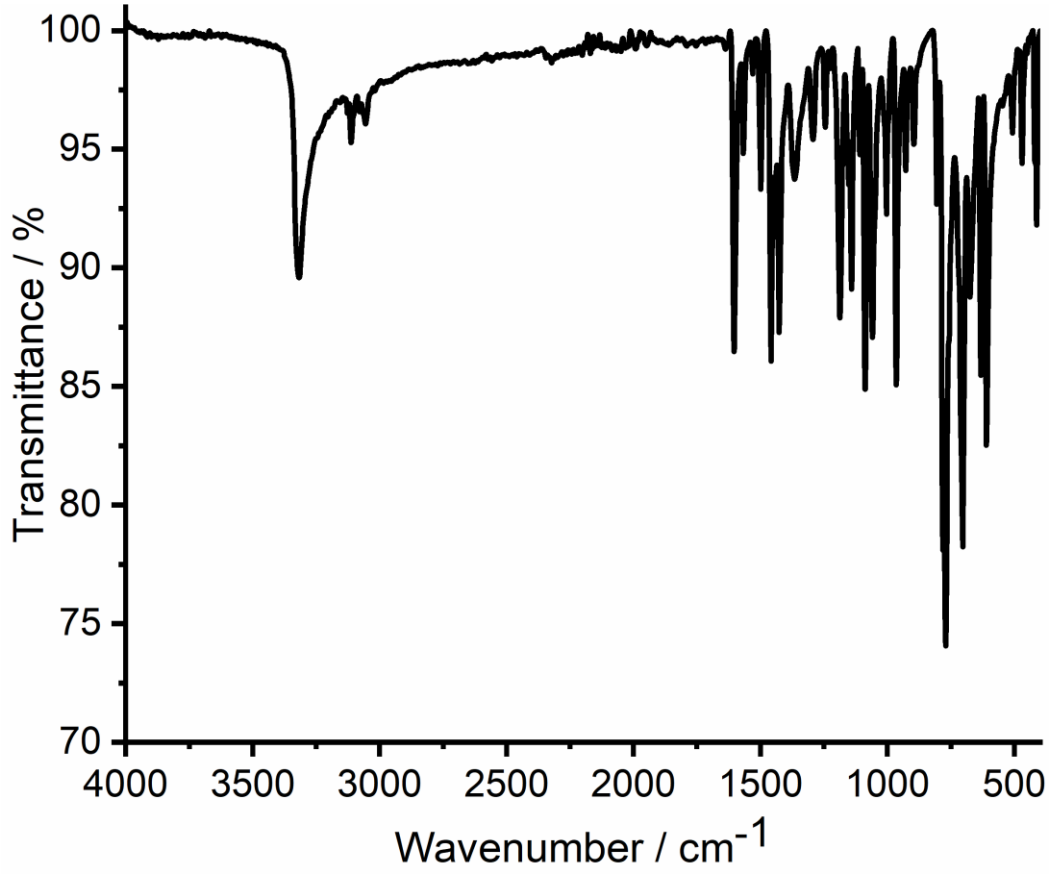

Figure S45. The infrared spectrum (ATR) of β–[Sm_2(2–PyPzH)$_4Cl_6$] (**8**).

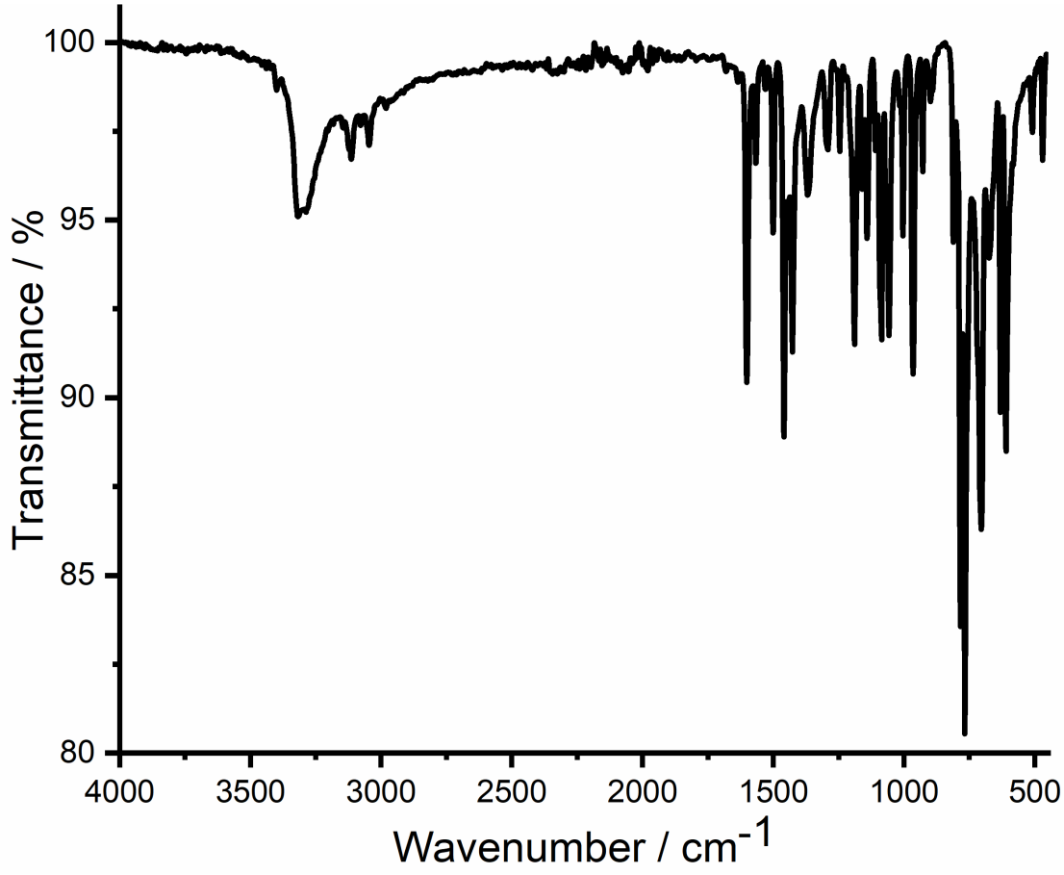

Figure S46. The infrared spectrum (ATR) of β–[Eu_2(2–PyPzH)$_4Cl_6$] (**9**).

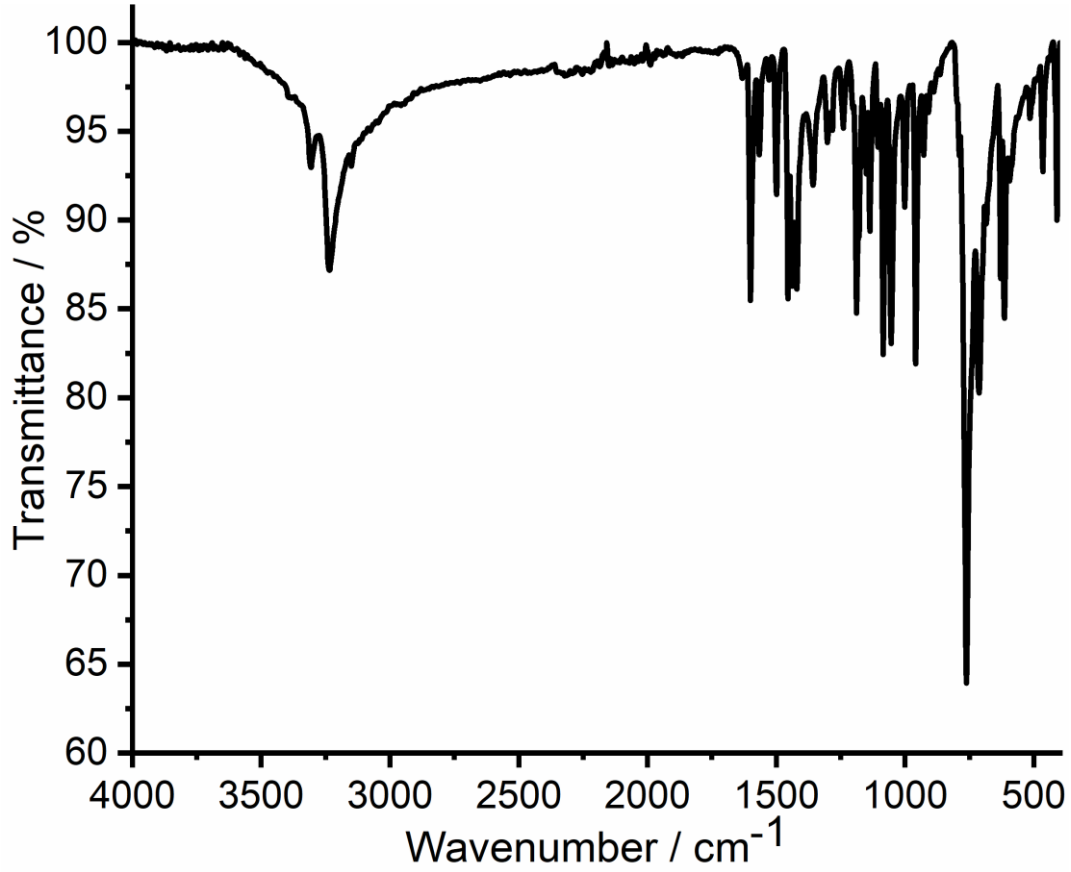

Figure S47. The infrared spectrum (ATR) of [Ce(2–PyPzH)$_3$Cl$_3$] (**11**).

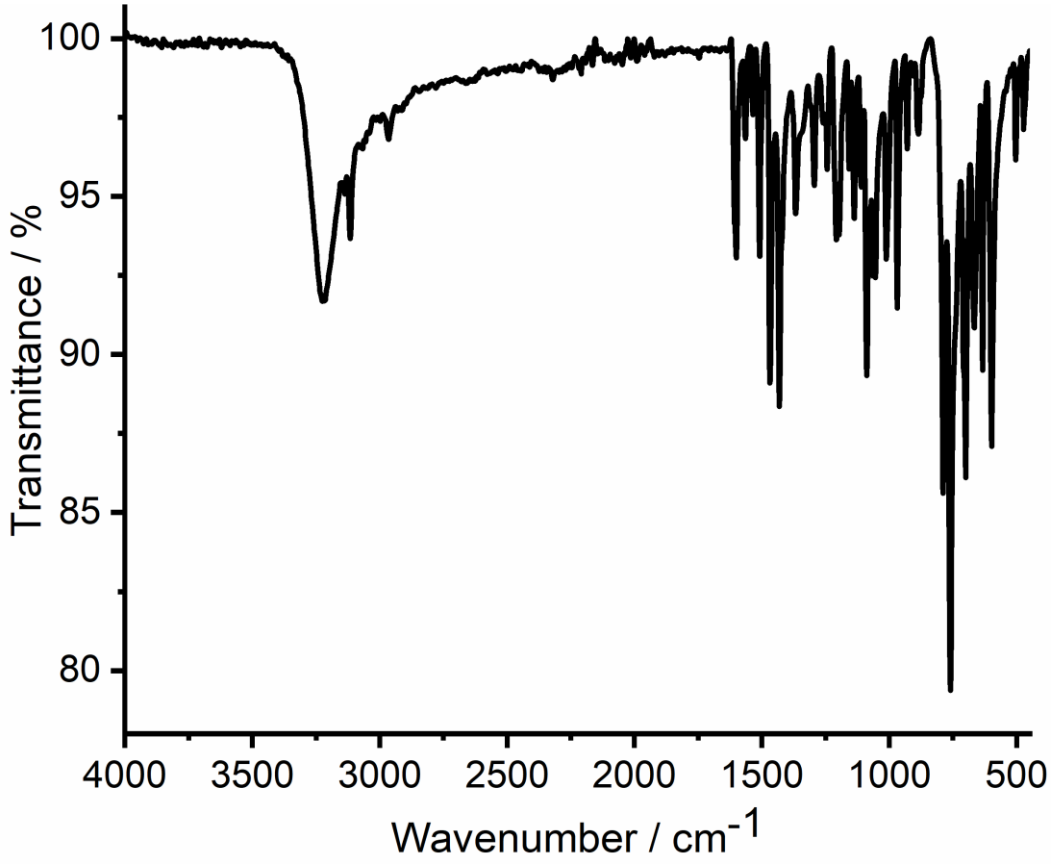

Figure S48. The infrared spectrum (ATR) of [Tb(2–PyPzH)$_2$Cl$_3$] (**12**).

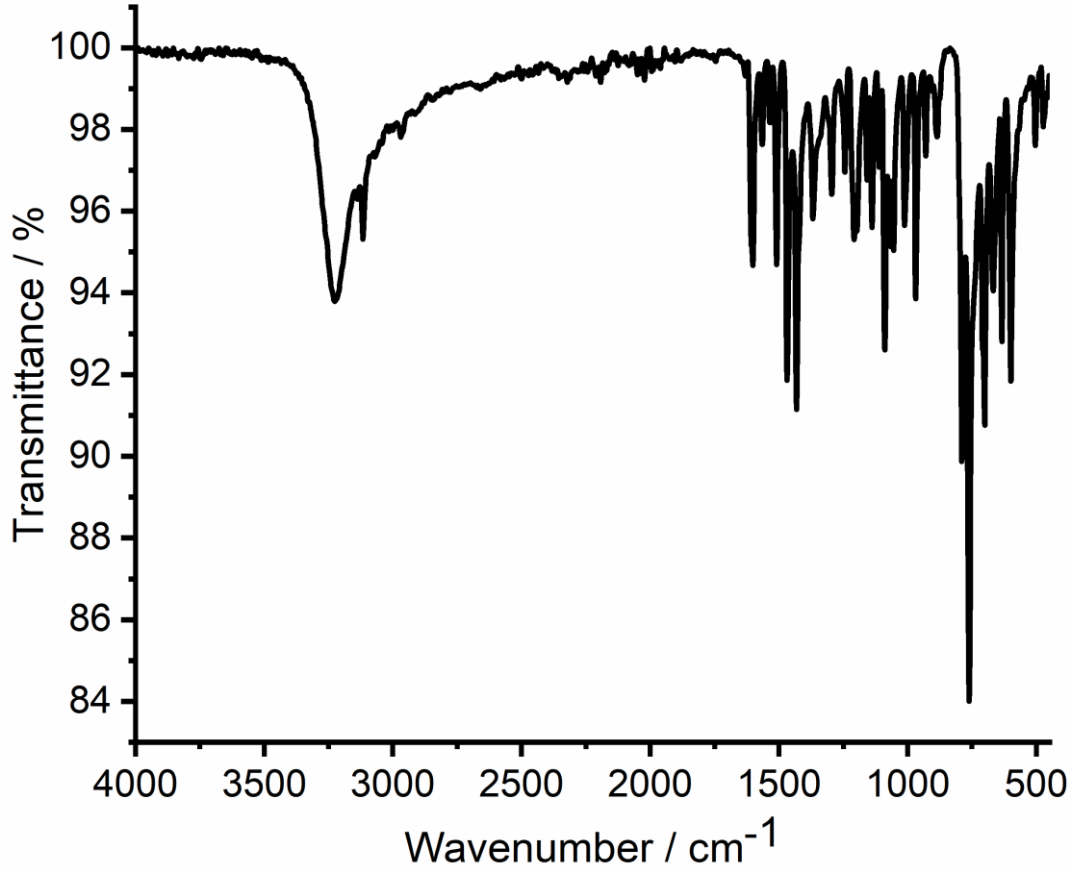

Figure S49. The infrared spectrum (ATR) of [Dy(2–PyPzH)$_2$Cl$_3$] (**13**).

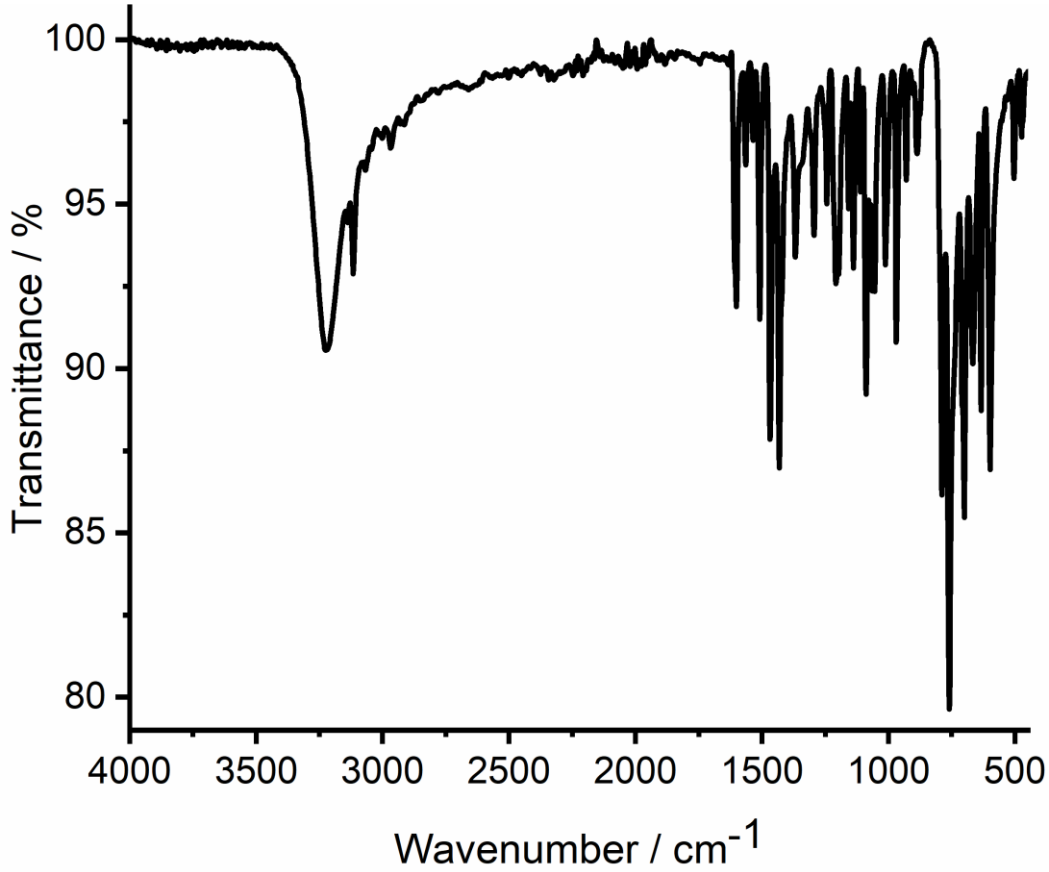

Figure S50. The infrared spectrum (ATR) of [Ho(2–PyPzH)$_2$Cl$_3$] (**14**).

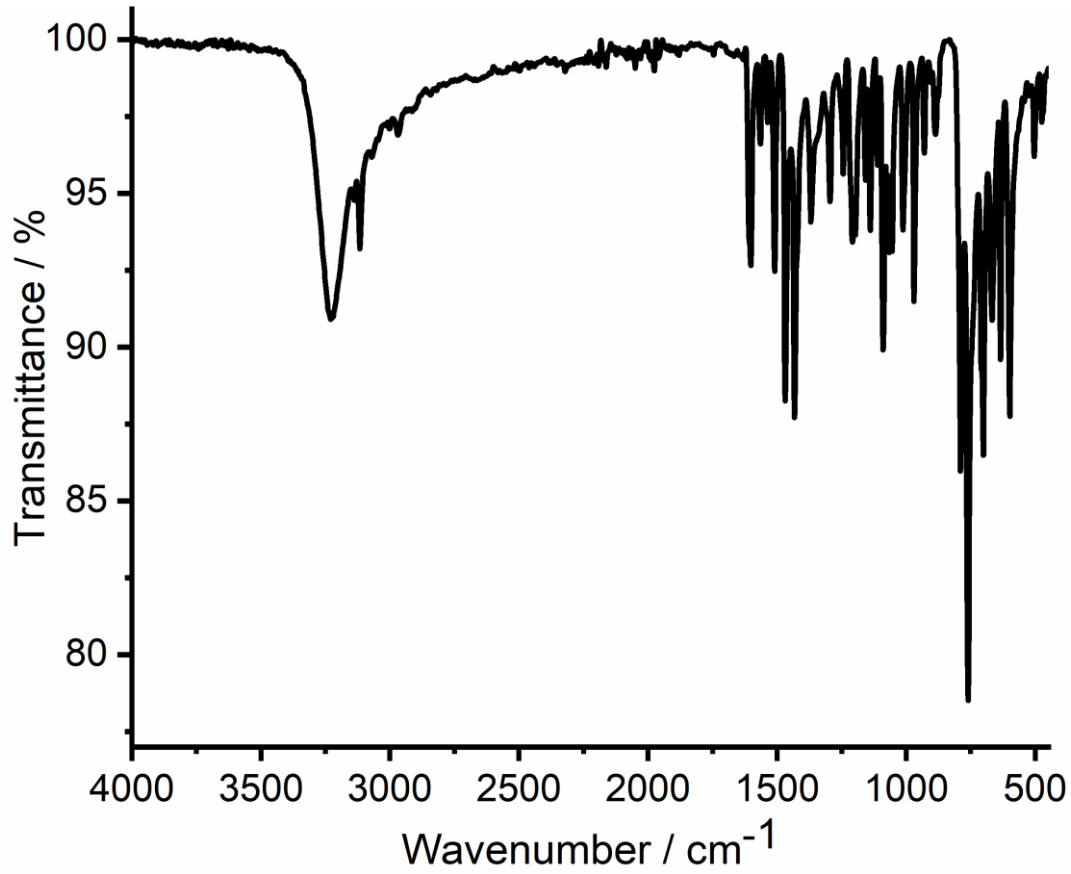

Figure S51. The infrared spectrum (ATR) of [Er(2–PyPzH)$_2$Cl$_3$] (**15**).